5-2002

Aquaporins and Aquaglyceroporins of Legume Nodules: Structure, Function, and Regulation

James F. Guenther
University of Tennessee - Knoxville

To the Graduate Council:

I am submitting herewith a dissertation written by James F. Guenther entitled "Aquaporins and Aquaglyceroporins of Legume Nodules: Structure, Function, and Regulation." I have examined the final electronic copy of this dissertation for form and content and recommend that it be accepted in partial fulfillment of the requirements for the degree of Doctor of Philosophy, with a major in Biochemistry and Cellular and Molecular Biology.

Daniel M. Roberts, Major Professor

We have read this dissertation and recommend its acceptance:

John Dunlap, Wesley Wicks, Albrect Von Armin, Jim Hall

Accepted for the Council:
Dixie L. Thompson

Vice Provost and Dean of the Graduate School

(Original signatures are on file with official student records.)

To the Graduate Council:

I am submitting herewith a dissertation written by James Guenther entitled, “Aquaporins and Aquaglyceroporins of Legume Nodules: Structure, Function, and Regulation.” I have examined the final electronic copy of this dissertation for form and content and recommend that it be accepted in partial fulfillment of the requirements for the degree of Doctor of Philosophy, with a major in Biochemistry and Cellular and Molecular Biology

Daniel M. Roberts

We have read this dissertaion and recommend its acceptance:

John Dunlap

Wesley Wicks

Albrect Von Armin

Jim Hall

Accepted for the Council:

Anne Mayhew

Vice Provost and Dean of Graduate Studies

(Original signatures are on file in the Graduate Studies Office.)

AQUAPORINS AND AQUAGLYCEROPORINS OF LEGUME NODULES: STRUCTURE, FUNCTION, AND REGULATION

A Dissertation
Presented for the
Doctor of Philosophy
Degree
The University of Tennessee, Knoxville

James F. Guenther
May 2002

ACKNOWLEDGMENTS

Through my years building up to this point I have changed much and I have many people that I have encountered along the way that I will remember long after I am free of this place. I would like to start off with Daniel Roberts, my major professor who has a dark sense of humor that is as warped and twisted as my own. I have often wondered what I would take in memories from him when I leave this place, I hope that I will take a more detailed first hand understanding of how a scientific mind operates together with a sense of satisfaction and passion for the work that I do, and the understanding that what ever I may do in my life it should be in line with the goals that I set for myself. In respect to this, I hope that I never look back and wonder what has brought me to the end of this road. It has been a strange time knowing Dan over the years, he has challenged me while at the same time retaining the difficult job of remaining my friend, to this extent I have thought that I would surely kill him many times before I finished at Tennessee.

The next people who snap to my mind when thinking about my time in Tennessee are my committee members who have brought a barrage of knowledge and skills to my work; I would like to thank, Gary Stacey, John Dunlap, Pete Wicks, Albrecht Von Arnim, and Jim Hall for testing me and offering specialized advice which has allowed me to investigate new areas of my present research and to broaden my field of interests.

My interactions in the lab have been diverse and many people have contributed to my growth. The first person I would like to mention is Derik

Smiley who is a purist in the sense of research and a cruel friend. Over the years I have known many people that have come and gone in the lab during my time that deserve recognition, Scott Harding, who initially worked with me in the Roberts lab. I have made several friends in the lab along the way and each of them have contributed in their own way to my work, Rob Dean, Jennifer Cobb, Tina Randolph, Nouth Chanmanivone, Rana Ferrebee, Burnette Crombie, Dave Wills, Christa Niemietz, and Lenka Nezbith navathalovar. Recently, I have been lucky to work with three people in lab that are driven, the first was Manker Galetovic who walked in one day looking for a job and started washing dishes after the unexpected absence of the last lab dishwasher. It quickly became apparent that Manker was capable of much more involved skills and eventually he was placed working with me on the last part of my project dealing with generation of the phosphorylation-specific antibody for nodulin 26 and the physiological regulation of phosphorylation of this protein. All I can say is that, it has been a pleasure to work with someone who is talented and driven. The next person who I thank for their time and help is Ian Wallace who I first met while he was working in Pete Wicks lab where he showed a dedication and interest for the work he was doing which reminded me what dedication to ones work was even though I had thought I had long lost that spark. Molecular modeling of the LIMP1 and LIMP2/Nod26 proteins was done by and large by Ian without concern for credit, but with the self-fulfillment that I think would shame most scientists. I would also like to thank Eric Vincill for his interest in taking over the one of the

projects I have worked on while in Dan's lab. I think it is a great compliment to know that the research I have worked on over the years will be continued, hopefully elucidating a greater understanding of these processes. He has already shown that he has the hands for this line of work, I am sure that he will grow into an excellent scientist.

Next I would like to thank my family who have stood by me over the long years that I have been away from them in Tennessee: my mother, father, brother and grandmothers who have given me so many viewpoints to consider and so much support and advice which I have used to navigate through life keeping my back to the wind. I would also like to mention two my closest friends over the years that I have known since childhood, Joseph Brinz and Bryan Gallo, they have always been there for me when I thought I could not take anymore of this abuse. Finally, I would like to thank my friends back in New Orleans and abroad who have given me their unending and unregulated support over the years I know that I would not have come this far without the hope that I will come back to them when the time is right. These people need no name-wise mentioning because they are always in my thoughts and in my heart.

I could be laughing or spitting up blood right now, for all I know.

ABSTRACT

By isolating RNA from mature nodules of the legume *Lotus japonicus* and employing an RT-PCR approach, two new cDNAs were characterized whose open reading frames code for members of the MIP (Major Intrinsic Protein) family of membrane proteins. These two genes products were termed (Lotus Intrinsic Membrane Protein 1 and 2) LIMP1 and LIMP2. Both LIMP1 and LIMP2 display all the hallmarks of the MIP protein family including, six putative transmembrane domains based on hydropathy plots, and the invariant NPA (asparagine-proline-alanine) signature motifs located symmetrically on two loops, which connect transmembrane helix 3-4 and transmembrane helix 5-6. Based on sequence information, LIMP1 is placed in the TIP (Tonoplast membrane Intrinsic Protein) subfamily of plant MIP proteins. Based on localization within the cells, TIPs are typically found on the tonoplast membrane of plant vacuoles. Functional characterization of LIMP1 by expression in *Xenopus* oocytes has demonstrated that it is a water-selective aquaporin. Using Northern blot techniques combined with immunolocalization, the expression patterns for LIMP1 were analyzed. The results indicate that LIMP1 is expressed predominately in nodules and roots. Based on Western blot analysis, however the highest LIMP1 protein levels are found in roots. LIMP1 appears to be regulated by diurnal cycling conditions, with expression increasing during the day hours, but falling off at the beginning of the night cycle. Increases in LIMP1 expression precedes the

time of the diurnal cycle when the plant rate is the highest. This finding suggests that LIMP1, similar to other aquaporins, is regulated in response to the need for trancellular water uptake and transport from the soil during times of high transpiration stream activity.

Although the LIMP2 protein shows some sequence similarity to LIMP1, it displays several features which distinguish it. Based on primary sequence identities, LIMP2 is classified in the plant NIP (Nodulin-like Intrinsic Protein) subfamily of MIP proteins which takes its name from the patriarch protein, nodulin 26. Nodulin 26 is a soybean nodule protein localized exclusively to the symbiosome membrane which surrounds the symbiotic bacteria during the nitrogen fixation process. Comparison of the LIMP2 protein sequence with other MIP family members shows that it shares the highest sequence identity (68%) with nodulin 26. In addition to structural similarity, nodulin 26 and LIMP2 also share the ability to facilitate the transport of water as well as small uncharged solutes (e.g. glycerol) upon expression in *Xenopus* oocytes. Analysis of the tissue distribution of LIMP2 by Northern blot and immunolocalization reveal that the LIMP2 transcript is expressed only in nodule tissue and that this protein, like nodulin 26, is present on the symbiosome membrane.

LIMP2 and LIMP1 both show the ability to transport water, but the rate of transport is several-fold lower than that observed for high water transport MIP proteins such as mammalian aquaporin 1 (AQP1). Based on the crystal structures of AQP1 and the bacterial glycerol facilitator protein (GlpF), models

of the selectivity filter for LIMP1 and LIMP2 were generated and analyzed in order to resolve the underlying characteristics for these observed differences. The proposed selectivity filter for LIMP2 displays a pore large enough to accommodate the passage of glycerol. Further, three key residues, a tryptophan in helix 2 and a valine in helix 5 and an arginine in the second NPA loop, form an amphipathic signature similar to the selectivity filter of the glyceroporin GlpF and are proposed to account for the glycerol permeability of nodulin 26 and LIMP2. In silica modeling of the predicted pore for LIMP1/TIPs shows a unique set of features. It shows a higher hyrdrophobic character than AQP1 and unusual substitutions, a histidine in helix 2 which replaces an invariant phenylalanine, an isoleucine in helix 5 which substitutes for a histidine, and a valine in the second NPA loop which substitutes for an invariant arginine. These substitutions suggest that the pore structure of LIMP1 is quite unlike the two models (AQP1 and GlpF), and further insight into factors that contribute to its rate and selectivity will have to await more detailed structural analysis.

In addition to sequence and functional similarities, both nodulin 26 and LIMP2 share a conserved phosphorylation motif for CDPK (Calcium Dependent Protein Kinase) located on the cytosolic carboxyl terminal tail. In vitro assays using the carboxyl terminal sequence of LIMP2 suggest that similar to nodulin 26, it is phosphorylated by CDPK and is likely a target for calcium-dependent phosphorylation. Using an antibody which specifically recognizes the phosphorylated form of nodulin 26, a developmental pattern of

phosphorylation is observed, where immature nodules show no or very low levels of phosphorylation and very old nodules show no phosphorylation of nodulin 26 although the protein is present in both young and old nodules at the same level as in mature nodules. Using this phosphorylation-specific antibody it was also determined that in mature soybean nodules the inherent level of phosphorylation is stimulated in response to osmotic stress (drought and salinity).

Taken together, these results show that *Lotus japonicus* nodules have two MIP proteins. LIMP1 is a member of the TIP family of plant MIP proteins which is found predominately in root tissues where it forms a water selective channel, and its expression is controlled by diurnal variation. Its role in roots and nodules remains unknown, but it could play a role in transcellular water flow and cell volume regulation as proposed for other TIPs. In contrast, LIMP2 appears to be the *Lotus japonicus* ortholog of nodulin 26, an aquaglyceroporin that is localized on the symbiosome. LIMP2 and nodulin 26 are phosphorylated and likely regulated by calcium signaling through a symbiosome membrane CDPK. Previous studies show that phosphorylation of nodulin 26 enhances its water permeability. The present work suggests that phosphorylation by a calcium-dependent kinase is stress regulated and that phosphorylation of nodulin 26 may be among the osmoregulatorry responses of nodules necessary for stress adaptation, possibly by facilitating rapid water/solute flow to buffer the infected cell cytosol and symbiosome to fluctuations in osmotic gradients.

TABLE OF CONTENTS

LIST OF FIGURES

CHAPTER I

INTRODUCTION

Cell compartmentation and water transport across biological membranes

Water is the most abundant molecule found in all living cells, and the molecular processes that define life take place largely in an aqueous environment. One of the remarkable results of life in an aqueous environment was that it facilitated the production of membrane structures that allow compartmentation of biological processes. This need for primitive cells to generate a microenvironment within an enclosed volume is theorized to be fulfilled by the first crude amphipathic molecules which were capable of forming bilayers in aqueous media (Deamer et al., 1994). The lipid bilayer provides a simple but highly effective structure which can form spontaneously under aqueous conditions, and it provides a selective environmental barrier allowing for the transport of necessary metabolites into the cell and the export of waste and cellular byproducts out of the cell. During the course of evolution, specific protein molecules were generated which allow for the selective transport of the necessary compounds into and out of the cell to maintain cellular processes, thus enhancing the capabilities of the membrane. As a result of this flux of metabolites, the transport of water across membranes became more complex, and the need for osmoregulation to maintain osmotic balance and cell volume became critical.

For many years it was believed that the transport of water across biological membranes occurred by simple passive diffusion through the lipid bilayer. However, some membranes exhibited such high water permabilities which could not be explained by simple diffusion leading to the hypothesis of proteinaceous membrane components which could facilitate the rapid low energy transport of water across the bilayer (Finkelstein, 1987).

Two biophysical measurements of membranes can be used to experimentally determine if protein-facilitated transport of water is taking place: the osmotic permeability coefficient (P_f) and the diffusive permeability coefficient (P_d). P_f represents the permeability of a membrane in response to an imposed osmotic or hydrostatic gradient, while P_d reflects the diffusive properties of a membrane to water under isoosmotic conditions (Finkelstein,1987). Taken together the ratio of P_f to P_d indicates the presence ($P_f/P_d>1$) or absence ($P_f/P_d\approx1$) of a facilitated (proteinaceous) water channel activity.

Arrhenius energy of activation ($E_{act}<5$ kcal mol^{-1}) is indicative of channel mediated transport of water which is similar to the calculated diffusion of water in an aqueous environment. This also implies that even though water is transported through a pore-like structure through the hydrophobic interior of the membrane, the interior of the pore is similar in nature to the environment of water in an aqueous state. (King and Agre, 1996). In comparison, simple diffusion across membranes involves the movement of water from an aqueous environment through the hydrophobic

inner lumen of the lipid bilayer. This diffusive transport through the hydrophobic interior of the membrane is accompanied by a high energy of activation (E_{act}>10 kcal mol^{-1}) needed to solvate highly polar water molecules within the non polar environment of the lipid bilayer (King and Agre 1996).

Other evidence for protein facilitated transport of water across biological membranes came from the use of mercurial compounds that blocked transport and raised the E_{act} barrier. These compounds, such as $HgCl_2$ and a subset of various organomercurials, could reversibly inhibit water transport, presumably by interactions with free sulfhydryls located on or near the pore structure.

Although the protein component of water transport in membranes was not biochemically characterized at the time (Macey, 1984), the diffusive and protein facilitated component of a membrane could be separated biophysically based on Arrhenius energy of activation (E_{act}) plots, P_f and P_d measurements, and transport inhibition by mercuric compounds. These biophysical measurements raised strong evidence that protein transporters of water did exist at least in some membranes and that these proteins were responsible for mediating the rate of water flow across these barriers (Finkelstein, 1987; King and Agre, 1996).

Discovery of aquaporins

It had been hypothesized that in certain specialized membranes, the high rate of water conductance was caused by proteinaceous membrane channels, but the molecular characterization of these channels remained

elusive until the latter part of the 20th century. A breakthrough in our understanding of protein- based water transport came in the early 1990's with the discovery of the protein CHIP 28 (**C**hannel-forming **I**ntegral **P**rotein of 28 kDa). CHIP 28 was first discovered as a contaminating band in the isolation of the Rh blood group antigen found on red blood cells (Agre et al., 1987). Cloning and characterization of this contaminant lead to the discovery that it was a member of a functionally undefined family of putative membrane channel proteins which included the **M**ajor **I**ntrinsic **P**rotein (MIP) of bovine lens. Early work conducted on bovine MIP had shown that it was a major protein constituent of lens fiber membranes (approx. 50%). Based on reconstitution experiments it was believed to have large conductance channel activities similar to those displayed by gap junctions (Gooden et al., 1985b; Zampighi et al., 1995; Ehring et al., 1990). This view was challenged however by the pioneering work of Preston et al. (1992). They found that microinjection of cRNA coding for CHIP 28 into *Xenopus* oocytes resulted in a large increase in osmotic water permeability when compared to control water injected oocytes (Preston et al., 1992). CHIP 28 was found to satisfy the traditional requirements which had been biophysically documented for protein facilitated transport of water across membranes including: 1) A target size of 28 kDa which was similar to the predicted size of the hypothesized water channel found on renal vesicles by radiation inactivation studies (van Hoek et al., 1991), 2) Displays a low E_{act} (5 kcal mol^{-1}, Zeidel et al., 1992), 3) Reversible inhibition by $HgCl_2$ (Zeidel et al., 1992), 4) a P_f/P_d >>1 (Mathai et

al., 1996). The discovery that many other MIP proteins display similar functional properties has prompted the renaming of CHIP 28 to reflect the more functional name of aquaporin 1 (AQP1) as directed by the Human Genome Nomenclature committee (Agre, 1997).

MIP phylogeny and functional diversity

This discovery of the aquaporin properties of the MIP family of proteins has lead to a relative explosion of activity in the field of cellular water relationships. Investigators in many fields have now cloned MIP proteins from a large variety of living organisms from bacteria to man, thus underscoring again the importance for regulation of water homeostasis in single cells as well as multicellular organisms.

Over 300 MIP gene sequences have been logged into the databases with members found in all five biological kingdoms (Froger et al., 1998; de Groot and Grubmuller, 2001). In humans 10 MIP sequences have been identified so far, while the *Arabidopsis* genome sequencing project has elucidated 36 MIP-like sequences dispersed throughout the genome (Johanson et al., 2001; The *Arabidopsis* Genome Sequencing Initiative, 2000). In plants, the relatively large numbers of putative aquaporin proteins indicates the need for tightly controlled water homeostasis for maintenance of metabolic processes, turgor-driven development, and adaptation to stress (Chaumont et al., 2001; Quigley et al., 2001). It is not surprising that within this large family, many subfamilies have been demonstrated both by sequence analysis and distinct functional properties.

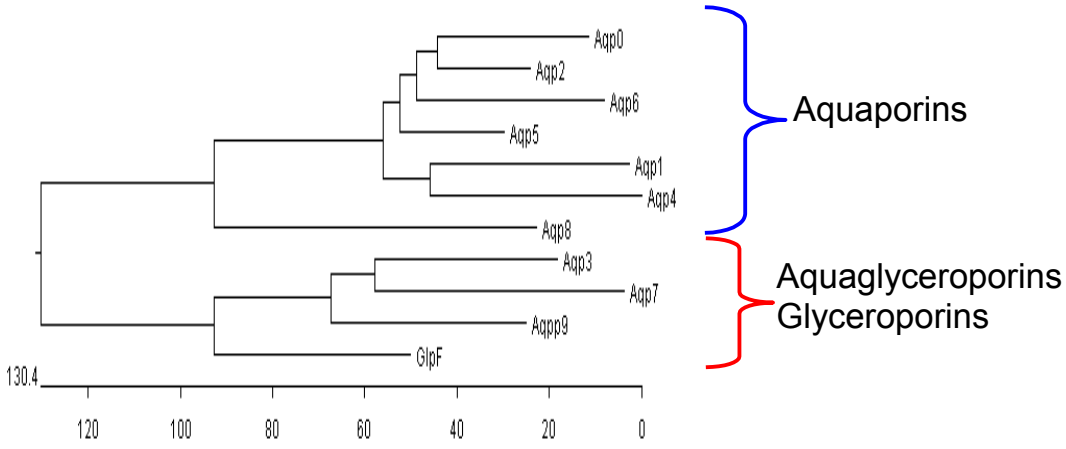

Figure 1. Phylogenetic alignment of human MIP proteins and the *E. coli* GlpF glyceroporin. MIP proteins can be broken down into three classes, aquaporins, glyceroporins, and aquaglyceroporins, based on sequence identity and limited functional analysis. The scale beneath the tree measures the distance between sequences. Units indicate the number of substitution events.

The family can be functionally broken down into three broad subclasses, the aquaporins, the glyceroporins, and the aquaglyceroporins (**Fig. 1**) (Agre et al., 1998). The aquaporin subclass is typified by the patriarchs of the MIP family AQP0 and AQP1. Both of these proteins have been shown to be functional transporters with a high degree of specificity for water (Preston et al., 1992; Mulders et al., 1995). Strikingly, these two proteins appear to have large contrasts in the rate at which they flux water (Borgnia et al., 1999). AQP0 has a relatively low conductance rate for water, an order of magnitude below the rate at which AQP1 fluxes water, while still retaining the same degree of substrate specificity as AQP1 (Preston et al., 1992; Chandy et al., 1997). Other mammalian members of the water-selective aquaporin subfamily of MIP proteins include aquaporins 2,4,5,6,8 (Borgnia et al., 1999). Water selective aquaporins in other organisms include, the bacterial AQPZ (Calamita et al., 1995; Borgnia and Agre, 2001), yeast AQY1 and AQY2 (Carbrey et al., 2001), and several members of the PIP and TIP subfamilies found in plant tissues (discussed below).

The subtle difference in the classes of MIP family members is further underlined by the transport properties of the glyceroporins, such as the bacterial transporter protein GlpF (Heller et al., 1980; Maurel et al., 1994) and the *Saccharomyces cerevisiae* glycerol transporter Fps1 (Luyten et al., 1995). These proteins show selectivity for glycerol as a substrate over water and are therefore predicted to transport only very small amounts of water because of competitive hydrogen bonding within the pore region (Jensen et al., 2001;

Nollert et al., 2001). Physiologically, GlpF serves as the major entry way of glycerol as a carbon source for bacterial cells, and is also important in adaptation to osmotic stress (Heller et al., 1980; Borgnia and Agre, 2001; Jensen et al., 2001). The yeast glyceroporin Fps1 has been demonstrated to be important during the mating process in maintenance of osmotic balance required for the process of proper cell fusion, and also for tolerance to osmotic shock (Luyten et al., 1995; Tamas et al., 1999; Philips and Herskowitz, 1997).

The third group of MIP proteins transport both water and small uncharged solutes. This family, termed the “aquaglyceroporins “, has been proposed to be a functional blend of the aquaporins and glyceroporins. Sequence alignments and functional data seem to support this, since aquaglyceroporins have hybrid sequences of the aquaporin and glyceroporin classes (Froger et al., 1998). Examples of the aquaglyceroporins include the mammalian AQP3, 7, 9, (Borgina et al., 1999), and some plant MIP proteins such as soybean nodulin 26, and tobacco Nt-AQP1 (Dean et al., 1999; Biela et al., 1999). Interestingly, no members of the aquaglyceroporin subclass have been found within yeast, bacterial, or unicellular algae genomes, either by sequence alignments or by functional analysis (Borgnia et al., 1999).

Although functional transport of water and small polyalcohols seems to be the major substrates of the MIP proteins, one cannot rule out other possible transport features. Some MIPs have been implicated in the transport of various other compounds such as CO_2, O_2, NH_3, H_2O_2, micronutrients such

as boric acid, and heavy metals such as antimonite (for review see Tyerman et al., 2002).

The size of the families of aquaporins and aquaglyceroporins found in many organisms has prompted the investigation into the reasons why these large numbers of MIP gene products are necessary. Localization studies performed with probes specific for the individual MIP homologs have revealed complex networks and arrays of multiple MIPs expressed in subcellular populations of tissues. This networking to generate an overall water balance within tissues is exemplified by well-studied systems such as, kidney, eye, airways, and brain, where water homeostasis is critical (reviewed in Borgnia et al., 1999). One example of this is the eye where five aquaporins (AQP0, 1, 3, 4, 5) reside in different populations of cells (Hamann et al., 1998). In the eye AQP0 is located exclusively in lens fiber cells; AQP1 is present in aqueous humor secretory epithelium, lens epithelium, corneal keratocytes, and endothelium; AQP3 is present in bulbar conjunctival epithelium; AQP4 is expressed within the end feet of ocular glial cells; and AQP5 is expressed in lachrymal gland and corneal epithelium (Hamann et al., 1998). This complex array in tissues such as the eye is probably reflective of the individual substrate and transport rate properties of each AQP isoform, and provides a mechanism for coordinated flow of water through various tissues.

The importance of aquaporins/MIP proteins in regulation of water homeostasis is clear from pathophysiological states and gene knockout studies. These loss of function mutations have implicated various aquaporins

in several physiological disorders. For example, mutations in AQP0 in mouse models have been linked to the formation of cataracts leading to the hypothesis that AQP0 is involved in maintaining the fluidity and elasticity of the lens (Berry et al., 2000). Mutations in human AQP2 have been studied in detail because of its implications in a rare form of diabetes insipidus (see regulation section below). Aquaporin 4 conducts water at the highest rate of the mammalian aquaporins (Yang et al., 1997), and is expressed in multiple tissues including the corti of the inner ear where it has been suggested to play a role in maintaining cellular water balance and precise volume regulation in epithelial cells involved in auditory signal transduction (Li and Verkman, 2001). In accordance with this, AQP4 null mice are hearing deficient providing further evidence that this protein is involved in hearing (Li and Verkman, 2001).

MIP structure

Despite the functional diversity apparent in the MIP/AQP superfamily, comparison of the primary structures and recent elucidation of high resolution structures for representative family members show highly conserved domains that likely form a conserved structural fold. Sequence predictions show that the percent identity for members of the MIP protein family is about 32% overall, and that several common features appear to be conserved (Pao et al., 1991; Park and Saier, 1996; Froger et al., 1998).

All MIP members are predicted to have an overall membrane topology consisting of six transmembrane spanning alpha helical domains (1-6)

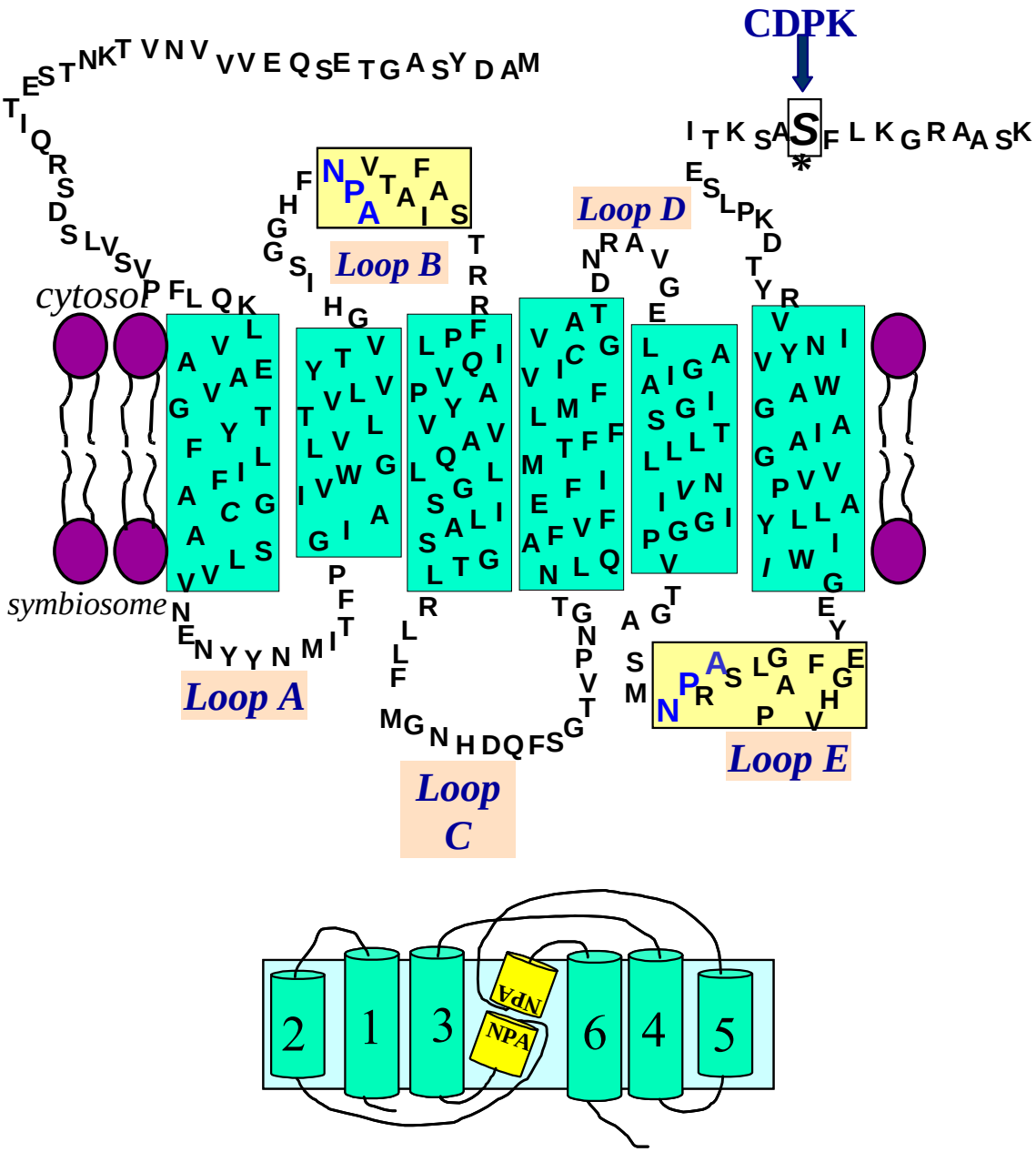

Figure 2. Proposed membrane topology for the MIP protein nodulin 26. The MIP protein soybean nodulin 26 has a predicted topology representative of the MIP class of proteins consisting of cytoplasmic carboxyl and amino terminal domains, and 6 helical transmembrane spanning domains (1-6) connected by 5 loop structures (A-E). Within loops B and E are the invariant NPA motifs which form half helices and are proposed to fold back in the membrane forming a kinked seventh transmembrane domain (bottom diagram). Nodulin 26 contains a CDPK phosphorylation motif located in its carboxyl terminal domain and is specifically phosphorylated at Ser 262 (boxed residue).

connected by five loop regions (A-E) (**Fig. 2**)(reviewed in Unger, 2000). This membrane topology was originally proposed based on hydropathy analysis, and was confirmed by proteolytic studies of AQP1 and glycosylation tagging of AQP2 (Preston et al., 1992; Bai et al., 1996). The primary sequence analysis of MIP proteins further reveals an internal homology where the amino terminal half of the sequence is homologous to the carboxyl terminal half by an obverse two fold symmetry, and from this it is proposed that the MIP family evolved from an ancient genetic duplication event (Reizer et al., 1993). Each MIP protein is predicted to be homotetrameric in nature consisting of four functional monomers displaying p422 symmetry in addition to the quasi twofold-related transmembrane symmetry (Fu et al., 2000; Sui et al., 2001; Borgnia and Agre, 2001). This tetrameric assembly was first proposed based on gel filtration, analytical ultracentrifugation, and electron microscopy studies (Smith and Agre, 1991; Verbavatz et al., 1993). This was later supported by the crystal structures of AQP1 and GlpF (Walz et al., 1997; Fu et al., 2000; Sui et al., 2001). The highly conserved NPA motifs are symmetrically oriented sequences of asparagine-proline-alanine that reside in loops B and E. The NPA regions have become the signature motifs for the MIP family and have allowed the subsequent cloning and identification of many new family members (Reizer et al., 1993). Based on site-directed mutagenesis of the NPA loops, combined with modeling of the potassium ion channel structure, the “hourglass model” for aquaporins was proposed (Jung et al., 1994). In this model the NPA loops fold back into the membrane and

form part of the pore structure (Jung et al., 1994). This structure of half transmembrane spanning helices is reminiscent of the P- loop structures found in some ion channels which are considerably hydrophobic and dip back into the membrane (Sansom and Law, 2001).

The first high resolution evidence for the hourglass structure of MIP proteins came from the three dimensional electron diffraction studies of AQP1 crystals with 6 Å resolution (Walz et al., 1997). This study provided for a three dimensional overview of each monomer and assignment of each of the 6 transmembrane helical regions (Walz et al., 1997). In addition to these overall features a region of high electron density was observed in the center of each monomer which could not be readily assigned at this relatively low resolution. However, it was thought to be composed of the two NPA loops folded back into the lipid bilayer in accordance with the proposed “hourglass model”.

Recently the high resolution atomic structures of the *E. coli* glycerol facilitator protein GlpF (2.2 Å, Fu et al., 2000) and mammalian aquaporin 1 (3.8 Å and 2.2 Å, Murata et al., 2000; Sui et al., 2001), were published, and revealed the remarkable accuracy of the hour glass model. As shown in **Fig. 3**, MIP proteins assume a structure with wide entry vestibules at either side of the membrane that constrict to a narrow pore (20 Å in length). The two NPA loops dip into the membrane, each half helix forming a seventh transmembrane domain forming the lining of the pore (**Fig. 3**). The NPA

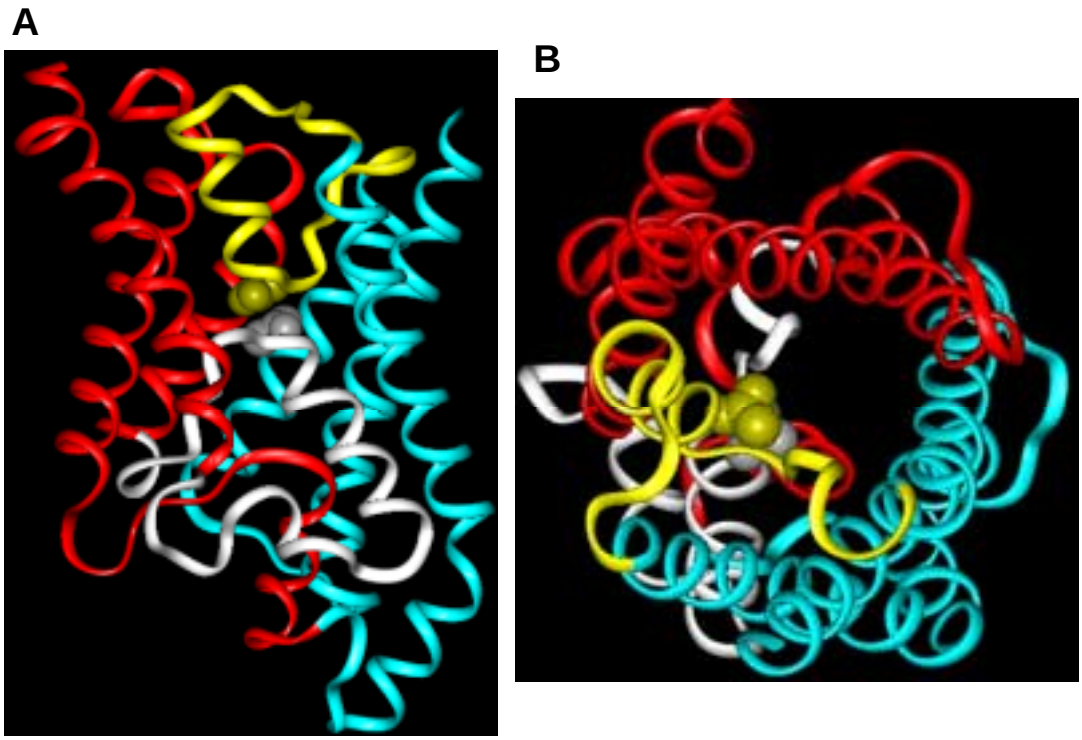

Figure 3. Structural organization of MIP proteins. The basic MIP fold is shown using the GlpF monomer (Fu et al., 2000) A**)** Ribbon diagram of GlpF monomer (Fu et al., 2001), viewed in the plane of the lipid bilayer. Transmembrane helices 1, 2, and 3 are depicted in blue, and symmetrical transmembrane helices 4, 5, and 6 are shown in red. NPA loops are shown in yellow and white and hydrogen bonded asparagine residues in NPA motifs are depicted as space filling. **B)** Same structure shown in panel **A** tilted 90º looking down from the cytoplasmic side through the pore.

regions interact via hydrogen bonds and van der Waals interactions at the central point of the membrane (**Fig. 3**).

Although MIP family members show functionally distinct profiles, structural analysis shows that the overall fold of the proteins in the lipid bilayer are strikingly similar. Thus, the overall structure of MIP proteins may be conserved throughout the family, and the observed functional differences between MIP proteins may be due to subtle residue substitutions which modify the properties of the channel without changing the overall fold (Unger, 2000).

Plant MIP proteins

In plants the need to maintain carefully regulated water homeostasis becomes readily apparent when one considers their sessile nature and the need to adapt to changing environmental conditions. However, historically it was assumed that water transport in plants was conducted without the need for a protein facilitated pathway. This view was held since plants have no specialized organs (e.g. such as the kidney in animals) which require the rapid transport of water across membranes. This view was first challenged by measurements of the hydraulic resistance of internodal cells of *Nitellopsis obtusa* (Wayne and Tazawa, 1990). High water conductance that was inhibited by mercurial compounds was observed, providing the first evidence for protein water channels in plants. More definitive evidence for water channels in plant tissue was provided by the landmark study of Maurel et al.

(1993) which showed that *Xenopus* oocytes expressing cRNA for a plant MIP protein γTIP showed an increase in P_f over water-injected oocytes.

This has lead to a refinement of the composite model for plant water relations. In this model, water is taken up through the roots and travels through plant tissues by three major pathways: (1) from cell to cell by the symplast, (2) transcellular, and (3) apoplast. In the composite transport model for plant tissues water flow through the tissues is analogous to electrical flow through a circuit where resistors arranged in parallel or in series determines the overall pathway taken by water and the conductivity of the tissue (Steudle, 1994; Steudle, 1997). The symplastic pathway component is defined by water transport through plasmodesmata and does not involve cellular membranes. The transcellular pathway involves the crossing of cellular membranes within a given tissue, and hence this pathway is most likely to be affected by the presence or activity of transmembrane water channels.

The final pathway is termed the apoplastic pathway and involves direct flow of water through cell walls and intracellular spaces and does not involve transmembrane water flow. Water flow can occur through any of these pathways and will take the path of least resistance down its hydraulic gradient. The plant can modify the rate of transcellular water flow by modifying the permeability of cell membranes, by expression and regulation of water channels (Steudle, 1997; Tyerman et al., 1999). The main bulk of water flow in plant tissues occurs where water is taken up through the roots,

and flows through the vascular tissue where it enters into a circuit which drives activities such as phloem loading, and photosynthate production in the leaves (Steudle, 1994; Tyerman et al., 1999). This transpiration is considered to constitute the major bulk of water movement in the plant system and is critical for photosynthesis. However, many other equally important roles have been proposed for water transport driven by hydraulic and osmotic gradients, including: cellular elongation, reproduction, regulation of cell turgor and volume, uptake of mineral nutrients, phloem loading, and adaptation to biotic and abiotic stress (for review see Weig et al., 1997; Maurel and Chrispeels, 2001). As a result of these multiple roles of water in plant physiology, plant membrane permeability to water is tightly modulated and can vary over three orders of magnitude (Maurel, 1997; Tyerman et al., 1999). The expression and regulation of MIP proteins is an essential part of this control of membrane permeability.

Plant MIP phylogeny

The first MIP proteins found in plants were discovered based on their overall abundance in particular tissues and membranes. For example, αTIP was originally detected in seeds and bean cotyledons as a major membrane protein component (Johnson et al., 1990). From the original plant phylogenetic comparison of Weig et al. (1997), and the more recent analysis of the complete *Arabidopsis* genome complement of MIP proteins (Johansen et al., 2001), and from the MIP family found in maize (Chaumont et al., 2001), four distinct subclasses of plant MIPs (**Fig. 4**) have been recognized from

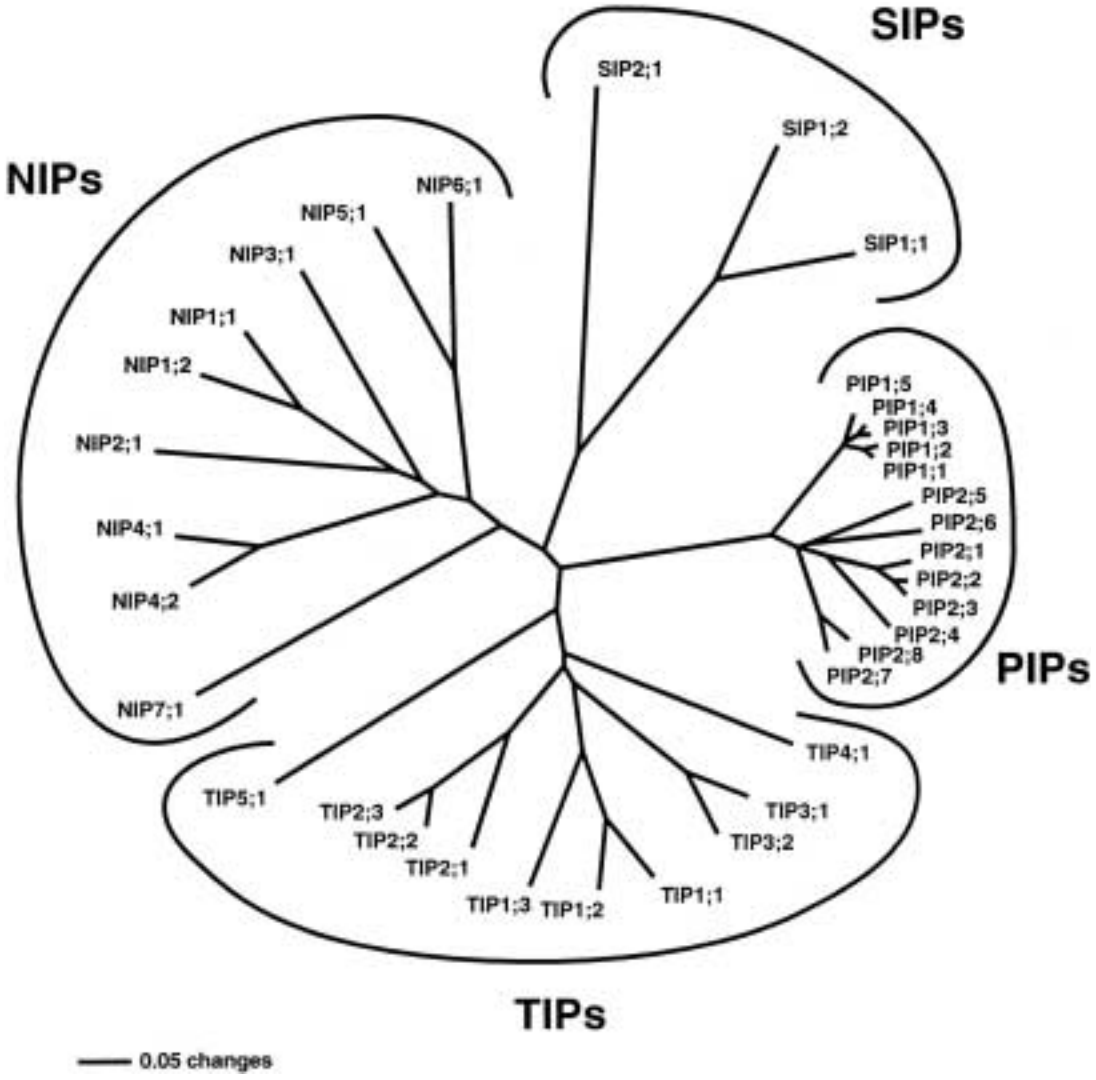

Figure 4. Phylogenic tree of *Arabidopsis thaliana* MIP proteins. The four branches of proposed MIP proteins, NIPs, TIPs, PIPs, TIPs are shown. The bar indicates the mean distance of 0.05 changes per amino acid residue. Copyrighted material by the American Society of Plant Biologists, reprinted with permission (Johanson et al., 2001).

sequence comparisons and on a more limited basis on functional and tissue distribution. These subclasses include the TIPs, PIPs, NIPs, and SIPs (Chaumont et al., 2001; Johanson et al., 2001).

The **T**onoplast **I**ntrinsic Membrane **P**roteins (TIPs) are predominately localized within the tonoplast membrane of vacuoles of most plant cells. The vacuole can account for a large percentage of the cell volume (50-90%), and serves as a reservoir for amino acids, sugars, ions, and toxic wastes (Mohr and Schopfer, 1995). The vacuole has a high osmotic capacity and has been proposed to serve as a buffering system for the water content and volume of the cytosol. Also, it has been proposed to be involved in cellular expansion processes by generating a sustained water influx into the cell (Johansen et al., 2000). In agreement with its role for cellular enlargement and expansion, several TIPs have been shown to be expressed in zones where cell expansion is taking place (Ludevid et al., 1992; Barrieu et al., 1998). TIPs have also been demonstrated to have a temporal and spatial expression patterns which, combined with other key features such as size and cellular localization, have been used to classify subclasses of vacuoles (Jauh et al., 1999). Two examples are the lytic vacuoles found in most mature cells and the protein storage vacuoles found in developing tissues and seeds which can be identified based on their expression of γTIP or αTIP (Höfte et al., 1992; Karlsson et al., 2000). Overall, the TIPs appear to play an important role in maintaining proper tonoplast osmotic potential in response to the changing needs of the cellular cytosol.

The **P**lasma membrane **I**ntrinsic **P**roteins (PIPs) subclass of plant MIP sequences can be further separated into two distinct subcategories, PIP1 and PIP2 based on sequence comparisons and transport activity (Chaumont et al., 2000; Kammerloher et al., 1994). A generalization can be inferred from the work conducted on the PIPs from several plant species indicating that the PIP1 subclass in general has a lower rate of facilitated water transport when compared to the PIP2 subclass (Chaumont et al., 2000). This difference in rate could imply other different functional roles, or regulation of the transport rate for the individual PIP subclasses (discussed below) (Chaumont et al., 2000). PIPs are predominately localized to the plasma membrane of plant cells (Chaumont et al., 2000), although some exceptions have been noted in the literature (Barkla et al., 1999). Due to localization, the PIP family is proposed to be critical in the fine tuning of the transcellular pathway of water flow through plant tissues. Experiments conducted on plasma membrane vesicles have demonstrated relatively low facilitated water transport activity compared to vacuoles (Maurel et al., 1997; Niemietz and Tyerman 1997; Dordas et al., 2000). Given the nature of the plasma membrane, and the need to maintain cellular volume, this low water permeability observed for plasma membranes is reasonable under conditions of osmotic stress where plant cells would possibly limit cytosolic water loss by reducing the permeability of the plasma membrane to water (Tyerman et al., 1999; Tyerman et al., 2002).

The majority of the PIP and TIP members characterized to date display water selectivity traits, however the tobacco Nt-TIPa displays glycerol conductivity upon expression in *Xenopus* oocytes (Gerbeau et al., 1999), and three PIPs, tobacco Nt-AQP1, Bo-PIP1b1, and Bo-PIP1b2 from *Brassica oleracea* (Biela et al., 1999; Marin-Oliver et al., 2000), also show multifunctional transport. Thus, similar to mammalian MIPs, the intrinsic water transport rates and specificity of plant MIPs can vary greatly and could be subject to regulation as discussed below.

NIPs (**N**odulin like **I**ntrinsic membrane **P**roteins) take their name from their subfamily patriarch, nodulin 26, which is found in symbiosomes of nitrogen fixing nodules of soybean. NIPs are discussed in detail in the following section.

The final subclass of plant MIP proteins are the **SIP**s (**S**mall basic **I**ntrinsic **P**roteins). This subclass has only recently been characterized by analysis of the *Arabidopsis* genome and maize expressed sequence tag libraries (Chaumont et al., 2001; Johanson et al., 2001). This subclass shows the most sequence divergence from the other plant MIP family members. In particular, the loop B region which contains the first NPA motif (**Fig. 2**) shows a remarkable amount of divergence both in the NPA box and the surrounding loop region displaying either NPT or NPL for the maize SIPs, and NPT, NPC, or NPL for the *Arabidopsis* SIPs (Chaumont et al., 2001; Johanson et al., 2001). Since this region is predicted to form part of the channel pore lining (Fu et al., 2000; Sui et al., 2001), it is possible that the transport selectivity

and rate of these SIPs differ from other MIPs. The localization and transport properties of the SIPs are not yet known, but the high amount of sequence divergence argues that they may have evolved separately from an ancestral gene (Chaumont et al., 2001; Tyerman et al., 2002).

MIP regulation

Experimentally, it has been shown that certain membranes exhibit large variance in their permeability to water under different assay conditions. It was not until the functional identification of MIP proteins that a protein component was identified which could account for these changes. In plants, changes in membrane permeability to water had been hypothesized to be necessary for physiological functions discussed above. These rapid changes in membrane permeability could be accomplished by several different mechanisms or combinations of mechanisms working in parallel to regulate membrane permeabilities. Coordinated regulation of systems of aquaporins, such as those described for the human eye, can control or redirect the overall flow of water through tissue and organs. Indeed the large number of MIP proteins found in plants may allow considerable regulation of membrane permeability to water and/or solutes in response to developmental and environmental cues. Multiple means of regulation have been demonstrated for various members of the MIP protein family.

Regulation by changes in protein trafficking

One mechanism of altering membrane permeability is by changing the localization pattern of the MIP protein constituents. Perhaps the best studied

case for this type of regulation is vasopressin-sensitive AQP2, which is found in the collecting duct principal cells of mammalian kidney. The antidiuretic hormone arginine vasopressin activates the vasopressin type 2 receptor located on the basolateral surface of principle cells of the kidney collecting duct causing an increase in the intracellular messenger cAMP. This increase in cAMP activates protein kinase A, which in turn phosphorylates AQP2 located in intracellular vesicles, causing a change in routing to the apical cell membrane where they fuse (Nielsen et al., 1995). This increase in AQP2 on the apical cell surface dramatically changes the membrane permeability to water allowing for the concentration of urine. Upon removal of the vasopressin signal, AQP2 is dephosphorylated and is returned back into intracellular vesicles by endocytosis, restoring the membrane to a relatively water-impermeable state. In humans, mutations in AQP2 are responsible for some forms of nephrogenic diabetes insipidus (NDI). NDI is characterized by an inability of the individual to concentrate urine leading to the excretion of large volumes of dilute urine regardless of stimulation by vasopressin (Deen et al., 1994). In addition to these means of control for aquaporin 2, a vasopressin response element has also been detected in the promoter region of the AQP2 gene, implying another overlapping level of control for regulation of membrane permeability by AQP2 (Hozawa et al., 1996).

In addition to AQP2, it now appears that AQP8 may have a similar mechanism of stimulated vesicle delivery. AQP8 is expressed in hepatocytes where it may be involved in water fluxes during bile secretion. Treatment of

cultured rat hepatocytes with dibutyryl cAMP showed a redistribution of AQP8 to the plasma membrane which was accompanied by an increase in membrane permeability (Garcia et al., 2001). Trafficking of AQP1 in specific tissues also has been theorized, and evidence has been presented that AQP1 may undergo redistribution to the plasma membrane when stimulated with secretin in cultured cholangiocytes (Marinelli et al., 1999).

Regulation by change in expression

One possible means of regulating the osmotic permeability of a membrane is by modifying the density of MIP proteins expressed per unit area of the membrane. This can be accomplished by changes either at the mRNA transcript level, or changing the turnover rate of the protein component. In plant tissues there is abundant evidence for the increase or decrease of MIP transcripts and proteins under a variety of physiological conditions (Johanson et al., 2000; Tyerman et al., 2002). Increased levels of the MIP proteins γTIP and δTIP have been found in tissues where cellular growth and elongation are taking place indicating that these proteins may be involved in water uptake during turgor-driven cellular expansion (Ludevid et al., 1992; Balk and deBoer, 1999; Barrieu et al., 1998; Karlsson et al., 2000). Changes in diurnal expression of PIP genes have also been shown either directly by monitoring changes in MIP transcript levels, or indirectly by recording changes in tissue hydraulic conductivity and inferring diurnal aquaporin regulation of membrane permeability (Henzler et al., 1999; Clarkson et al., 2000). Transcript levels of a sunflower TIP (sunTIP7)

expressed in guard cells, has been shown to have diurnal fluctuations which reflect the pattern observed for stomatal gating. In agreement with this, transcript levels of sunTIP7 increase in response to drought conditions during which stomata are closed (Sarda et al., 1997).

Water deficiency generated either by desiccation (drought) or by osmotic stress such as salinity has also been shown to cause changes in the expression of other MIP proteins by changes in protein levels or by inducing changes in mRNA transcript levels. For example, the functional aquaporin BobTIP26-1 is found in cauliflower florets and shows increased expression upon water deficit which can be correlated cytologically with apparent vesiculation of the central vacuole (Barrieu et al., 1999). The level of messenger RNA for five MIP genes found in *Nicotiana glauca* (three TIP homologs and two PIP homologs) was monitored and varying expression patterns for tissues monitored by Northern blot analysis. Overall these genes showed the highest expression in root tissue and stem tissue but appeared to decrease in response to drought stress (Smart et al., 2001). Hormonal regulation of MIP proteins have been implicated in some cases such as *Arabidopsis* PIP1b which is induced by blue light, ABA and gibberellins (Kaldenhoff et al., 1996). Regulation of the *Brassica* MIP-MOD gene has been linked to alterations in the hydration of pollen grains as part of the self-incompatible response (Dixit et al., 2001). Initial studies of several MIP-like transcripts from the common ice plant showed that upon salt stress, these genes showed a transient decrease in expression which recovers back to

pretreated levels within two days (Yamada et al., 1995). Changes in the overall MIP protein levels in response to salt stress has also been observed in the ice plant *Mesembryanthemum crystallinum* by using immunocytological techniques (Kirch et al., 2000). These observations suggest that alterations of MIP protein levels by genetic regulation may be important during the initial phases of water deficient stress adaptation. One other striking modulation in MIP genes in plants was shown by the wounding and feeding of the root-knot nematode *Meloidogyne incognita* which modulates the expression of the MIP gene *Tob*RB7 in the large feeding cells "giant cells" produced during the infection process (Oppermann et al., 1994). It has been proposed that this gene product participates in the swelling process of these cells accompanying feeding (Oppermann et al., 1994).

Taken together the regulation of these MIP genes reflects the need to modify overall membrane permeability in various tissues in response to various developmental and environmental stresses.

Regulation by post translational modification

Recently it has been shown that some aquaporins can be directly regulated by changes in pH. This effect is presumably the result of changes in ionization state of key residues thus causing a localized or global changes in protein structure that leads to altered transport properties. Such is the case for three mammalian aquaporins (AQP0, 3, 6), which show modified activity at various pH values (Németh-Cahalan and Hall, 2000; Zeuthen and Klaerke, 1999; Yasui et al., 1999). Experiments conducted on AQP0 of the lens fiber

cells have demonstrated a switch from a low to a high conductance water channel upon stimulation by decreasing pH. In these experiments, lowering the pH of the bath in AQP0 expressing *Xenopus* oocytes caused a change in channel properties which manifests itself at pH 6.5 by an 3-4 fold increase in water channel activity (Németh-Cahalan and Hall, 2000). This finding implicates that MIP proteins may be modulated by changes in pH which may reflect changes in biological activity through the activation or inactivation of proton pumps and ATPases. Interestingly, chelation of Ca^{+2} within the oocyte cytosol also appeared to enhance the rate of water transport by AQP0, which combined with the use of calmodulin inhibitors, indicates a possible role for calmodulin in regulating the channel activity of this MIP (Németh-Cahalan and Hall, 2000). This is supported by finding that calmodulin interacts with the carboxyl terminal region of AQP0 in a calcium-dependent manner (Louis et al., 1990).

In contrast, AQP3, which is permeable to water, glycerol, and small solutes such as urea, undergoes gating to a closed state upon acidification of the medium to pH<6 (Zeuthen and Klaerke, 1999). Aquaporin 6 however appears to undergo a specificity change at pH<5.5 allowing permeation by both water and chloride ions (Yasui et al., 1999). Other aquaporins, such as the archetype AQP1, are completely insensitive to these agents. Thus, while MIP proteins may have a similar structure and function, their regulatory properties can vary substantially.

Posttranslational modification by phosphorylation has been demonstrated to affect membrane localization of some aquaporins (discussed above), but evidence supporting direct modification of channel properties by phosphorylation has also been collected for several aquaporins. For example, treatment of oocytes expressing AQP4 with the protein kinase C agonist TPA (phorbol-12-myristate-13-acetate) resulted in a decrease in water permeability, suggesting that phosphorylation inhibits transport (Han et al., 1998). In plants, αTIP is phosphorylated in planta at ser 7 located in its amino terminal domain (Johnson et al., 1992). In oocytes, phosphorylation of αTIP in response to treatments with agents that elevate cAMP levels increases the P_f of oocytes by a factor of 2-3 fold (Maurel et al., 1995). The spinach leaf PIP PM28a has been shown to be phosphorylated both in vivo and in vitro at ser 274 located in the carboxyl terminal domain. This phosphorylation event induces an increase in osmotic water permeability in oocytes expressing PM28a (Johansson et al., 1998). In vivo, this phosphorylation appears to be in response to changes in apoplastic water potential, and is catalyzed by a plasma membrane associated protein kinase and is dependent on submicromolar concentrations of Ca^{+2} indicating possible regulation through a calcium dependent protein kinase (CDPK) (Johanson et al., 1996). This regulation is proposed to be a stress response that increases the water retention in cells undergoing osmotic shock (Johansson et al., 1996). Recently, two lentil seed TIPs have been shown to be phosphorylated by a Ca^{+2} kinase in response to temperature changes and

pH changes (Harvengt et al., 2000). Chemical crosslinking of these two proteins indicates that these proteins form a hetero-oligomer (Harvengt et al., 2000). Nodulin 26 was the first plant MIP to be studied with respect to protein phosphorylation (Weaver et al., 1991), and its properties are discussed below.

Symbiotic nitrogen fixation in legumes

During conditions of limiting soil nitrogen, legumes are capable of becoming infected by bacteria of the *Rhizobiaceae* family. This process triggers an exchange of signals between the plant and the bacteria which involves a preset developmental program culminating in the formation of a specialized organ called the nodule that engages in the reduction and fixation of molecular nitrogen (**Fig. 5**). Legume nodules can be morphologically placed into two distinct classes: determinant and indeterminant. Indeterminant nodules such as those of pea are typified by the presence of a persistent meristem that grows away from the root endodermis. Apart from the meristematic tissue there are four major developmental zones that are spatially oriented between the meristem and the root endodermis. These are the zones of cellular expansion, symbiosis development, nitrogen fixation, and senescence (Werner, 1992). In contrast, the determinant nodule (such as those formed on soybean or *Lotus japonicus* roots) do not have a persistent meristem and the various processes of symbiosis have no spatial relationship but appear to be temporally regulated for the whole nodule (Franssen et al., 1992).

Figure 5. *Lotus japonicus* nodulated root structure. Root systems of *Lotus japonicus* can be colonized by species specific free living soil bacteria forming nodule organs.

Classically, the development of nitrogen fixing nodules can be broken down into three stages (1) pre infection (2) infection and nodule formation (3) nodule function and maintenance (Franssen et al., 1992; Kijne, 1992). Although not fundamentally recognized in the typical staging of the nitrogen fixation symbiosis process, a fourth stage can be characterized, the senescence stage during which the process of nitrogen fixation is terminated. Within each of these stages various physiological and biochemical changes are taking place. During the pre infection stage, the plant secretes species-specific flavonoid and isoflavonoid compounds that attract *Rhizobia* soil bacteria to the root system where they attach to root hairs (Aguilar et al., 1988). Upon attachment, the bacteria secrete species-specific lipo-chitin Nod factor signals which induce root hair deformation into the “shepherds crook” pattern (Van Brussel et al., 1986). The second stage begins when the bacteria enclosed within the root hair are then released into the growing infection thread through break down of the root hair cell wall. The infection thread is a cell wall-enclosed structure that serves as a conduit for the bacteria allowing access to the growing nodule primordium where cortical cell divisions are taking place. Where the infection thread reaches the nodule primordium, the infection thread releases the bacteria into the infected cell in a drop wise fashion within a membrane of host origin, the symbiosome membrane (SM)(Roth et al., 1988). During the third stage of this process the bacteria undergo differentiation into the nitrogen fixing bacteroid form. Within the senescence stage the process of nitrogen fixation is terminated usually

when the plant switches over to a reproductive stage and resources are shunted away from nodule maintenance.

During the process of nodule formation, the bacteria become enclosed within a specialized subset of cells referred to as infected cells within the core of the nodule (**Fig. 6**). These infected cells are larger than most plant cells and are morphologically distinct having no detectable vacuole in most cases, and have specialized carbon and nitrogen metabolic requirements (Udvardi and Day, 1997; Day and Copeland,1991). Most of the cytosolic volume of these cells is occupied by large numbers of organelles referred to as symbiosomes (Roth et al., 1988). The symbiosome consists of three major components: the nitrogen fixing *Rhizobia* bacteroids, the external symbiosome space, and a membrane of plant organ referred to as the symbiosome membrane.

This symbiosome membrane by definition must mediate all of the exchanges between the host plant and the bacterial symbiont (reviewed in Day et al., 2001; Udvardi and Day, 1997). The plant host supplies part of its photosynthate to the bacteria as a fuel source for the nitrogen fixation process. It is generally accepted that sucrose is metabolized to phosphoenolpyruvate (PEP) by glycolysis in the plant cytosol, and by the action of PEP carboxylase (Chollet et al., 1996) PEP is converted to C_4-dicarboxylates, which are transported to the bacteria (Udvardi et al., 1988; Chollet et al., 1996). Strong evidence for the role of dicarboxylic acids as the fuel source for nitrogen fixation come from the observation that *Rhizobia* that

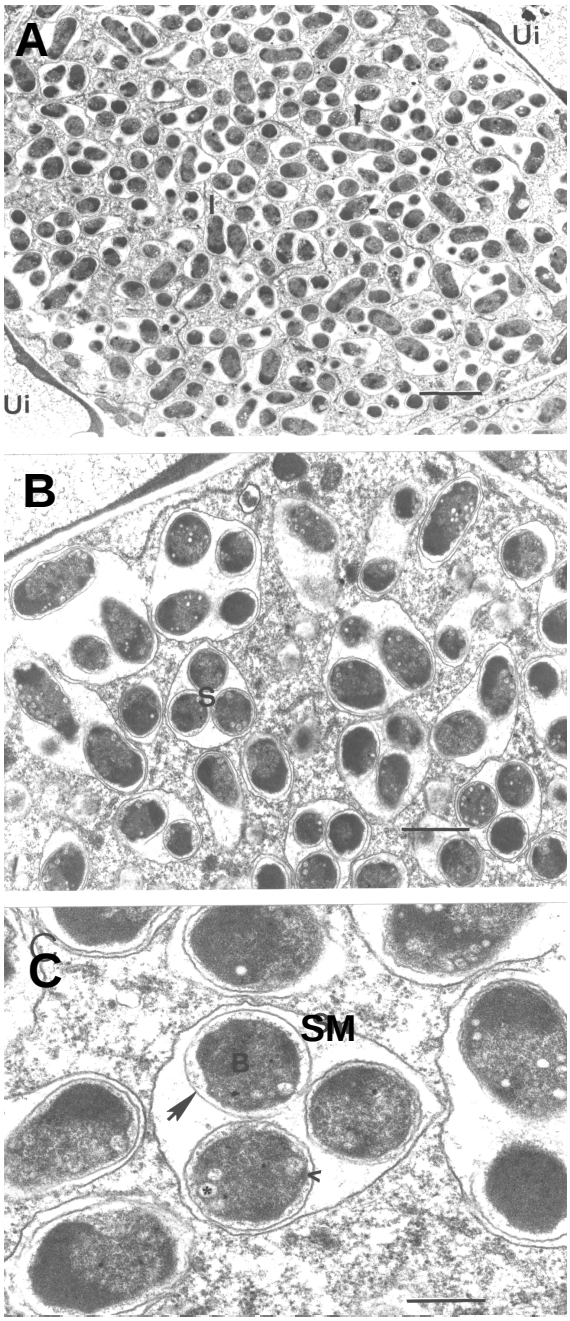

Figure 6. Electron micrographs of infected cells of *Lotus* nodules. **A**) Low magnification image of cells within the nodule showing an infected cell in the center (**I**) and two uninfected cells (**Ui**); **B**) higher magnification image of an infected cell showing multiple symbiosomes (**S**); **C**) High magnification of an infected cell showing detailed structural features of the symbiosome membrane (**SM**), bacteroid (**B**), Outer bacteroid membrane (**closed arrow head**), inner bacteroid membrane (**open arrow head**), and Poly-β-hydroxybutyrate (*****). Scale pars represent 2 μm in **A**, 1 μm in **B**, and 0.5 μm in **C**.

result in a defect in transport or metabolism of dicarboxylic acids results in a Fix^- pheontype (Engelke et al., 1987). Biochemical support for the metabolic importance of malate in the symbiosis came with the demonstration of a selective malate transporter on the symbiosome membrane (Udvardi et al., 1988; Ou Yang et al., 1990). Recently, molecular approaches for the study of nodulation have uncovered a potential candidate for a dicarboxylate transporter in *Lotus japonicus* (LjNod70), which shows sequence homology to bacterial transporters that flux dicarboxylates (Szczyglowski et al., 1998; Szczyglowski et al., 1997).

The bacteroids use malate as a fuel source to drive the reaction which breaks down dinitrogen N_2 into ammonia which is then exported to the plant cytosol. The bacterial nitrogenase complex which breaks down dinitrogen is exquisitely sensitive to elemental oxygen and the pO_2 of the infected cell cytosol is maintained at a low level (10 nM) (Werner, 1992). As a result, diffusion of oxygen into the infected cells to support respiration is the rate-limiting step of nitrogen fixation (Hunt and Layzell, 1993) and is the primary means of regulation for this process (Fischer, 1994). One of the main oxygen diffusion barriers within the nodule is the ring of cortical cells which surround the zone of infection. In the electroosmotic model (Denison and Kinraide, 1995; Sinclair and Serraj, 1995) osmotic gradients from ion fluxes and accompanying water movement is proposed to modulate cortical cellular volume which in turn regulates the nitrogen fixation process affecting O_2

diffusion into the infected zone. Modulation of MIP proteins might be important in this regulation (Serraj et al., 1998).

After fixation by nitrogenase, reduced nitrogen in the form of either NH_3 or NH_4^+ is transported across the symbiosome membrane either by diffusion through the lipid bilayer or through protein-mediated transport (Day et al., 2001; Tyerman et al., 1995; Roberts and Tyerman, 2002; Udvardi and Day 1997). Once within the plant cell cytosol it is quickly converted to glutamine maintaining a low cytosolic concentration of ammonia, and providing a concentration gradient to drive export from the symbiosome (reviewed in Udvardi and Day, 1997). Besides serving as a metabolic interface between the host and symbiont, another important role for the symbiosome membrane is the sequestering of the bacteroids from the host cytosol providing protection from the plant defense responses. This was exemplified in experiments by the use of ineffective nodulation strains where the symbiosome membrane appears to break down and is quickly followed by characteristic defense response reactions (Parniske et al., 1990).

During the infection process, a subset of host genes are specifically up regulated for initiation and maintenance of the symbiotic process. These gene products are referred to as nodulins (Legocki and Verma, 1980). These nodulins can be broken down into two broad classes, the early nodulins (ENODs), and the late nodulins, based primarily upon their temporal induction in relation to nodule formation (Franssen et al., 1992). Most of the ENOD proteins are thought to be involved in the early stages of nodule formation

either serving in signaling processes, or by serving structural roles in generating the nodule organ. In contrast, the late nodulins are generally thought to participate in the metabolic processes that accompany nitrogen fixation (Franssen et al., 1992).

Among the late nodulins are a specific subset of gene products that are specifically targeted to the symbiosome membrane. A partial cDNA encoding a symbiosome membrane protein designated nodulin 26 was discovered (Fortin et al., 1987), and subsequent full length cloning and comparisons to known sequences revealed similarities to the MIP protein (later termed AQP0) of bovine lens (Shiels et al., 1988; Sandal and Marcker, 1988).

Nodulin 26 and nodulin-like intrinsic membrane proteins

Specific antibodies generated to nodulin 26 have shown it to be a major protein component of the symbiosome membrane where it constitutes between 10-15% of the total membrane protein (Weaver et al., 1991; Dean et al., 1999). From the deduced sequence of nodulin 26 (Fortin et al., 1987; Sandal and Marcker, 1988), it appeared that the carboxyl-terminal sequence contained a putative phosphorylation consensus motif for calmodulin-dependent protein kinase II and a calcium dependent-calmodulin independent plant kinase (CDPK) (Weaver et al., 1991; Harmon, 1994). Using the synthetic peptide CK15 containing the last 14 residues of nodulin 26, it was demonstrated that both the peptide and a symbiosome membrane protein corresponding to the predicted molecular size of nodulin 26 were

phosphorylated both in vivo and in vitro (Weaver et al., 1991). The exact site of phosphorylation was then determined for native nodulin 26 to be ser 262 located in the carboxyl-terminal domain and on an analogous site on the synthetic peptide CK-15 (Weaver and Roberts, 1992; **Fig. 2**). Based on the putative membrane structures of the MIP proteins it was originally proposed that nodulin 26 was a metabolite transporter for the symbiosome membrane (Ou yang et al., 1991; Weaver et al., 1994). Consistent with this, incorporation of nodulin 26 into artificial lipid bilayers demonstrated that it was capable of forming a large symmetrical nonselective ion channel that fluxes several ionic species including malate (Lee et al., 1995; Weaver et al., 1994) similar to early studies with AQP0 (Ehring et al., 1990).

However, upon expression in *Xenopus* oocytes, nodulin 26 did not form an ion channel but rather displayed aquaporin-like properties (Rivers et al., 1997). The *Xenopus* results were supported by analysis of native purified nodulin 26 reconstituted into proteoliposomes and analyzed by stopped flow fluorimetery (Dean et al., 1999). From this work the unitary water conductance (p_f) for nodulin 26 was determined to be ($3.8 \pm 2.5 \times 10^{-15} cm^3/s$) (Dean et al., 1999). Unitary conductance (pf) is a measurement of the amount of water each channel can transport per unit time, assuming that each nodulin 26 monomer contains one aqueous pore (Dean et al., 1999; Jung et al., 1994). Interestingly, this number was found to be 30-fold lower than the single channel conductance rate obtained for AQP1 (117×10^{-15} cm^3/s)(Ziedel et al., 1992; van Hoek and Verkman, 1992), and was similar to

the low conductance rate observed for AQP0 (Chandy et al., 1997 Zampighi et al., 1995; Yang and Verkman, 1997).

The ratio of P_f/P_d was calculated for nodulin 26 (P_f/P_d = 18.2) and compared to the published values of AQP1 (P_f/P_d =13, AQP1) (Rivers et al., 1997). Based on the theory of Finkelstein (1987), it was suggested that within the channel of nodulin 26 eighteen water molecules line up while within the channel of AQP1 thirteen waters are aligned in single file (Rivers et al., 1997; Mathai et al., 1996; Finkelstein, 1987). While this argument has been challenged in theory (Hill, 1995) and by the actual AQP1 structure (Sui et al., 2001), the P_f/P_d data of Rivers et al. (1997), suggests that differences in the pore structure between nodulin 26 and AQP1 could account for an intrinsic difference in transport rates. Even though nodulin 26 has been shown to have a low single channel conductance rate, it is present in sufficient amounts within the native symbiosome membrane to account for the high rate of water transport observed for purified symbiosome membrane (0.05 cm/s compared to 0.001 cm/s for a bare lipid bilayer)(Rivers et al., 1997; Dean et al., 1999).

In addition to water transport, nodulin 26 was found to facilitate the flux of glycerol both upon expression in *Xenopus* as well as in proteoliposomes (Dean et al., 1999), and can account for the high permeability of the symbiosome membrane to this solute (Rivers et al., 1997). The data, taken together with the low E_{act} and reversible mercury sensitivity found for purified nodulin 26 argues strongly that nodulin 26 is capable of facilitating the transport of this compound at rates observed for purified symbiosome

membranes (Dean et al., 1999; Rivers et al., 1997). Additionally, based on the observation of a mercurial-sensitive NH_3 transport pathway in isolated symbiosome membranes, and similarity in structure and size between H_2O and NH_3, it was proposed that nodulin 26 might also be responsible for the flux of fixed ammonia through the symbiosome membrane (Niemietz and Tyerman, 2000).

The finding that nodulin 26 is a major symbiosome membrane component and functions as an aquaglyceroporin argues for a role in the establishment and maintenance of the symbiosis. Whether it serves an osmoregulatory role (via water or solute transport) or a role as a metabolite exchange protein (NH_3) remains unknown.

In 1997, Weig and co-workers first showed the presence of a protein with a high identity to nodulin 26 in *Arabidopsis* (Weig et al., 1997). This finding was the first indication that the occurrence of nodulin 26-like proteins in plants were much broader than previously suspected giving rise to a new family of MIPs which were labeled the NLMs (later termed NIPs) based on structural similarity to nodulin 26 (Weig et al., 1997; Chaumont et al., 2001; Johanson et al., 2001). This finding of a class of MIPs which showed many of the characteristics of nodulin 26 argued that they may play broader roles in water homeostasis in non-nodulated plant tissues. The *Arabidopsis* sequencing project has determined 10 sequences which fall into the NIP family (Johanson et al., 2001). The few members which have been functionally characterized using heterologous expression systems show

aquaglyceroporin activity similar to nodulin (Weig et al., 1997; Weig and Jakob, 2000).

Lotus japonicus

Nodulin 26 was first characterized in soybean root nodules. Soybean confers several advantages as an experimental system including the ability to extract large amounts of relevant tissue, relatively short generation times for biological sample preparation, and a large reservoir of biochemical information on the establishment and maintenance of root nodules. Although soybean has advantages which make the study of nodulation in this system desirable, it also has limitations that prevent the facile use of modern methods of plant molecular biology (tetraploid, large genome, difficulty obtaining efficient transgenic plant production). In recent years *Lotus japonicus* has emerged as a genetic model legume for the study of the biology of nitrogen fixing symbioses (Handberg and Stougaard, 1992). *Lotus japonicus* has several features that make it better suited for modern biochemical and genetic techniques including, small genome size (0.5 pg per haploid complement), short generation time (approximately 3 months), the ability to generate transgenic plants with high efficiency for reverse genetic studies, large banks of mutants with defined nodulation phenotypes, and a dedicated genomic and proteomic research thrust in the plant research community (Handberg and Stougaard, 1992; Stiller et al., 1997; Stougaard, 2001). Thus, *Lotus japonicus* presents several potential advantages over soybean in allowing for the direct investigation of a physiological role for nodulin orthologs in *Lotus*

nodules through the use of modern techniques of plant molecular biology and genetics.

The extensive biochemical and biophysical analyses of nodulin 26 has led to the proposal of multiple biological functions, but its role in legume symbioses still remains unknown. To take advantage of the modern biochemical and genetic tools available for *Lotus japonicus* for the study of MIP function in legume symbiosis, it is first necessary to identify and characterize these proteins in this model organism. In the present work the identification and characterization of the structure and function and regulation of two MIPs from *Lotus japonicus* nodules was pursued.

CHAPTER II

MATERIALS AND METHODS

Materials

Synthetic oligonucleotides were purchased from Sigma Genosys Biotechnologies, IDT Biotechnologies, or Gibco/BRL. Synthetic oligopeptides were purchased from Bio-synthesis, INC., Sigma Genosys Biotechnologies, or Research Genetics. γ^{32}PATP (4500 Ci/mmol), and α^{32}PATP (800 Ci/mmol) were purchased from ICN. [1,2,3-^{3}H]-glycerol (80 Ci/mmol) was purchased from NEN™ Life Science Products, Inc. MBS-activated keyhole limpet hemocyanin (KLH), Ellman's reagent, BCA Protein assay reagent, albumin standards and *m*-Maleimidobenzoyl N-hydroxysuccinimide (MBS) were from Pierce Endogen Chemicals. Freund's complete and Freund's incomplete adjuvant were purchased from Gibco/BRL. *pfu* polymerase was purchased from Stratagene, *taq* polymerase was purchased from Fisher Scientific, Promega, or Eppendorf. Restriction enzymes were purchased from New England Biolabs, Promega, or Takara. New Zealand White rabbits were purchased from Harlan Sprague Dawley, and *Xenopus laevis* frogs were purchased from *Xenopus* Express. Other reagents were purchased from standard commercial sources and were of reagent grade or better.

Rhizobia cultures and growth conditions

Prior to inoculation of *Lotus japonicus, Mesorhizobium loti* (NZP-2235) (Stiller et al.1997; Szczyglowski et al. 1998), bacteria were inoculated into

200 ml of Bergenson's minimal medium: 270 mg/L $NaH_2PO_4 \cdot 7H_2O$; 80 mg/L $MgSO_4 \cdot 7H_20$; 3 mg/L $FeCl_3 \cdot 6H_2O$; 3.7 mg/L ferric monosodium EDTA; 30 mg/L $CaCl_2 \cdot 2H_2O$; 0.0025 mg/L $MnSO_4 \cdot 4H_2O$; 0.03 mg/L H_3BO_3; 0.03 mg/L $ZnSO_4 \cdot 7H_2O$; 0.0025 mg/L $NaMoO_4 \cdot 2H_2O$; 0.1 mg/L biotin; 1 mg/L thiamine; 10 g/L mannitol; 0.5 g/L sodium glutamate; 0.5 g/L yeast extract; pH 6.8-7.1. *M. loti* bacterial cultures were grown shaking at 30ºC for three days before inoculation of plants. For soybean inoculation, *Bradyrhizobium japonicum* strain USDA 110 was cultured as above for 5 to 7 days before use.

Lotus japonicus **growth conditions**

Lotus japonicus B-129-56 'gifu' seeds were briefly scarified with 100 grit sand paper until the seeds turned light gray. For routine bulk growth of *Lotus japonicus* plants for nodule production, seeds were planted directly in a 1:1 mix of sand and vermiculite. The seeds were then watered on the day of planting with a three day old culture of *M. loti* diluted 1:1 with Herridges nutrient solution (K_2HPO_4, 22 mg/L; KH_2PO_4, 17 mg/L; KCl, 19 mg/L; $MgSO_4 \bullet 7H_2O$, 250 mg/L; $CaCl_2 \bullet 2H_2O$, 37 mg/L; ferric monosodium EDTA, 9 mg/L; H_3BO_3, 0.71 mg/ml; $MnCl_2 \bullet 4H_2O$, 0.45 mg/L; $ZnCl_2$, 0.03 mg/L; $CuCl_2 \bullet 2H_2O$, 0.01 mg/L; $NaMoO_4 \bullet 2H_2O$, 0.005 mg/L). For transgenic plant and developmental studies, seeds were surface sterilized and pre-germinated on filter paper as described by Handberg and Stougaard (1992). Seeds were surface sterilized by treatment in 2% (v/v) hypochlorite, 0.02% (v/v) Tween 20 for 20 min followed by 4 rinses in sterile H_2O. Plants were allowed to germinate on sterile filter paper for 7 days and were inoculated with an

undiluted 3 day old culture of *M. loti* (5 ml/plate) for 24 h before planting in sand/vermiculite.

After seven days, the plants were re-inoculated with *M. loti*, and were subsequently watered on alternative weeks with water or Herridge's solution. For non-nodulated *Lotus japonicus*, seeds were germinated and grown as described above in the absence of *M. loti* and with Herridge's solution supplemented with 5 mM KNO_3. Growth of *Lotus japonicus* was routinely done under standard greenhouse conditions. However, for transgenic plants and growth of wild type plants for developmental studies, plants were grown in a Percival growth chamber (RE-16BH, AR-60L, or AR-66L) under a 18 hr light period, (22˚C) followed by a 6 hr dark period, (19˚C).

Soybean growth conditions

Seeds of *Glycine max* cv. Essex were surface-sterilized by soaking for 1 hr in a solution of 0.03% (v/v) sodium hypochlorite, followed by rinsing in water for 1-3 hr. The seeds were then soaked in a liquid culture of *Bradyrhizobium japonicum* USDA 110 for 1 hr followed by plating onto 150 mm culture plates on filter paper pre wetted with *B. japonicum*. The seeds were germinated for three days before planting in vermiculite and watering with a culture of *B. japonicum* diluted 1:5 with Herridge's solution. Plants were then watered on alternating weeks with water or Herridge's unless otherwise specified. For standard symbiosome membrane preparations used for nodulin 26 isolation, plants were grown under greenhouse conditions as previously described (Weaver et al., 1991; 1994). For analyses of the effects

of developmental state and stress on nodulin 26, plants were grown in a Percival growth chamber as described above for *Lotus japonicus* plants.

Drought stress was administered by withholding water from 28 day old soybean plants for a period of 14-20 days. Control plants were grown under identical conditions except that they were well watered. Salinity stress was administered by watering soybean plants with 0.3 M NaCl. Nodules were collected, quick frozen on dry ice and were stored at -80˚C until membrane extraction and analysis.

Nucleic acid isolation

Total RNA was isolated from *Lotus japonicus* plants using a guanidinium thiocyanate procedure (Chirgwin et al., 1979), and was purified by differential LiCl precipitation (Ausubel et al., 1987). In cases where tissue was limiting, such as in the analysis of transgenic lines and diurnal expression analysis, total RNA was isolated by extraction in hot phenol chloroform followed by differential LiCl precipitation (Verwoerd et al., 1989). Genomic DNA was isolated from *Lotus japonicus* plants using the TRIzol® Reagent (Gibco/BRL), following the manufacturers protocols for differential DNA isolation.

For standard plasmid preps, *E. coli* was grown in Luria Broth (LB) media cultures with 100 μg/ml ampicilin (or 50 μg/ml tetracycline for bacteria containing the pGA941 plasmid), with shaking at 37°C overnight. Cells were collected by centrifugation at 5000g for 10min. Plasmids were prepared by using the

Promega Wizard Miniprep kit or the Qiagen QIAprep Spin Miniprep kit. Final plasmid products were stored at -20°C.

RT-PCR and cDNA cloning of *Lotus japonicus* MIPs

Purified total RNA (5 μg) from 9 week old *Lotus* nodules was used for first strand cDNA synthesis by using reverse transcriptase, an oligo dT primer and a 3' Rapid Amplification of cDNA Ends (RACE) system and the manufacturer's protocol (Gibco BRL). Ten microliters of this reaction was amplified by touchdown PCR with the NPA forward and reverse primers (**Fig. 7**). PCR was done with a Perkin Elmer GeneAmp® PCR system 2400 with the following cycling conditions: denaturation 94°C, 1 min: annealing 30 sec; extension 72°C 2 min. The annealing temperature was decreased in two degree steps every third cycle from 48°C to 40°C, followed by three cycles at 39°C, and a final fifteen cycles with an annealing temperature of 48°C. An aliquot of the final product was re-amplified by PCR with the following conditions: denaturation 94°C, 1 min: annealing 48°C, 2 min: elongation 72°C, 5 min, final elongation 72°C, 7 min.

The PCR product was cloned by ligation into the pCR 2.1 cloning vector (Invitrogen) by using the manufacturer's protocol for the original TA cloning kit . Plasmids from twenty separate transformants were restriction mapped (*Eco* RI; *Xho* I and *Hind* III; *Xho* I and *Hind* III and *Pvu* II; *Eco* RI and *Pvu* II; or *Rsa* I). Products were resolved by agarose electrophoresis in Tris-borate-EGTA (TBE)(Sambrook et al., 1989).

NPA forward 5'-GGTGG[CT]CA[CT][TG]T[CT]AA[CT]CC[AT]GCTGT[CG]AC-3'
NPA reverse 5'-CTTCT[AG]GC[CT]GG[AG]TTCAT[TG]GATGC[AT]CC-3'

LIMP 2 forward 5'-GAAGATCTTGTTTTAGCTAGTGAGTG-3'
LIMP 2 reverse 5'-GAAGATCTAACCACTAGGCGTCTAGGC-3'

LIMP 1 forward 5'-GAAGATCTCGTTTTCCTACAGTCGCCGG-3'
LIMP 1 reverse 5'-GAAGATCTCATTTTCACTTTCACTTCCC-3'

NPT II 196 forward 5'-GTGGAGAGGCTATTCGGCTA-3'

NPT II 745 reverse 5'-CCACCATGATATTCGGCAAG-3'

Figure 7. Oligonucleotide primers used for PCR reactions. NPA forward, NPA reverse; degenerate primers used to amplify MIP cDNAs from *Lotus japonicus* nodules. **LIMP2 forward, LIMP2 reverse;** primers for cloning the LIMP2 open reading frame into the pXβG *Xenopus* expression plasmid, and the pGA941 *Agrobacterium* transformation vector. **LIMP1 forward, LIMP1 reverse;** primers for cloning the LIMP1 open reading frame into the pXβG *Xenopus* expression plasmid, and the pGA941 *Agrobacterium* transformation vector. **NPT II 196 forward, NPTII 745 reverse;** NPT II primers for PCR amplification of the NPTII gene from the pGA941 vector and transgenic plants.

Partial cDNA products for two *Lotus* MIPs were used to probe a cDNA library prepared from mature *Lotus japonicus* nodules and cloned into λ Uni-ZAP™ XR (Stratagene) (graciously supplied by Dr. Jens Stougaard, University of Aarhus, Denmark). For library screening, 0.6 ml of a mid-logarithmic *E. coli* culture (SURE strain, Stratagene) was infected with 50,000 pfu of the cDNA library by shaking at 37°C for 20 min. The cells were plated onto NZCYM agar plates and grown overnight at 37°C. The plates were overlaid with nitrocellulose transfer membranes and were screened by the procedures outlined by the manufacturer (Custom Lambda Phage Libraries, Stratagene). Membranes were denatured for 2 min by submerging in 1.5M NaCl, 0.5 M NaOH followed by neutralization for 5 min in 1.5 M NaCl, 0.5 M Tris-HCl pH 8.0 and rinsed in 0.2 M Tris-HCl pH 7.5, 2xSSC (Sambrook et al., 1989). Nucleic acids were immobilized on the membranes by baking in a vacuum oven at 80˚C for 1.5 hr. Membranes were prehybridized in 50% (v/v) formamide, 5x SSPE (Sambrook et al., 1989), 5X Denhardt's solution (Sambrook et al., 1989), 0.1% (w/v) sodium dodecyl sulfate (SDS), 100 μg/ml denatured salmon sperm DNA, and then were hybridized in the same solution containing 10^6 cpm probe/ml at 42ºC for 16 hr. Radiolabeled probes were generated by nick translation using α^{32}PATP and the Promega Nick Translation Kit (Cat.No. U1001). After hybridization, the filters were washed in 2X SSC, 0.1% (w/v) SDS and then with 1X SSC, 0.1% (w/v) SDS (Sambrook et al.1989).

Positive plaques, identified by autoradiography, were selected and re-screened until plaque purified. Plasmids containing the cDNAs were excised by using protocols outlined in the ZAP-cDNA® SYNTHESIS KIT manual (Stratagene), using the ExAssist™/SOLR™ system. Phage stocks were incubated with the ExAssist helper phage and XL-Blue cells for 15 min at 37˚C for 15 min, then incubated at 37˚C for another 2.5 hr. Cells were then lysed by heating to 70˚C for 15 min. The rescued phagemid were allowed to infect SOLR cells, and selection for colonies containing the rescued pBluescript plasmid was done by growing on LB plates containing antibiotic ampicillin (100 µg/ml).

For expression analysis in *Xenopus* and for the production of transgenic *Lotus* plants, the LIMP1 and LIMP2 open reading frames were subcloned into other expression vectors. The open reading frame of LIMP1 and LIMP2 was amplified by PCR with *Pfu* polymerase with primers homologous to regions flanking the open reading frame of the two cDNAs (**Fig. 7**). In addition, the primers were designed to introduce two new *Bgl* II sites to facilitate subcloning. The LIMP 1 and LIMP 2 PCR products were gel purified by electroelution into dialysis bags (Sambrook et al., 1989), and were digested with *Bgl* II, prior to being cloned into the *Bgl* II site of the pXβG-ev1 plasmid (Preston et al., 1992) downstream of the T3 RNA polymerase promoter and flanked by 5' and 3' untranslated sequences of the β-globin gene. It has previously been shown that the presence of these sequences allow high expression in *Xenopus* oocytes (Preston et al., 1992).

Bgl II-digested LIMP1 and LIMP2 cDNAs were also ligated into the *Bgl II* cloning site of the pGA941 binary transformation vector (a gracious gift from the lab of Dr. Gary Stacey, University of Tennessee, Knoxville). The vector construct was then transformed into *E. coli* JM101. Orientation of the LIMP1 and 2 constructs relative to the cauliflower mosaic virus 35S promoter (CaMV35S) was then determined by restriction mapping,

DNA sequence analysis

Automated DNA sequencing was performed on a Perkin Elmer Applied Biosystems 373 DNA sequencer at the University of Tennessee Molecular Biology Research Facility (Knoxville, TN, U.S.A.). Sequencing reactions were prepared with a Prism Dye Terminator Cycle sequencing kit (Perkin Elmer Applied Biosystems). Sequence alignments, and phylogenetic comparisons were performed using the Clustal algorithm default settings using the megaAlign package of the DNAstar program (Guenther and Roberts, 2000). Hydropathy plots (Kyte and Doolittle, 1982) were generated by using the Protean program of DNA star.

Determination of water and glycerol permeability in *Xenopus* oocytes

cRNA was synthesized by in vitro transcription as previously described (Rivers et al.,1997). pXβG-ev1 plasmids containing cloned LIMP1, LIMP2 , AQP1 (a gift of Dr. Peter Agre, Johns Hopkins School of Medicine, Baltimore), GlpF (a gift of Dr. Christopher Maurel, CNRS, Montpellier, France), or nodulin 26 (Rivers et al., 1997), were digested with *Xba* I or *Sma* I. The linearized plasmid was used in an in vitro transcription reaction using T3 polymerase

according to the manufacturer's instructions (mCAP^{TM} RNA capping kit, Stratagene), to generate capped cRNA. The DNA template was then degraded with RNAse-free DNAse, and was purified by phenol chlorform extraction followed by ethanol precipitation. The final cRNA product was quantitated spectrophotometrically and RNA quality and integrity was assessed by electrophoresis on a 1% (w/v) agarose gel. The final product was stored at -80°C.

Xenopus laevis oocytes were prepared as previously described (Dean et al.1999) by surgical removal of oocyte sacks from mature female oocyte positive frogs. Oocyte sacks were treated with 2 mg/ml collagenase in Ringers solution without calcium (96 mM NaCl, 2 mM KCl, 5 mM $MgCl_2$, 5 mM HEPES-NaOH, pH 7.6,) for 2-3 hr at room temperature. Oocytes were washed until the solution turned clear (usually 4-5 times, 40 ml each) with Ringers solution (96 mM NaCl, 2 mM KCl, 5 mM $MgCl_2$, 0.6 mM $CaCl_2$, 5 mM HEPES-NaOH, pH 7.6, 100 μg/ml pennicillin-streptomycin) and stage V and VI oocytes were selected under a dissecting microscope. Oocytes were incubated in Ringers solution for 1 hr prior to cRNA injection. Oocytes were injected with 40-50 ng of cRNA or 46 nl of DEPC-treated water as a negative control using a Drummond “nanoject” automatic injector (Drummond Scientific Company). The oocytes were cultured for 72 hr in 96 well microtiter plates at 16°C in Ringers solution. Media was removed and replenished every 24 hr until the oocytes were assayed.

The osmotic water permeability (P_f) of oocytes was measured by assaying the initial rates of oocyte swelling upon rapid dilution of external media from isoosmotic (202 mOsm/kg) Ringer's solution to hypoosmotic (59 mOsm/kg) dilute Ringer's solution. Solution osmolarities were determined by freezing point depression changes using an Osmette A Automatic Osmometer (Precision Systems). Swelling was measured by video microscopy on a Nikon Alphaphot YS microscope equipped with a Pro-Series High Performance CCD Camera. Images were captured and digitized by the Image-Pro Plus™ software (Media Cybernetics Silver Spring, MD). The cross sectional area of the oocyte was determined, and used to calculate the overall oocyte volume by using the following equation.

$$\left(\frac{\mathbf{A}}{\mathbf{A_0}}\right)^{\frac{3}{2}} = \frac{\mathbf{V}}{\mathbf{V_0}} \quad \textbf{(Eq. 1)}$$

Where **A** is the cross sectional area at a given time; $\mathbf{A_0}$ is the cross sectional area at the initial time point; **V** is the oocyte volume at a given time, $\mathbf{V_0}$ is the initial oocyte volume. The change in oocyte volume ($\mathbf{V/V_0}$) was measured over time to determine an initial swelling rate, $\mathbf{(dV/V_o)/dt}$. This rate was used to determine the osmotic water permeability $\mathbf{P_f}$ by the following equation:

$$\mathbf{P_f} = \frac{(\mathbf{V_0/S_0})(\mathbf{dV}/\mathbf{V_0})/\mathbf{dt}}{(\mathbf{S_{real}}/\mathbf{S_{sphere}})\mathbf{V_w}(\mathbf{osm_{in}} - \mathbf{osm_{out}})} \qquad \textbf{(Eq. 2)}$$

Where, $\mathbf{S_o}$ is the geometric surface area of the oocyte at time zero, $\mathbf{osm_{in}}$ is the osmolarity in the oocyte, $\mathbf{osm_{out}}$ is the osmolarity of the media, $\mathbf{V_w}$ is the partial molar volume of water (V_w=18), $\mathbf{S_{real}}$ is the actual area of the oolemma and $\mathbf{S_{sphere}}$ is the area calculated by assuming a sphere. $\mathbf{S_{real}/S_{sphere}}$ is taken as 9 for all permeability measurements (Rivers et. al., 1997; Zampighi et. al., 1995).

^{3}H-Glycerol permeability measurements of *Xenopus* oocytes were performed as described in Dean et al. (1999). Glycerol solutions were prepared in a Ringers base solution (without penicillin-streptomycin) in which NaCl concentrations were varied so that the osmolarity of medium was maintained between 205/215 mOsm/kg. Oocytes were incubated for ten min at room temperature in 50, 100, 150, or 200 mM glycerol with 60 μCi/ml of ^{3}H glycerol. The oocytes were then quickly washed twice in 6 ml of ice cold Ringers solution. The oocytes were then lysed in scintillation vials with 200 μl of a 2% (w/v) SDS solution overnight. Scintisafe (Fisher) scintillation cocktail (10 ml) was added and ^{3}H uptake was determined by liquid scintillation counting on a Beckman LS3801 counter.

Agrobacterium transformation

Agrobacterium tumefaciens strain *AGL1* (Lazo et al., 1991) was electroporated with the pGA941 vector containing either the LIMP1 or LIMP2 antisense constructs. Electroporation was performed using a BioRad pulse controller connected to a BioRad gene pulser. Electrocompetent *Agrobacterium* were generated by sedimenting a logarithmic phase culture at

10,000 g for 5 min at 4°C. Cells were resuspended in ice cold sterile H_2O three times, and finally in sterile 10% (v/v) glycerol. Electrocompetent *Agrobacterium* was placed in a BioRad Gene Pulser cuvette with 100 ng of LIMP1 and LIMP2 constructs in pGA941 and were electroporated using the following operational settings: set volts 250; Resistance 200 Ω; Capacitance 25 μFD. Transformants were identified by selection on LB agar containing 50 μg/ml tetracycline.

Plant transformation and selection

Lotus japonicus transformation was done using the hypocotyl transformation technique as described by Stiller et al. (1997). *Lotus japonicus* B-129-56 'Gifu' seeds were scarified, sterilized, and germinated on sterile filter paper as described above. Hypocotyls from one week old etiolated seedlings were then dissected and incubated with *Agrobacterium tumefericus* AGL1 carrying the desired construct. Hypocotyls were plated on co-cultivation media (0.1X Gamborgs B5 without sucrose, 0.1X B5 vitamins, 5 mM MES, pH 5.2, 0.5 μg/ml 6-benzylaminopurine [BAP], 0.05 μg/ml α-naphthaleneacetic acid [NAA]) for one week. Hypocotyls were then transferred to regeneration medium (1X Gamborgs B5 2%(w/v) sucrose, 1X B5 vitamins, 0.6% (w/v) agar, 5 mM MES pH5.2, 0.5 μg/ml BAP, 0.05 μg/ml NAA, 5 mM $(NH_4)_2SO_4$, 300 μg/ml cefotaxime) for 5 days. Hypocotyls were subsequently transferred onto selection media (regeneration media with 1.2% (w/v) agar, 5 μg/ml geneticin). During the selection process green calli were

separated from the brown untransformed tissue and plated separately on selection media. Undifferentiated calli were then transferred onto shoot induction medium (1X Gamborgs B5 1.2% (w/v) sucrose, 1X B5 vitamins, 1.2% (w/v) agar, 5 mM MES pH5.2, 0.5 μg/ml BAP, 0.05 μg/ml NAA, 5mM $(NH_4)_2SO_4$, 150 μg/ml cefotaxime, 5 μg/ml geneticin) and then to shoot elongation medium (shoot induction media with 0.2 μg/ml BAP). The growing shoots were then clipped and transferred onto a root induction medium (0.5X Gamborgs B5 1% (w/v) sucrose, 0.5 X B5 vitamins, 1.2% (w/v) agar, 0.5 mM NAA) until sufficient roots were generated before transfer to root elongation medium (root induction media without NAA). Plantlets were then transferred to Pro-Mix soil (Premier) and allowed to produce seeds; these plants were termed the primary transformants, T_0 lines.

T_1 *Lotus* line production

Seeds harvested from the T_0 lines were sterilized and germinated on filter paper as above. After 1-3 days, seedlings were transferred onto agar plates containing 0.5 X Gamborgs B5 medium and 0.5 X B5 vitamins, 3% (w/v) agar, 2% (w/v) sucrose, supplemented with 60 μg/ml kanamycin for selection of transformed seedlings. Seedlings were grown on selective medium for approximately two to three weeks before scoring. Plants were inoculated with *Mesorhizobium loti* and grown in growth chambers as described above.

Northern and Southern blot analyses

Total RNA samples were resolved by electrophoresis on 1.2 % (w/v) agarose gels in the presence of 5.6% (w/v) formaldehyde as described by Sambrook et al. (1989). RNA was blotted onto Zeta-Probe (Biorad) membranes under vacuum. The membranes were washed in 2X SSC and dried overnight. The membranes were crosslinked by using a UV Stratalinker 2400 (Stratagene) and were prehybridized with 0.5 M $NaPO_4$, pH 7.2, 7% (w/v) SDS for ten min at 65°C. The membranes were hybridized in 5 ml of the same solution containing 10^6 cpm/ml of various nick-translated radiolabeled probes: the cloned PCR fragments of LIMP 1 or LIMP 2 described above, or a rice 17S rRNA probe as a control (Zarembinski and Theologis, 1993). The membranes were washed twice at 65°C in 1 mM EDTA, 40 mM $NaPO_4$, pH 7.2, 5% (w/v) SDS for 30 min and were exposed to X ray film at -80°C.

Southern blotting of total genomic DNA extracted from 21 day old *Lotus japonicus* plants was carried out using standard protocols supplied with the BioRad Zeta-Probe Blotting membranes. Total genomic DNA was digested using *Xba* I overnight at 37°C before phenol chloroform extraction followed by ethanol precipitation (Sambrook et al., 1989). Between 1 and 10 μg of recovered genomic DNA was digested with *Xba* I and resolved by electrophoresis on a 0.8% (w/v) agarose gel buffered with TBE (Sambrook et al., 1989). After electrophoresis, the DNA was blotted onto BioRad Zeta-Probe membranes. A PCR fragment of the NPT II gene was generated from

the vector pGA941 by using the NPT II primers (**Fig. 7**), and was radiolabeled using the Promega Nick translation system. All hybridizations and washes were conducted on the membrane according to the standard protocol for Zeta-Probe membranes which were the same as listed for Northern blotting except that the prehybridization and hybridization solution consisted of 1 mM EDTA, 0.5 M Na_2HPO_4, pH 7.2, 7% (w/v) SDS.

Antibody generation and purification

The synthetic peptides used in the present study to generate antibodies against the various proteins are shown in **Figure 8**. Synthetic peptides were engineered with an additional cysteine at the amino terminus to facilitate coupling to carrier proteins. Peptides were coupled to MBS-activated KLH according to the manufacturer's protocols (Pierce Endogen Chemicals). Coupling efficiency was monitored by Ellman's Reagent (Ellman, 1959). The conjugated peptide was purified by gel filtration through a Sephadex G25 column in 137 mM NaCl, 2.7 mM KCl, 9.6 mM NaH_2PO_4, 1.5 mM K_2HPO_4, pH 7.2 (PBS), and was quantitated using the BCA protein assay. After coupling 100 μg of total conjugate was diluted into 300 μl of PBS and mixed 1:1 with Freund's complete adjuvant and injected into New Zealand White female rabbits subcutaneously. After 1 week, the rabbits were injected with the same amount of conjugate mixed 1:1 with Freund's incomplete adjuvant. All subsequent injections of the antigen were done with 100 μg of conjugate in 600 μl of PBS. Blood was harvested and processed as described in Harlow and Lane (1988). Blood was allowed to clot for 30-60

CI-14: C-R-E-I-T-K-N-V-S-F-L-K-G-I

GC12P: C-E-I-T-K-N-V-S(PO4)-F-L-K-G

CK-15: C-T-K-S-A-S-F-L-K-G-R-A-A-S-K

CA-15: C-A-P-Q-E-A-T-H-P-D-T-L-R-S-A

CY-14: C-I-G-S-Q-T-H-E-Q-L-P-T-T-D-Y

Figure 8. Synthetic peptides used for generation of antibodies. **CI-14:** synthetic peptide corresponding to the carboxyl terminal 13 amino acids of LIMP2; **GC12P:** synthetic peptide of LIMP2 residues 259-269 with phosphorylated serine indicated; **CK-15:** peptide corresponding to the carboxyl terminal 14 amino acids of soybean nodulin 26; **CA-15:** synthetic peptide corresponding to residues 10-23 of LIMP1; **CY-14:** synthetic peptide corresponding to the carboxyl terminal 14 amino acids of LIMP1. The cysteine residue at the amino terminus is not part of the sequence but was included to allow coupling to KLH for antibody production.

min at 37°C before loosening the clot from the walls of the collection tube with a Pasteur pipette. The clot was allowed to contract overnight at 4°C, and was then separated from the sera by centrifugation in a table top clinical centrifuge (Sorvall GLC1). Sera was collected and stored at –20°C or -80°C until further use.

For affinity purification of antipeptide antibodies, affinity resins consisting of peptide antigen coupled to ω-aminohexyl-agarose (Sigma) were used. Peptides were coupled to resin by using the heterobifunctional crosslinking reagent MBS (Pierce Endogen Chemicals). Briefly, 1 ml of ω-aminohexyl-agarose was washed 3x in 15 ml of 0.01 M $NaPO_4$ pH 7.0 and resuspended in 2 ml of the same buffer. The resin was incubated with 15 mg of MBS dissolved in 100 μl of N,N-dimethylformamide for 30 min under constant shaking at room temperature. The reaction was then washed with 200 ml of 0.01 M $NaPO_4$ pH 7.0 using a 15 ml vacuum filter. After washing, 15 mg of the sulfhydryl containing peptide was added and allowed to react for 4 hr under constant shaking at room temperature then washed with 0.01 M $NaPO_4$ pH7.0 as described above. Coupling efficiency was assayed by using Ellman's reagent as described above for peptide conjugation to MBS activated KLH.

Antibodies were adsorbed to peptide agarose resins in 10 mM Tris-HCl, pH 7.5. The column was washed with 10 mM Tris-HCl, pH 7.5 and adsorbed antibodies were eluted sequentially with 100 mM glycine-HCl, pH 2.5 and 100 mM triethylamine, pH 11.5 as described by Harlow and Lane (1988). Eluents were neutralized with Tris and were concentrated on a

Centricon-10 ultrafilter (Amicon). The buffer was exchanged into PBS by using the Centricon filter. The final concentrated product was stored at –20°C.

In the case of phosphorylation-specific antibodies (against peptide GC12P, **Fig. 8**), antibodies were pre-adsorbed by passing the sera repeatedly over a resin of CI-14 (**Fig. 8**) in 10 mM Tris-HCl, pH 7.5 to remove antibodies reactive against unphosphorylated epitopes. The eluant from the CI-14 column was then passed over the GC12P-coupled resin as described above for antibody purification.

Antibodies against whole, gel purified soybean nodulin 26 were prepared as previously described (Zhang and Roberts, 1995). Anti-nodulin 26 antibodies were affinity purified by adsorbing to soybean nodulin 26 immobilized on nitrocellulose membranes. The symbiosome membranes were resolved by SDS-polyacrylamide gel electrophoresis on a 15% (w/v) polyacrylamide SDS gel and were then electrophoretically transferred to nitrocellulose. The region of nodulin 26 migration was determined by staining a flanking lane of symbiosome membrane with amido black (45% [v/v] methanol, 10% [v/v] acetic acid, 0.1% [w/v] amido black) followed by a brief destain in (90% [v/v] methanol 2% [v/v] acetic acid). The membrane region containing nodulin 26 was cut into small squares and incubated with anti-nodulin 26 sera in PBS for two hr at room temperature while shaking. The membrane squares were then washed with a large volume of PBS with 0.05% Tween 20 (PBST) followed with elution by 100 mM glycine-HCl pH 2.5 for ten

min at room temperature. The elutate was collected and was neutralized with Tris-HCl pH 8.0. The affinity purified anti-nodulin 26 sera was stored at -80°C.

Immunochemical techniques

Western blots were done by a modification of previous procedures (Weaver et al., 1991; Zhang and Roberts, 1995). After resolution by SDS polyacrylamide electrophoresis (SDS-PAGE), proteins were transferred onto polyvinylidene fluoride membranes (PVDF, Immobilon^{TM}-P, Millipore) overnight at 4ºC, 100 mA, using a BioRad trans-blot cell (transfer buffer: 0.2 M glycine, 0.025 M Tris base, 20% [v/v] methanol). After transfer, the membrane was placed in blocking buffer (10% [w/v] non fat dry milk, 1% [v/v] goat sera, in PBS) and incubated for two hr shaking at 37ºC. The membrane was then washed 3X for 5 min each in PBST. Membranes were incubated with the primary antibody solution diluted in 0.5% (w/v) non fat dry milk, 1% (v/v) goat sera for 1 hr at 37ºC with constant shaking. Membranes were then washed 3X in PBST for five min each. Blots were incubated for 1 hr with the secondary antibody solution at 37ºC with constant shaking. Secondary antibody solution consisted of 0.2 μg/ml horse radish peroxidase-labeled goat anti-rabbit IgG (Southern Biotechnology Labs) diluted in PBS, 0.5% (w/v) non fat dry milk, 1% (v/v) goat sera. Blots were then washed for 5 min in PBS, 0.05% (v/v) Tween 20, then 3x 5 min in PBS, 0.05% (v/v) Tween 20, 0.05% (w/v) SDS, 0.1% (v/v) Triton X-100. The membranes were then placed in 10 ml of developer substrate for 1 minute (equal volumes of 2.5 mM luminol 0.4

mM p-coumaric acid, 0.1M Tris-HCl pH 8.5; and 0.018% [v/v] H_2O_2, 0.1 M Tris-HCl pH 8.5). The blots were immediately exposed to X ray film (Fuji HR-HA 30).

Enzyme-linked immunosorbent assays (ELISA) were done as previously described (Weaver, 1994). ELISA plates were prepared by adsorbing 50 μl of 5 μg/ml unconjugated peptide in 50 mM sodium carbonate, pH 9.5 on polystyrene microtiter plates (Biotek) overnight at 4ºC. The plates were blocked for 2 hr with 2 mg/ml bovine serum albumin in 200 mM glycine, pH 7.0 (200 μl/well). Varying dilutions of primary antibodies were prepared in PBS, 0.5% (v/v) goat sera (50 μl/well) for 1 hr at room temperature. Plates were then washed 3X in PBS and incubated with secondary antibody, 0.4 μg/ml horse radish peroxidase-labeled goat anti-rabbit antibody (Southern Biotechnology Labs), in PBS, 0.5% (v/v) goat sera (50 μl/well) for 1 hr at room temperature. Plates were washed 3x in PBS and were developed by using the BioRad Horseradish Peroxidase Substrate kit (Cat.No.172-1064). Product was measured by absorbance at 414 nm on a Lab Systems Multiscan MCC/340.

Membrane and protein isolation

Symbiosome membranes were isolated from nodules harvested from 9 week old *Lotus japonicus* plants by a Percoll step gradient differential centrifugation technique (Weaver et al., 1991; Dean et al., 1999). *Lotus* nodules were crushed on ice in an 1.5 ml polypropylene eppendorf tube in

extraction buffer (20 mM MES-NaOH, pH 7.0, 20 mM sodium isoascorbate, 1% [w/v] BSA, 1% [w/v] PVP-40, 10 mM EGTA, 5 mM DTT, 1 μM leupeptin, 350 mM mannitol), the homogenate was then passed through Miracloth to remove large cellular debris and loaded onto a 6 ml gradient in a 15 ml Corex tube. Gradients consisted of equal parts 30% (v/v) Percoll, 60% (v/v) Percoll, 80% (v/v) Percoll in 10 mM MOPS-NaOH, pH 7.0, 3 mM $MgSO_4$, 350 mM mannitol, 1 μM leupeptin. Samples were centrifuged at 5,500 rpm, 15 min, in a HS-4 rotor, at 4°C, and the interface at 60-80% was harvested from the gradient and was resuspended in approximately 25 ml of wash buffer (20 mM MOPS-NaOH, pH 7.0, 350 mM mannitol, 3 mM $MgSO_4$). This sample was centrifuged at 4°C, 650g for 3.5 min to remove excess Percoll. The pellet was then resuspended in 20 mM MOPS-NaOH, pH7.0, 150 mM KCl and was passed through a 25 gauge needle 3 times. Bacteroids were removed by low speed centrifugation in an HS-4 rotor (6000 rpm, 10 min at 4°C). The supernatant fractions were then centrifuged for 1 hr at 100,000g at 4°C. Various isolated fractions were visualized by Nomarski imaging on an Olympus BX60 microscope under a 100X oil immersion lens and digitally collected using a Hamamatsu Color chilled 3CCD camera attached to a Hamamatsu controller C5810.

Symbiosome membranes were isolated from nodules harvested from soybean plants between 28 to 42 days of age by two phase partitioning as previously described (Christiansen et al., 1995). Nodulin 26 was purified by

solubilization in octyl glucoside and fast protein liquid chromatography using diethylaminoethyl cellulose fast flow as previously described (Weaver et al., 1994; Dean et al., 1999). Recombinant his-tagged nodulin 26 expressed in *E. coli* was prepared by a modification of a previously described procedure (Lee et al., 1995). Briefly, *E. coli* BL21 CodonPlus-RP cells (Stratagene) transformed with pRSETA (Invitrogen) containing the nodulin 26 cDNA were grown to mid-logarithmic phase and were induced with 1 mM isopropyl-ß-D-thiogalactoside. Cells were grown for 2 hr, and were collected by centrifugation. Cells were lysed and his-tag nodulin 26 was solubilized from the membrane pellet in octyl glucoside as previously described (Lee et al., 1995). Solubilized nodulin 26 was adsorbed to Ni^{2+}-nitrilotriacetic acid (Ni-NTA) superflow (Qiagen) in 1% (w/v) octyl glucoside, 100 mM HPO_4, 10% (v/v) glycerol, 5 mM 2-mercaptoethanol, 200 mM NaCl, 100 mM imidazole, pH 7.0. The column was washed extensively and was eluted with 1% (w/v) octyl glucoside, 100 mM HPO_4, 10% (v/v) glycerol, 5 mM 2-mercaptoethanol, 200 mM NaCl, 1 M imidazole, pH 7.0. Fractions containing nodulin 26 were concentrated on a Microcon-30 ultrafilter (Amicon) and stored at –80°C.

For analysis of the phosphorylation state of nodulin 26, a modified membrane purification protocol was adopted. Nodules were ground on ice with a pestle in an extraction buffer containing 250 mM sucrose, 50 mM *N*-2-Hydroxyethylpiperazine-*N'*-2-ethane-sulfonic acid (HEPES)/KOH pH 7.5, 20 mM EDTA, 20 mM EGTA, 10 mM sodium fluoride, 5 mM sodium orthovanadate, 1% (w/v) polyvinylpyrrolidone-40, 20 mM iso-asorbic acid,

0.2% (w/v) bovine serum albumin, 5 mM dithiothreitol, 5 mg/ml leupeptin, 0.5 mM phenylmethylsulfonyl fluoride. Extracts were centrifuged at 100g for 10 min. The supernatant fraction was then passed through a 25 gauge needle three times and was centrifuged at 700g for 20 min. The 700g supernatant was then centrifuged at 100,000g for 1 hr. The pellet was resuspended in 330 mM sucrose, 5 mM potassium phosphate pH7.8, 2 mM EDTA, 2 mM EGTA, 10 mM sodium fluoride, 5 mM sodium orthovanidate, 5 mg/ml leupeptin, 0.5 mM phenylmethylsulfonyl fluoride and was stored at -80°C until analysis.

Recombinant *Arabidopsis* calcium dependent protein kinase (CDPK) KJM23-62H was prepared by expression in *E. coli* and purified by nickel chelate chromatography followed by affinity chromatography on glutathione-Sepharose as previously described (Harper et al., 1994). Purified kinase was stored in aliquots at -80°C.

Yeast growth

Yeast strain YPH259 (Sikorski and Hieter, 1989) harboring the pHVX2 (Volschenk et al., 1997; Gietz and Sugino, 1988) plasmid containing the LjNod70 cDNA (Szczyglowski et al., 1998) downstream of the phosphoglycerate kinase promoter was grown on leucine- dropout media (Dropout Base supplemented with Complete Supplement Mixture –LEU, commercially purchased from BIO 101). Yeast cultures grown on leucine-dropout media were grown at 30°C and 1 ml aliquots were removed at various time points and stored at -80°C.

Analytical methods

Protein kinase assays were carried out with the phosphocellulose filter paper method as previously described (Weaver et al., 1991; Lee et al., 1995). Assays were conducted in 25 mM MOPS-NaOH, pH 7.0, 10 mM magnesium acetate, 7.5 mM 2-mercaptoethanol, 0.1 mM [γ^{32}P]ATP (980 dpm/pmol) and various amounts of a synthetic peptide substrate CI-14 (**Fig. 8**). In situ phosphorylation of nodulin 26 on symbiosome membranes was performed by incubation of membranes (1 mg/ml protein) in 50 mM ATP, 1 mM $CaCl_2$, 10 mM Mg-acetate, 25 mM MOPS-NaOH, pH 7.5 for 3 hr at 27°C. To monitor the extent of phosphorylation, a small aliquot of membranes was incubated under the same conditions except that γ^{32}P-ATP was included as previously described (Weaver et al., 1991). Dephosphorylation reactions were conducted with a duplicate sample of membranes by incubation with 6 units of calf intestinal alkaline phosphatase (Promega) in 50 mM Tris HCl pH 9.3, 1 mM $MgCl_2$, 0.1 mM $ZnCl_2$, 1 mM spermidine.

The phosphorylation status of nodulin 26 was determined by comparing the Western blot signals obtained with affinity purified anti-GC12P and anti-nodulin 26 antibodies using 20 μg of isolated membrane protein. The intensity of the Western signals on the blots was quantitated by densitometry using digitally scanned X-ray film and the Quantity One Version 4.3 software (BioRad). The index of phosphorylation was determined by taking the ratio of the anti-GC12P and anti-nodulin 26 for each treatment.

Protein analysis was done by using the BCA (Pierce Endogen Chemicals), or Peterson's assays (Peterson, 1977). SDS-polyacrylamide gel electrophoresis was performed using the buffer system of Laemmli (1970). Free sulfhydryl groups on peptides was determined by using Ellman's reagent (Ellman, 1959).

Accession numbers used for sequence alignments

AQP0 P3030, **AQP1** AAL87136, **AQP2** NP_000477, **AQP3** NP_004916, **AQP4** AAB26958, **AQP5** NP_001642, **AQP6** NP_001643, **AQP7** NP_001161, **AQP8** XP_047117, **AQP9** JC5973, **AQPZ** BAA35593,**AQY1** NP_015518, **FPS1** CAA 38096, **GlpF** 11514194, **PIP1;1** CAB71073, **PIP2;1** CAB67649, **TIP1;1** AAD31569, **TIP2;1** BAB01264, **NIP1;1** CAA16760, **NIP1;2** CAA16748, **NIP2;1** AAC26712, **NIP3;1** AAG50717, **NIP4;1** BAB10360, **NIP4;2** BAB10361, **NIP5;1** CAB39791, **NIP6;1** AAF14664, **NIP7;1** AAF30303, **SIP1;1** AAF26804, **SIP2;1** CAB72165,**LIMP2** AF82791, **LIMP1** AF82790, **Nodulin 26** PO8995, **SPCP1** JQ2287.

CHAPTER III

RESULTS

Isolation of LIMP 1 and LIMP 2 cDNA sequences from *Lotus japonicus*

To identify MIP proteins expressed in the nodules of *L. japonicus*, including nodulin-26 like proteins, an RT-PCR approach was taken, using degenerate primers based on the two highly conserved NPA motifs found in all members of this protein family (Reizer et al.1993; Froger et al.1998) (**Fig. 9**). RT-PCR of total RNA from nodules of 9 week old *Lotus japonicus* plants showed a major 370 bp product (**Fig. 10**) consistent with the predicted size of a DNA fragment expected based on the distance between MIP NPA boxes (110-130 a.a.). This PCR product was cloned into the pCR 2.1 vector. Restriction mapping of the resulting colonies showed that they clustered into three patterns. Sequence analysis of representative clones of each showed that two encode MIP-like proteins which were designated LIMP 1 and LIMP 2 (Lotus Intrinsic Membrane Protein 1 and 2) respectively. The third clone that was amplified was homologous to plant elongation factor EF1-alpha and showed little homology to MIP proteins. This product was not pursued further.

The cloned LIMP 1 and LIMP 2 PCR fragments were used to probe an *L. japonicus* nodule cDNA library. Successive screens produced plaque-purified stocks which were rescued into the pBluescript plasmid. Restriction

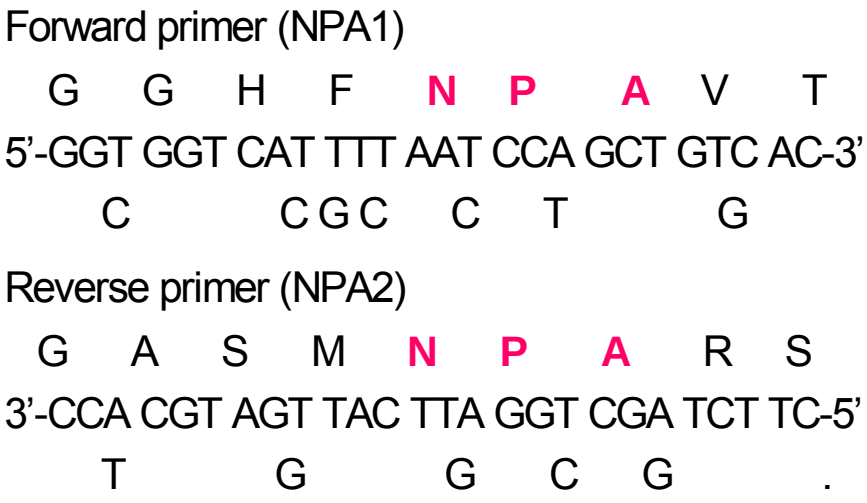

Figure 9. Degenerate primers designed to the NPA motifs conserved in MIPs. Based on sequences from several MIP proteins, a set of degenerate primers were designed to amplify MIP sequences expressed in *Lotus japonicus* nodules. Translated sequences are shown above the nucleotide sequences with the NPA motifs in red. Individual nucleotides positioned under the oligonucleotde primers indicate the degenerate nucleotide.

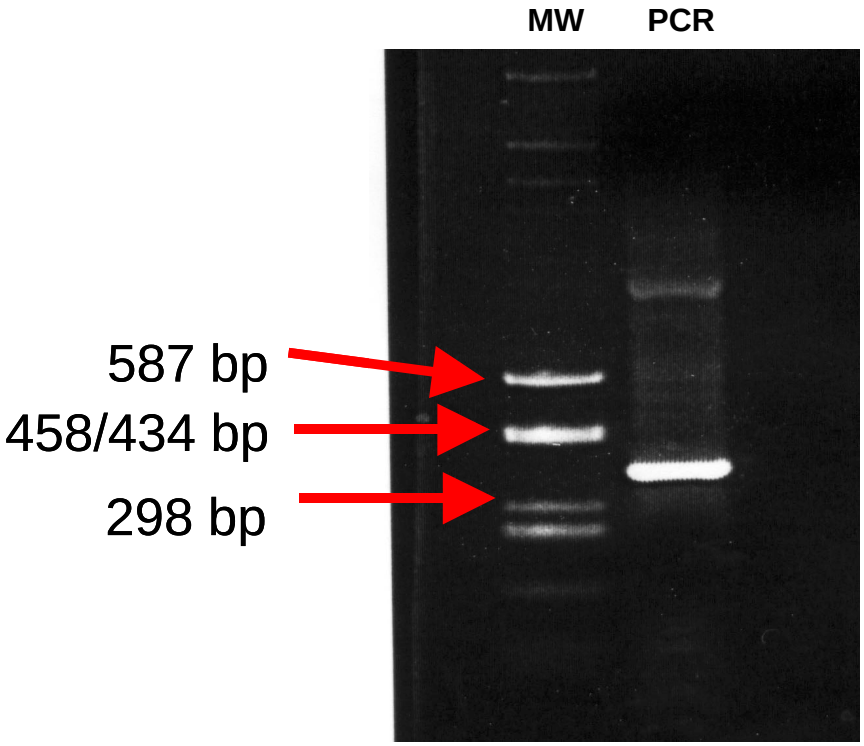

Figure 10. Reverse transcriptase coupled PCR of *Lotus* nodule RNA with degenerate primers. RT-PCR reactions of RNA from *Lotus* nodules with primers were performed and the products were resolved by electrophoresis on a 1% (w/v) agarose gel. **MW**, pUC18 plasmid *Hae* III digest molecular weight markers; **PCR**, RT-PCR product from 9 week old *Lotus japonicus* nodules.

digestion of these clones identified several different length inserts. The longest inserts for the LIMP1 and LIMP2 hybridizing probes were submitted for sequencing. Both strands of the clones were sequenced using successive gene specific primers based on the results of the previous sequencing reaction. Each sequencing run for both strands of the LIMP1 and LIMP2 clones were then aligned and compiled to generate the full length LIMP1 and LIMP2 sequences by using the Applied Biosystems Auto Assembler software ver. 1.4.0.

The LIMP 2 cDNA is 1211 bp in length and includes an 810 bp open reading frame that codes for a protein of 270 amino acid residues (**Fig. 11**). In addition, the LIMP 2 cDNA clone contains 91 bp of untranslated 5' sequence including 2 in-frame stop codons located upstream of the open reading frame start site, and 310 bp of untranslated 3' sequence. The LIMP 1 cDNA (**Fig. 12**) is 1162 bp in length, with an open reading frame of 753 bp that codes for a protein of 251 amino acid residues. The LIMP 1 clone also contains 59 bp of untranslated 5' sequence including an in-frame stop codon located upstream of the putative translational start site, and 350 bp of untranslated 3' sequence. These two MIP cDNAs were novel and had not been previously described in *Lotus japonicus* and were assigned GenBank Accession numbers AF275315 (LIMP1), and AF275316 (LIMP2).

Analysis of the deduced amino acid sequences show that LIMP 1 and 2 share only 23.5% amino acid identity, indicating the two proteins are highly divergent. The LIMP 2 protein shared the highest sequence similarity (68%

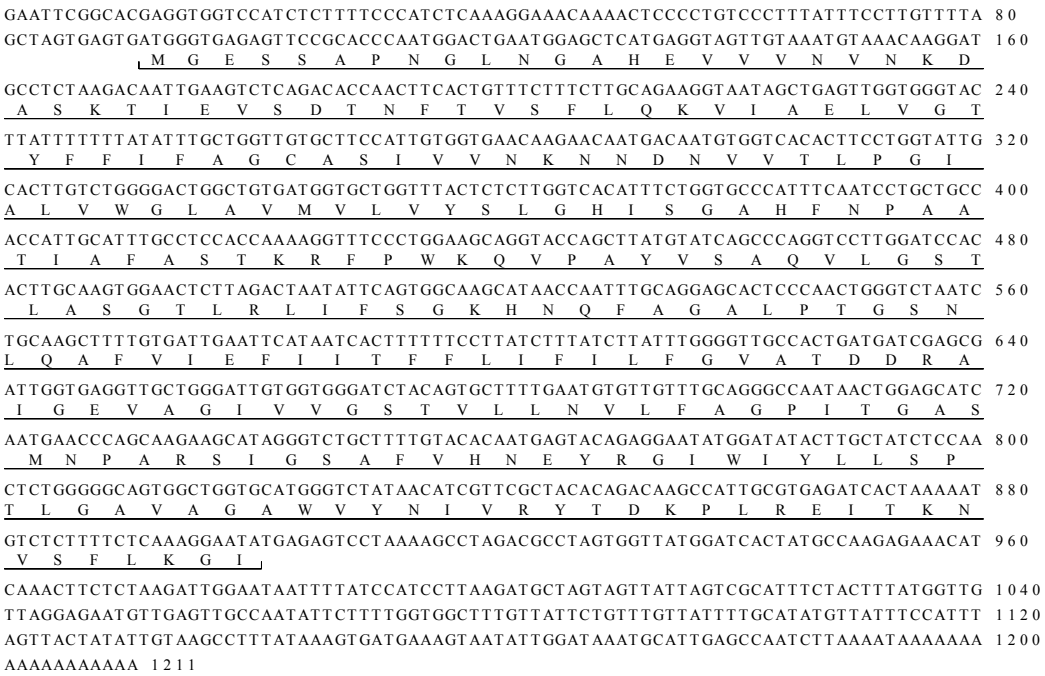

Figure 11. Sequence of full cDNA clone of LIMP 2. The sequence of the full length cDNA clone for LIMP2 that was isolated from a *Lotus japonicus* nodule cDNA library is shown. The predicted open reading frame is shown translated below the nucleotide sequence.

Figure 12. Sequence of the full length cDNA clone of LIMP1. The sequence of the full length LIMP1 cDNA clone isolated from a *Lotus japonicus* nodule cDNA library is shown. The predicted open reading frame is shown translated underneath the nucleotide sequence.

identity) with soybean nodulin 26 (**Fig. 13**). In contrast, the LIMP 1 open reading frame shared high identity (84% and 78% respectively) with the soybean SPCP 1 protein (Miao and Verma, 1993), and *Arabidopsis* γTIP (Höfte et al., 1992) (**Fig. 14**). Both proteins contain all the hallmarks of the MIP family (Reizer et al. 1993) including the highly conserved NPA regions and six transmembrane α-helical domains which is consistent with the hydropathy plots of the sequences (**Fig. 15**). The overall positioning and magnitude of these domains between LIMP2 and nodulin 26 (**Fig. 15**), and LIMP1 and SPCP1 (**Fig. 16**) are remarkably similar, further underscoring the high degree of structural relatedness between the proteins within each pair.

Expression of LIMP 1 and LIMP 2 mRNA in *Lotus japonicus* tissues

LIMP1 and LIMP2 represent the first two MIP family members isolated from *Lotus japonicus*. The representation of both sequences in the cDNA library suggests that these proteins are expressed in nodules, but it remains unclear whether they are nodule-specific proteins (i.e., nodulins). To test the tissue distribution of LIMP1 and LIMP2, total RNA from the aerial part of the plant (stems and leaves), nodules, and roots of 9 week old *Lotus japonicus* plants were analyzed by Northern Blot using LIMP1 or LIMP2-specific probes (**Fig. 17**). Northern blot analysis with a LIMP2-specific probe shows the presence of a hybridizing mRNA signal of the expected size in total RNA isolated from nodules of *L. japonicus* but no detectable message in either roots or leaves and stems (**Fig. 17A**). In contrast, LIMP1 shows high expression in roots and nodules, but its expression is markedly reduced in

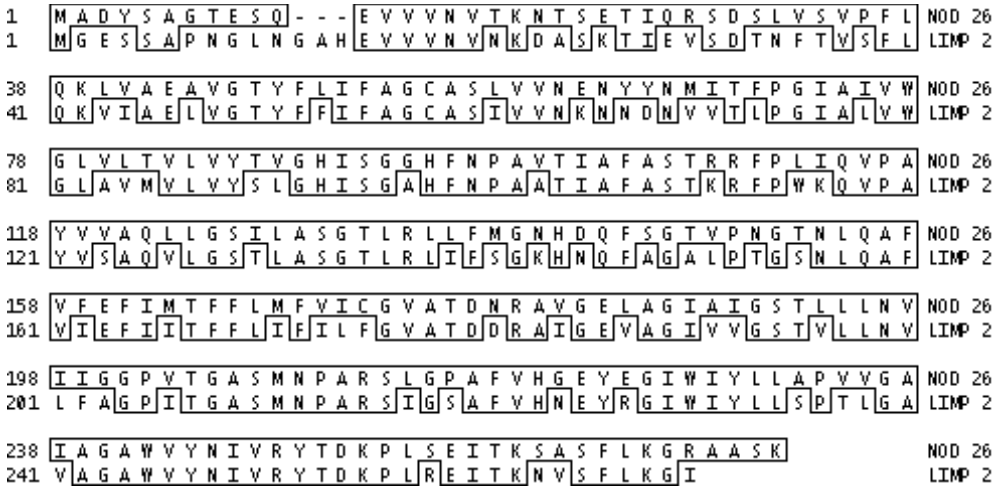

Figure 13. Sequence alignment between soybean nodulin 26 and LIMP2. The deduced amino acid sequence of LIMP2 and soybean nodulin 26 (Sandal and Marcker, 1988; Fortin et al., 1987), were aligned using the DNAstar program MEGALIGN and the clustal algorithm. Areas of identity are enclosed in boxes.

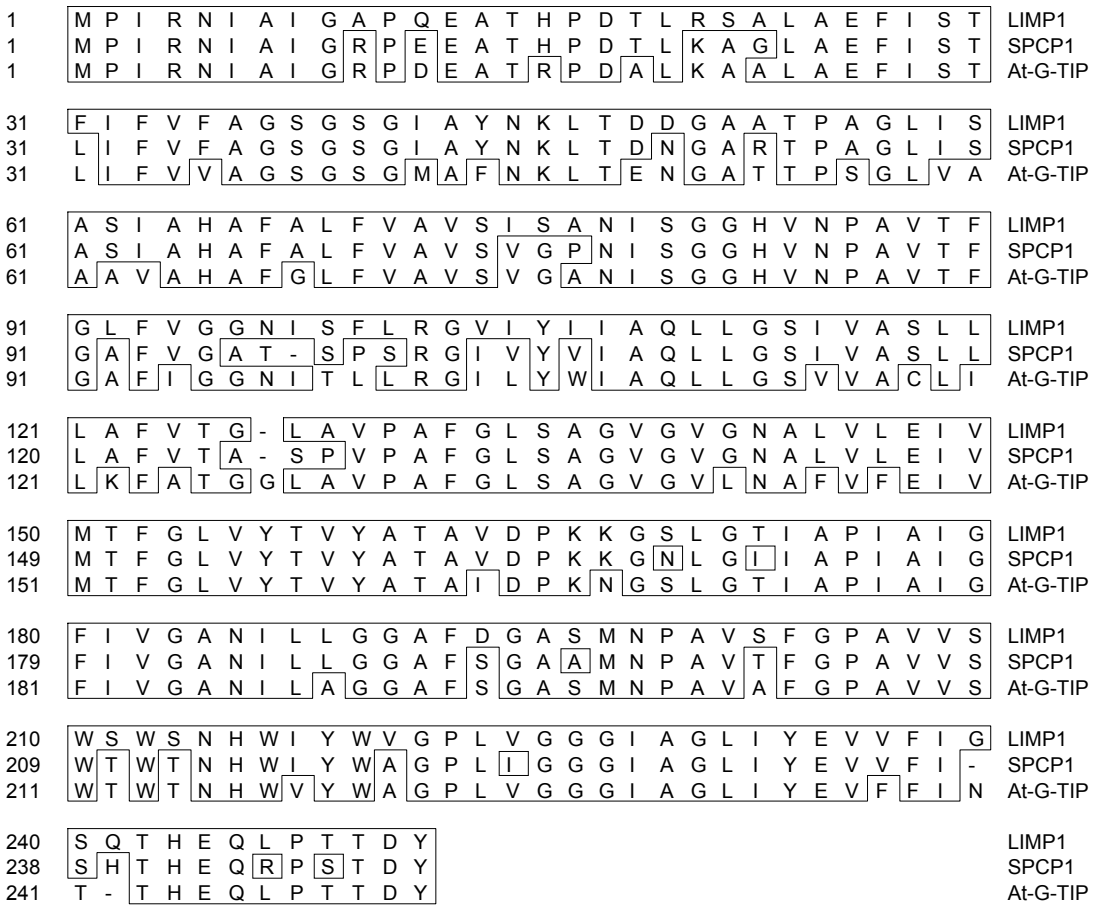

Figure 14. Amino acid sequence alignment between LIMP1, soybean SPCP1, and *Arabidopsis* γTIP. The deduced amino acid sequences of LIMP1, soybean SPCP1)(Miao and Verma, 1993), and *Arabidopsis* γTIP (Höfte et al., 1992), were aligned using the DNAstar program MEGALIGN and the clustal algorithm. Areas of identity are enclosed in boxes.

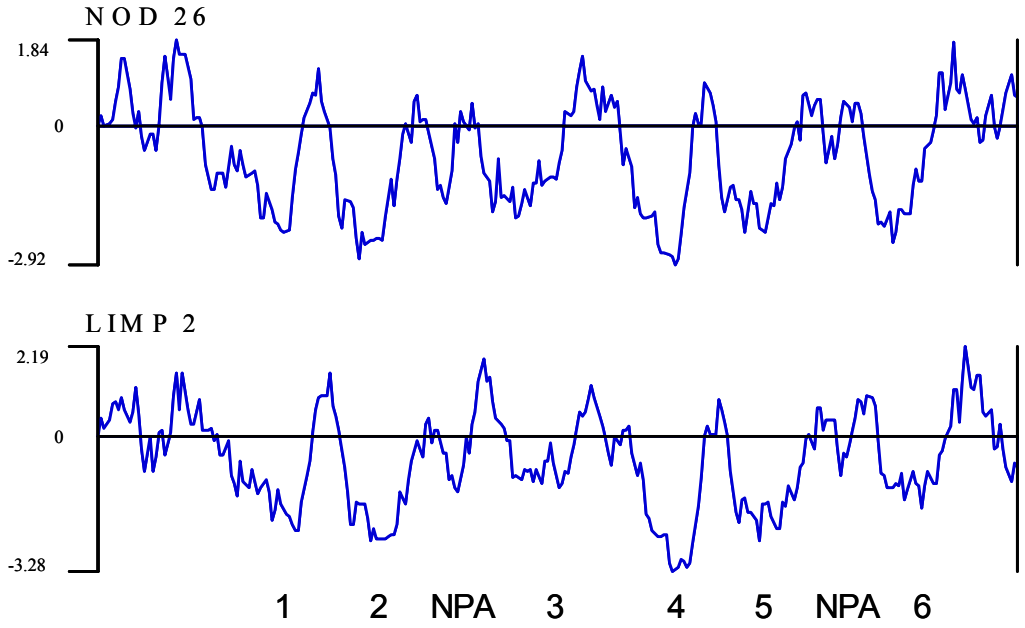

Figure 15. Hydropathy plots of soybean nodulin 26 and LIMP2. Hydrophobicity comparisons of LIMP2 with soybean nodulin 26 were done by using the DNAstar program Protean to generate a Kyte-Doolittle hydropathy plot with a window of nine amino acid residues (Kyte and Doolittle, 1982). The predicted transmembrane domains (1-6) and NPA loops are shown underneath the plots.

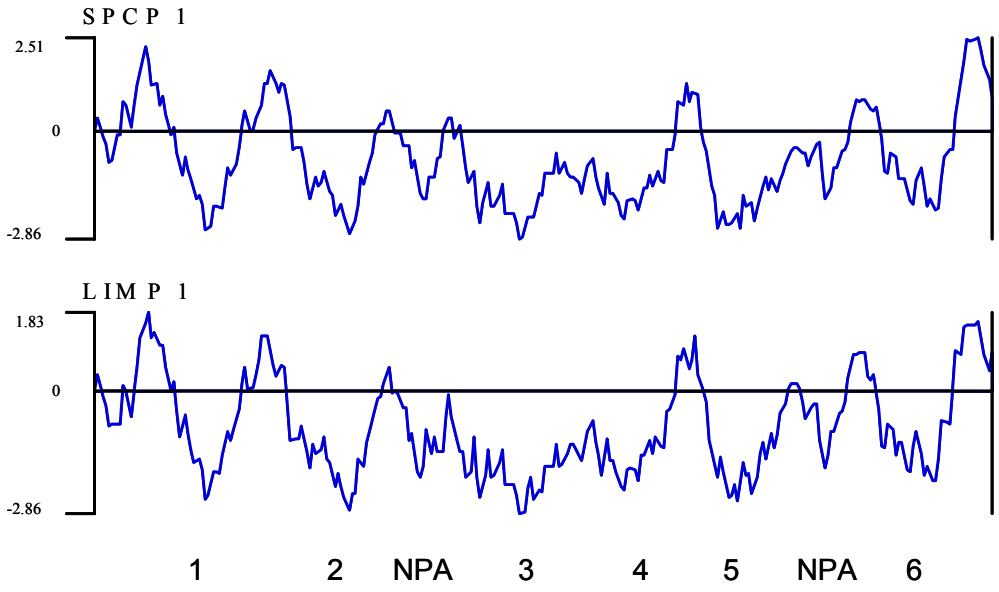

Figure 16. Hydropathy plots of LIMP1 and SPCP1. Hydrophobicity comparisons of LIMP1 with soybean SPCP1 were done by using the DNAstar program Protean to generate a Kyte-Doolittle hydropathy plot with a window of nine amino acid residues (Kyte and Doolittle, 1982). The predicted transmembrane domains (1-6) and NPA loops are shown underneath the plots.

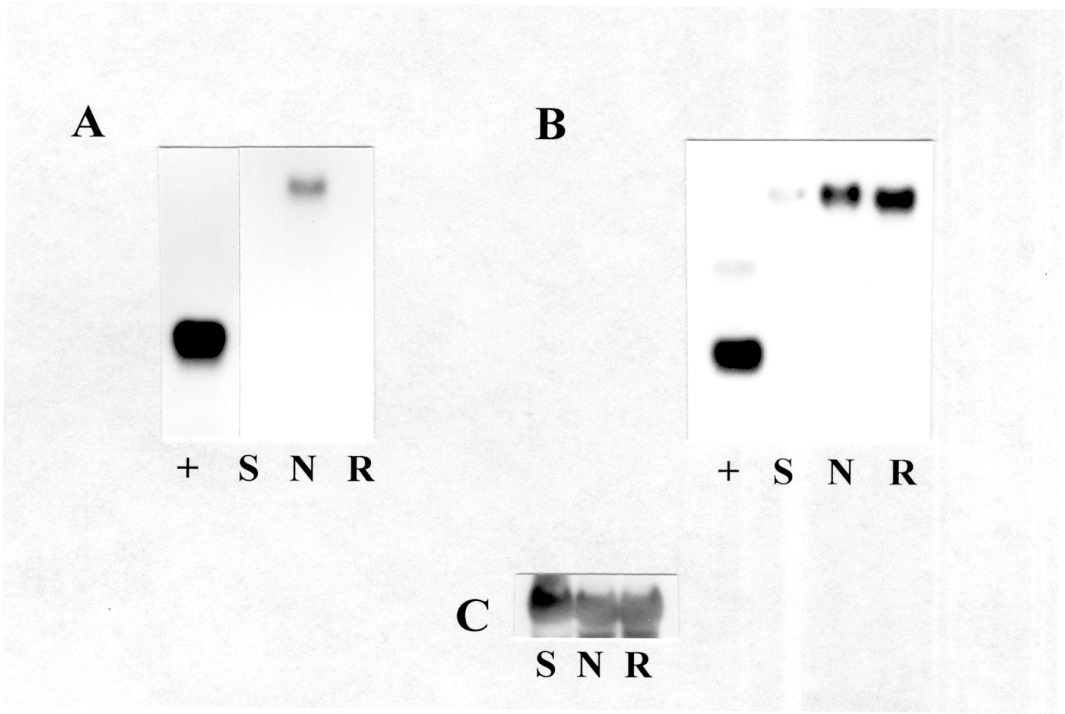

Figure 17. Northern blot of RNA from various *Lotus* tissues probed for the LIMP2 or LIMP1 transcript. Total RNA isolated from (**N**) nodules, (**S**) stem and leaves, and (**R**) roots of 9 week old *Lotus japonicus* plants was analyzed by a Northern blot protocol as described in the Materials and Methods. (**+**) Indicates a sample of the LIMP1 or LIMP2 PCR fragment loaded as a positive hybridization control. Blots were probed with the labeled cloned PCR fragments for (**A**) LIMP2. (**B**) LIMP1 or (**C**) with a labeled 18S rRNA probe (loading control). Each lane contains 10 μg of the respective total RNA.

leaves and stems (**Fig. 17B**). Overall, the data suggest that LIMP2 appears to be a *Lotus japonicus* nodulin whereas LIMP1 is expressed principally in roots and nodules.

Production of site-directed antibodies for immunodetection of LIMP1 and LIMP2 proteins in *Lotus japonicus*

To gain more specific information on the actual cellular localization of LIMP1 and LIMP2 it was necessary to generate specific antibody probes. Specific peptide sequences for LIMP1 and LIMP2 (**Fig. 8**) were commercially synthesized with an additional cysteine at the amino terminus to facilitate linkage to carrier proteins for increased antigenicity and also to allow immobilization to solid resins for use in affinity purification.

Antibodies to LIMP2 were generated according to standard protocols listed in Materials and Methods using the CI-14 peptide (**Fig. 8**) conjugated to KLH. High antibody titers against unconjugated CI-14 were measured in crude antiserum obtained from immunized rabbits as judged by ELISA analysis. Affinity purification of antibodies was done on a resin consisting of CI-14 coupled agarose. The resulting antibodies were used to probe fractions purified from *Lotus japonicus* nodules. To isolate *Lotus* symbiosomes, a Percoll step gradient approach (Weaver et al., 1991) was adopted. A discrete band was obtained at the 60%/80% Percoll interface, which is the position at which *Glycine max* symbiosomes sediment. Analysis by Nomarski microscopy showed organelles indicative of symbiosome structures (**Fig. 18**). To obtain purified symbiosome membranes, these structures were

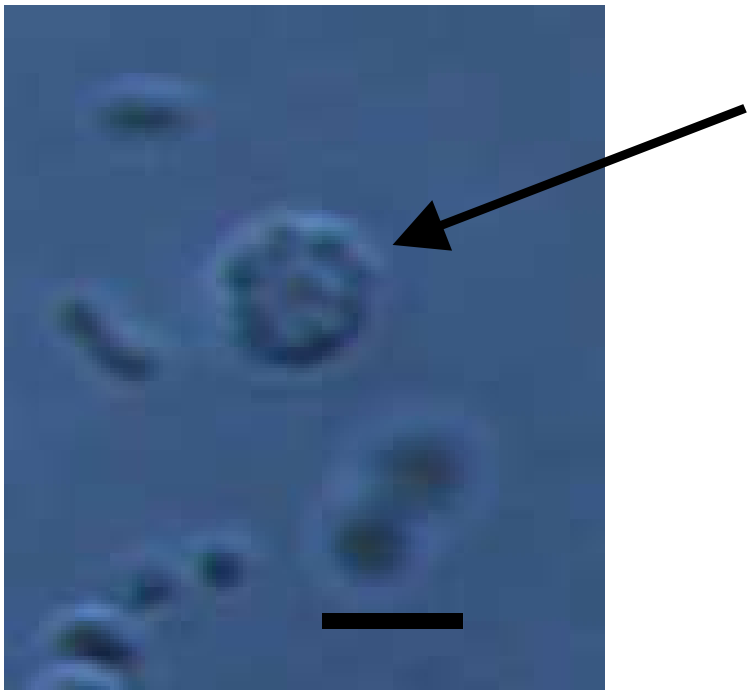

Figure 18. Nomarski light micrograph of isolated *Lotus japonicus* symbiosome. The 60%/80% Percoll fraction from *Lotus japonicus* symbiosome prep was visualized by Nomarski microscopy. Arrow depicts an intact symbiosome, bar represents 10μm.

mechanically ruptured and the bacteroids were separated from lighter symbiosome membrane fragments by differential centrifugation. Western blot analysis with anti CI-14 antibodies showed a band with an apparent molecular weight of 28 kDa in symbiosome membrane fractions (**Fig. 19**). This is consistent with the predicted molecular weight for LIMP2.

A similar approach for preparation of antisera against LIMP1 was adapted. Initially, an amino terminal sequence of the 13 amino acids at the carboxyl terminal end of LIMP1 was employed (**Fig. 8**). While high titers against KLH were obtained, these antibodies did not react with CA-15. A second peptide (CY-15) was produced and was conjugated to KLH and the coupled peptide/carrier was used for antibody production in the same rabbit. After several boosts, sera were collected that showed high antibody titers to the CY-15 peptide by ELISA. Further purification of CY-15-specific antibodies from the crude antiserum was done by affinity chromatography of the CY-15 peptide coupled to an agarose solid support. Western blots of *Lotus japonicus* microsomes probed with this affinity-purified antibody displayed a reactive band of 28 kDa which is the predicted size of the LIMP1 protein (**Fig. 20**). Much lower immunoreactivity was observed in microsomal fractions from nodules (**Fig. 20**), and no cross-reaction with the LIMP1 antibody was observed with symbiosome membrane samples (not shown). A larger MW band (110,000 kDa) was observed in the root microsomal fraction. The appearance of this band is variable, and it is proposed that it could represent a LIMP1 aggregate (i.e. tetramer). Aggregation of some MIP proteins during

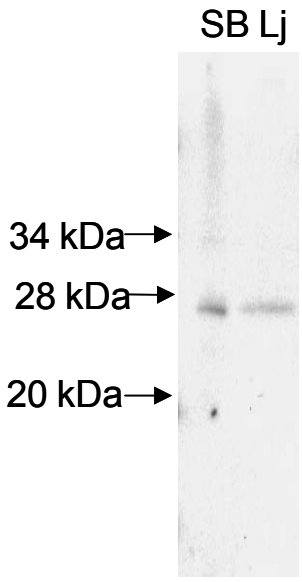

Figure 19. Western blot of symbiosome membranes probed with anti-CI-14 antibodies. **SB** soybean symbiosome membranes; **Lj** *Lotus* symbiosome membranes. Symbiosome membranes were resolved by SDS-PAGE on a 12.5% polyacrylamide gel and electrophoretically transferred to PVDF membranes for probing with anti CI-14 antibodies.

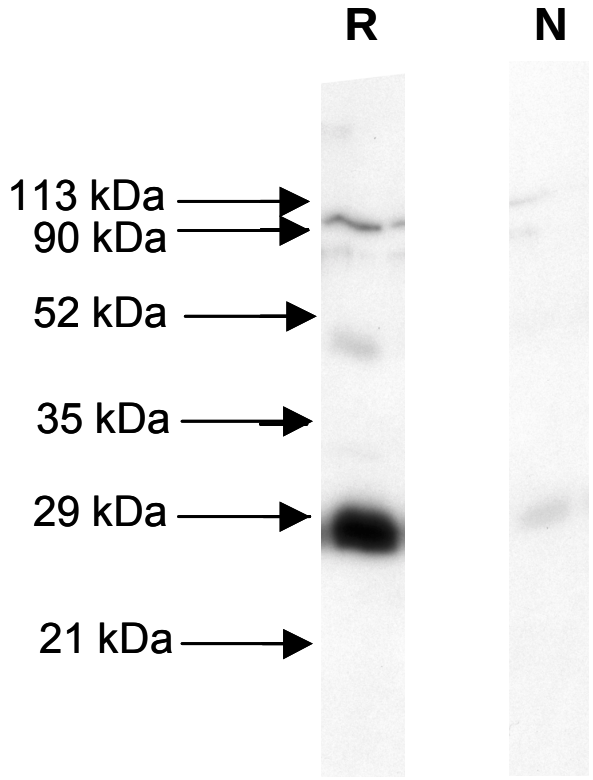

Figure 20. Western blot of *Lotus japonicus* microsome fractions probed for LIMP1 expression. Microsomal membranes (20 μg/lane) from five month old *Lotus* roots (**R**) and nodules (**N**) were probed with affinity purified antibodies raised against LIMP1 peptide.

SDS-PAGE is known to occur (e.g., Harvengt et al., 2000). Preimmunization sera from LIMP1 and LIMP2 rabbits showed no reaction with any fractions or samples tested.

Overall, the Northern blot and immunoblot data suggest that LIMP2 is a nodule-specific MIP protein localized to the *Lotus* symbiosome membranes, similar to nodulin 26. However, LIMP1 is more prevalent in root membranes than nodule membranes, is lacking from symbiosome membranes, and apparently is a *Lotus* TIP ortholog.

Immunolocalization of *Lotus japonicus* LjNod70

Lotus japonicus has been adopted as a model legume and a considerable focus has been placed on the genomics and proteomics of this organism, particularly on gene products involved in rhizobia symbiosis. A number of late nodulin gene products have been identified by using differential display techniques (Szczyglowski et al., 1997). The ability to isolate symbiosome membranes has allowed the investigation of whether other nodulin proteins in this library are localized to this critical symbiotic interface.

In collaboration with Dr. Krzysztof Szczyglowski (Michigan State University, presently at Agriculture and Agrifood, Canada), we have been investigating one particular late nodulin, LjNod70, which encodes a 575 a.a. putative membrane transporter with 12 predicted transmembrane α-helices (Szczyglowski et al., 1998). By using antibodies generated against a recombinant fragment of this protein, comprising 100 residues of the carboxyl

terminal region, *Lotus japonicus* symbiosome membranes were probed using the same procedure that was employed for LIMP2. Interestingly, reactivity was observed for two discrete entities within the symbiosome membrane fraction (**Fig. 21**). The smaller reactive species has a predicted molecular weight of 27 kDa and the larger reactive species has a calculated molecular weight of 64 kDa, which is consistent with the predicted molecular weight of LjNod70 (70 kDa). Western blot analysis of LjNod70 in a yeast expression system revealed only a single product with an apparent molecular weight of 60 KDa (**Fig. 21**). Whether the smaller product observed represents an alternative splicing product (Szczyglowski et al., 1998) or is a product of proteolysis remains unknown.

Overall the data suggests that LjNod70, similar to LIMP2 is also found on the symbiosome membrane and may participate in transport processes involved in the symbiosis.

Functional properties of LIMP 1 and LIMP 2 in *Xenopus laevis* oocytes

The similarity of LIMP1 and LIMP2 to MIP proteins suggest that they perform roles as water and/or solute channels on nodule membranes. To investigate transport properties, LIMP1 and LIMP2 were expressed in *Xenopus laevis* oocytes. Oocyte membranes have no endogenous water channels and are also electrophysiologically “quiet”. Because of these properties, and the fact that they are large, easy to culture and can be readily

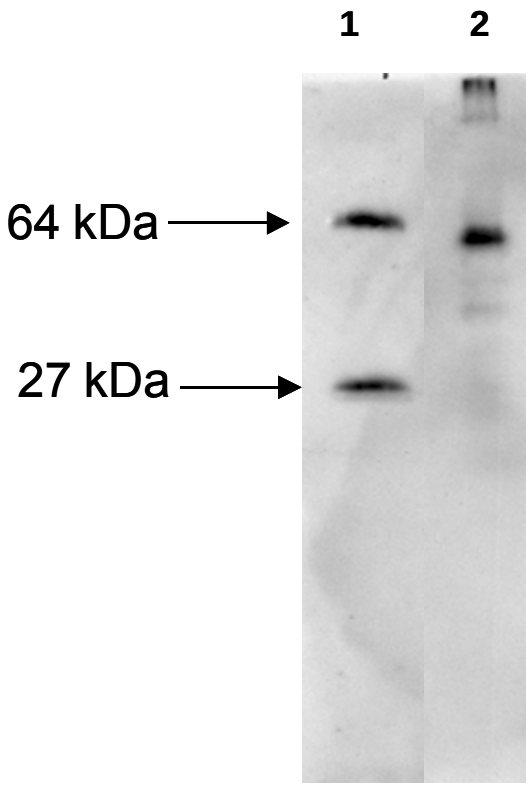

Figure 21. Western blot analysis of *Lotus japonicus* symbiosome membranes with antibodies against LjNod70. Lane 1, Symbiosome membrane fraction from *Lotus japonicus* nodules; **Lane 2**, Lysate of yeast strain YPH259 expressing full length LjNod70.

microinjected with RNA and DNA constructs, they are commonly used for heterologous expression to investigate channel function (Agre et al., 1998)

The water permeability of oocytes was investigated by an oocyte-swelling assay. Injection of capped LIMP1 and LIMP 2 cRNA into oocytes significantly enhanced the rate of oocyte swelling upon challenge with hypoosmotic media (**Fig. 22**). Calculation of the osmotic water permeability coefficient (P_f) shows that LIMP2 (3.2×10^{-4}cm/s) and LIMP1 (4×10^{-4} cm/s) injected oocytes display enhanced water permeability, at least 3-fold over control oocytes, and give P_f values similar to that observed for soybean nodulin 26 (3.5×10^{-4} cm/s) (Rivers et al.1997) (**Fig. 23**).

The glycerol transport activity of LIMP1 and LIMP2 was tested by the uptake of ^{3}H-glycerol by oocytes (**Fig. 24**). Nodulin 26 and LIMP2-injected oocytes showed a high rate of glycerol transport (**Fig. 24**), which was virtually identical to oocytes injected with the *E. coli* glycerol facilitator GlpF (data not shown). In contrast the LIMP1 protein did not show any significant flux of glycerol over water-injected control oocytes (**Fig. 24**), or oocytes expressing the water selective AQP1 (not shown).

Based on these results it is concluded that LIMP2 and nodulin 26 form multifunctional aquaglyceroporins that transport both water and uncharged solutes such as glycerol, whereas LIMP1 forms a water-selective aquaporin.

Lotus japonicus transgenic plant production

The findings that LIMP1 and LIMP2, form water and/or multifunctional channels respectively, and are found in *Lotus* nodules suggest that they play

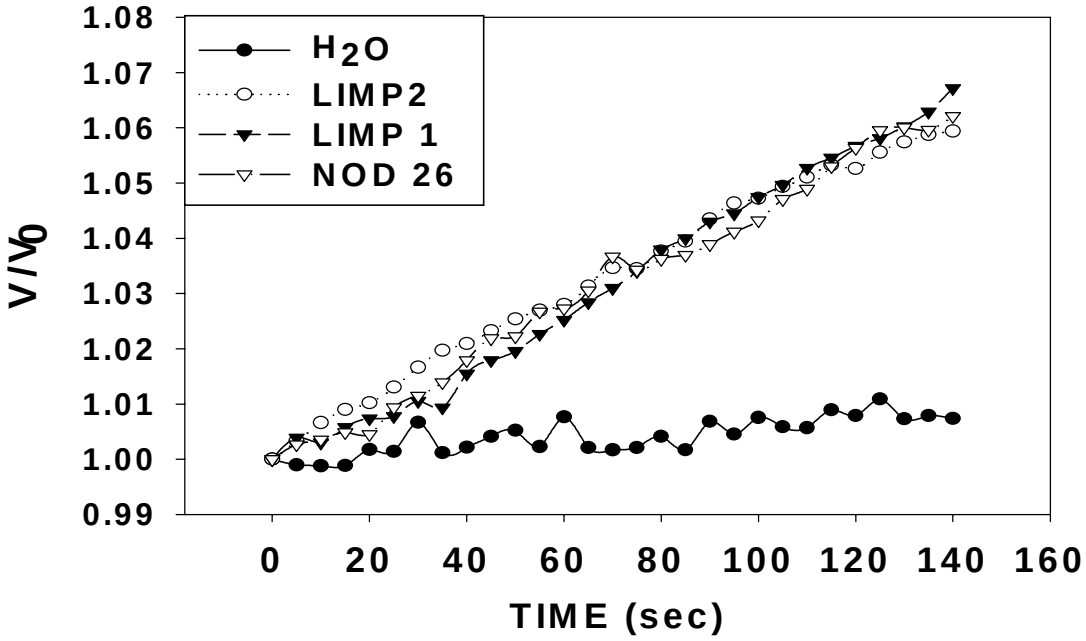

Figure 22. Swelling assay of *Xenopus* oocytes injected with cRNA constructs. The permeability of *Xenopus* oocytes injected with 50 ng of the indicated cRNAs (or sterile water control) was determined by lowering the osmolarity of the media (from 220 mOsm/kg to 59 mOsm/kg) and measuring the change in oocyte volume (V/V_0) per unit time.

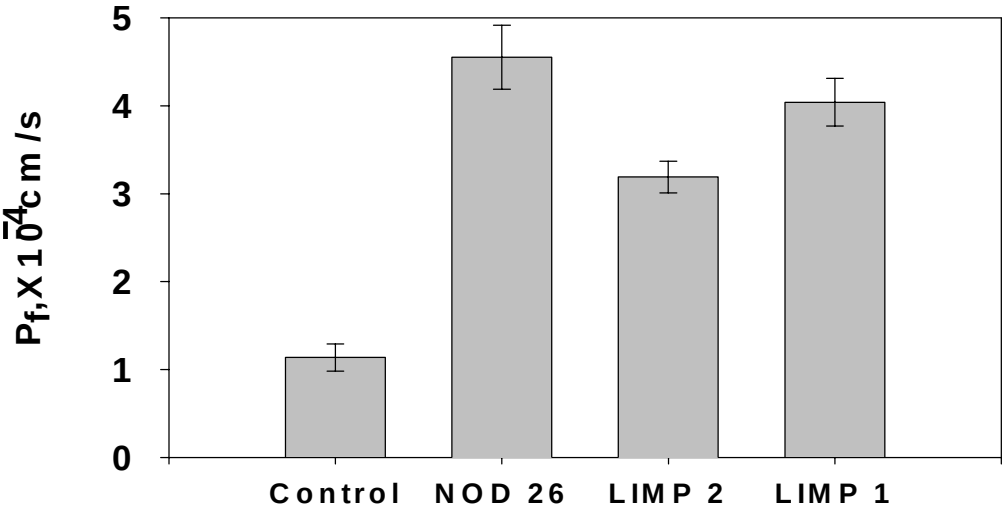

Figure 23. Calculated P_f values for cRNA-injected *Xenopus* oocytes. Osmotic permeability coefficients (P_f) were calculated from the time course of swelling for oocytes injected with LIMP 1, LIMP 2, or nodulin 26 cRNA, or nuclease free water by using the osmotic water permeability equation (Materials and Methods). Error bars show standard error for the mean (n=8).

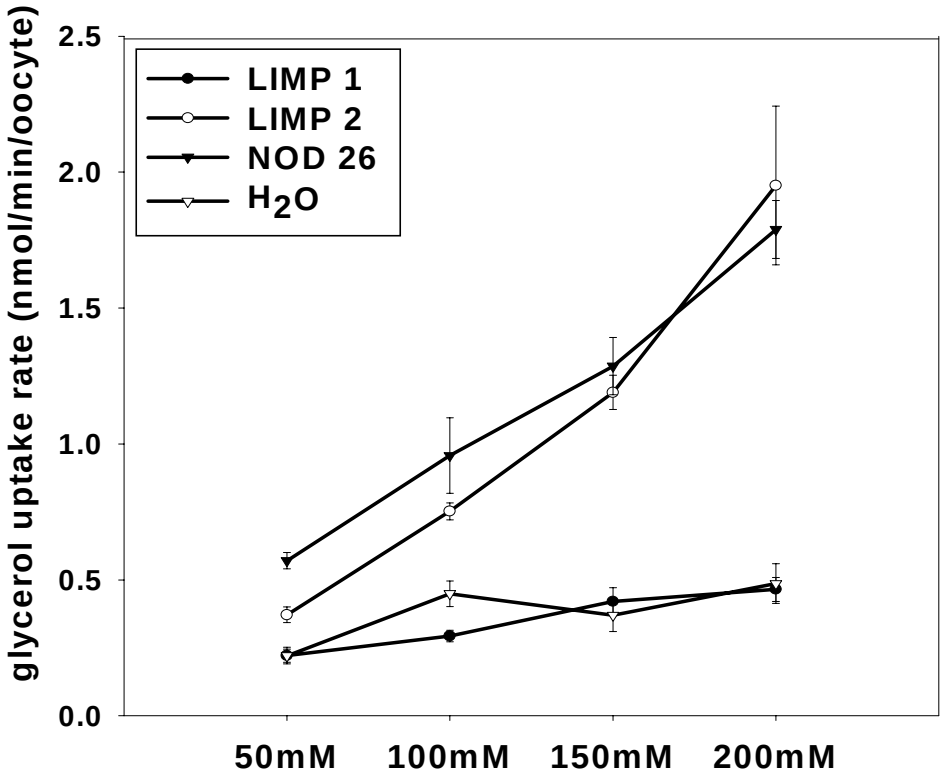

Figure 24. Glycerol uptake in LIMP1 and LIMP2 expressing oocytes. The uptake for ^{3}H glycerol was determined for oocytes expressing LIMP1 and LIMP2 under isoosmotic conditions in response to increasing concentrations of glycerol in media. Error bars show standard error of the mean (n=12).

a role in osmoregulation and possibly metabolite transport. To gain insight into these potential roles, a transgenic plant approach was attempted using LIMP1 and LIMP2 antisense constructs. Using the *Agrobacterium*-mediated genetic transfer method refined by Stiller et al, (1997), it is possible to generate transgenic *Lotus japonicus* lines which harbor genomic insertions of foreign genes/cDNAs. The LIMP1 or LIMP2 open reading frames were transformed into pGA941, an *Agrobacterium* binary transformation vector (**Fig. 25**). This vector construct contains the NPTII selectable marker, allowing for selection of transformed plant tissues using G418, or kanamycin antibiotics. The LIMP1 or LIMP2 ORFs were placed in an antisense orientation within the vector relative to the strong plant CaMV 35S promoter. Constructs were purified and transformed into *E. coli,* and electroporated into *Agrobacterium tumefaciens* strain AGL1.

Incubation of sectioned *Lotus* hypocotyls with cultures of *Agrobacterium* followed by transfer to selection media resulted in green calli resistant to the antibiotic G418. *Lotus japonicus* shoots and roots were regenerated as described by Stiller et al. (1997). Regenerated plants retaining resistance to G418 were transferred to individual pots and were allowed to produce seed (T_0 lines). Multiple separate transformed lines were generated for LIMP1 (26 lines), and LIMP2 (25 lines) antisense constructs.

Eleven lines of LIMP2 plants and thirteen lines of LIMP1 plants were selected for further study. Selection was performed by germinating seeds on

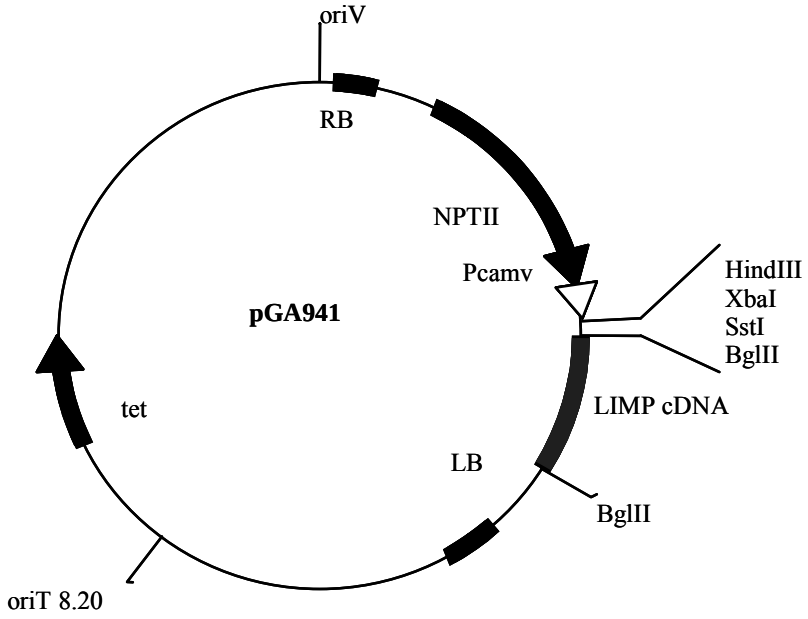

Figure 25. Constructs for production of LIMP1 and LIMP2 antisense *Lotus japonicus* plants. tet, tetracycline resistance gene for selection in *E. coli*; **NPT II**, neomycin phosphotransferase gene for selection of plants on kanamycin; **Pcamv**, Cauliflower Mosaic Virus 35S promoter; **RB,LB**, Right and left T-DNA borders; **LIMP**, site of insertion of LIMP1 and LIMP2 antisense cDNAs

media containing kanamycin (**Table 1**). Using this antibiotic, visual selection of transformed plants was based on stunting and curling of roots, and the appearance of chlorotic vegetative tissue. PCR analysis of genomic DNA from these lines with NPT II primers (specific for T-DNA) (**Fig. 7**) showed the presence of T-DNA in all T_1 lines tested. Further evidence was provided by genomic Southern blot analysis of selected lines which showed the presence of T-DNA (**Table 1**). Selection on kanamycin showed several lines with 3:1 selection ratios based on the presence of a single T-DNA insert. Some plants showed 2:1 selection, suggesting the possibility of a homozygous lethal, others showed a higher ratio, suggesting the possibility of multiple T-DNA insertions (**Table 1**).

Northern blot analysis of several of these lines was used to measure the RNA expression levels of the LIMP1 and LIMP2 transcripts in wild type and transformed nodules (**Fig. 26**). Although these experiments showed slight variations in the overall transcript levels of some transformed lines, no obvious gross changes in expression were observed. Further analysis of the growth and development of T_1 transgenic *Lotus* plants showed no significant change in growth and development, and form nodules with normal morphology. Previous work with this technology with other legumes (Schoenbeck et al., 2000) shows that effects of expression of antisense constructs even under the control of the strong CaMV promoter often results in a relatively modest effect on protein expression. In our case this might not

Table 1: Summary of LIMP1 and LIMP2 antisense transgenic plant lines

Transgenic line	Kanamycin selection Resistant : Sensitive[a]	Transgene verification by PCR/Southern blot[b]
LIMP2 antisense		
1A		+
7A	32:11	+
8A		+
9	19:8	+
11	All sensitive (no germination)	
12		+
15	27:9	+
17	24:4	+
18		+
36A		+
36B	28:7	+
LIMP1 antisense		
2B	22:10	
15B	34:10	
22	33:12	
23	19:11	
24A		+
24B	All sensitive (no germination)	
26B		+
27B	26:9	
28A	20:9	+
28B		+
30A		+
39B		+
41A	22:7	

[a] Kanamycin selectivity ratios obtained by germinating T_1 seed on kanamycin media.
[b] Indicates the presence of a transgene, detected by either PCR (by using the NPT II 196 forward and NPT II 745 reverse primers, **Fig. 7**) or by Southern blot of genomic DNA using NPT II DNA as a probe.

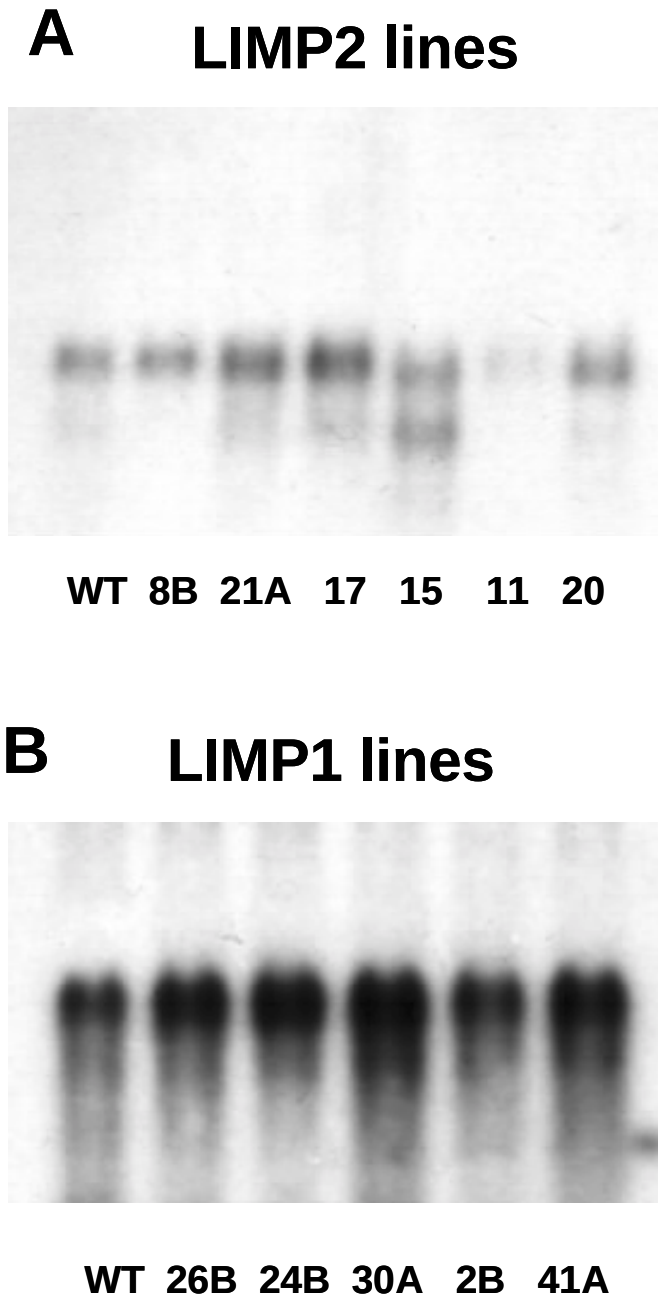

Figure 26. Northern blot analysis of total RNA extracted from *Lotus* transgenic lines. Total RNA was isolated from nodules of T_1 transgenic lines for comparison to wild type expression of **A** LIMP2 and **B** LIMP1. Individual transformed lines are designated by number and letter for each of the antisense constructs.

be enough to observe a phenotype particularly under normal growth conditions.

LIMP1 regulation by diurnal cycling

Plants depend on the capture of sunlight to generate photosynthate and to regulate the expression of a number of genes based on diurnal cycling conditions. In addition, day/night cycling conditions have a profound effect on the regulation of the transpiration stream (Parsons and Kramer, 1974; Clarkson et al., 2000). Microarray analysis conducted on *Arabidopsis* has revealed that a large number of the total genes (6%) appear to vary in expression in response to diurnal cycling conditions (Harmer et al., 2000).

Previous work has shown that plasma membrane intrinsic proteins in *Lotus* roots fluctuate during light/day cycling (Henzler et al., 1999; Clarkson et al., 2000). To determine whether nodule MIPs show a similar sensitivity, Northern blot analysis was used determine the expression levels for LIMP1 and LIMP2 over typical day/night cycling conditions. LIMP1 mRNA shows distinct variation (2-3 fold) during the day/night cycle. Messenger RNA levels begin to increase just before the start of the light cycle, and continue to increases reaching a maximum at 4-8 hr into the light cycle (**Fig. 27**). Levels decreased rapidly upon entry into the dark cycle, and began increasing again one hour before the start of the light period. LIMP2 showed a less distinct pattern, with levels slightly depressed during the dark period. Recent analysis of LIMP1 protein levels by Western blot using the affinity purified LIMP1 antibody also showed significantly enhanced LIMP1 protein in the light cycle

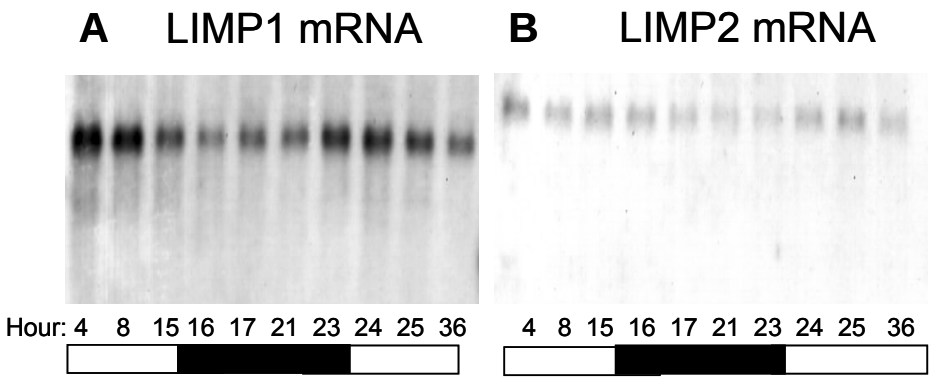

Figure 27. Control of LIMP1 and LIMP2 expression during a light dark cycle. Total RNA was extracted from nodules of 11 week old *Lotus japonicus* plants at various time points during a typical light-dark cycle (16hr light:8 hr dark) and was analyzed by Northern Blot probed for: **A.** LIMP1 expression; or **B.** LIMP2 expression. Time points corresponding to each individual lane are indicated and the bar shows the dark and light periods.

compared to the dark conditions (Vincill, Guenther, and Roberts, unpublished observations). Together, these results suggest that expression of LIMP1 in nodules is apparently under diurnal regulation.

Phosphorylation of LIMP2 by CDPK

Examination of the carboxyl terminal region of the LIMP 2 sequence (Fig. 28) revealed a potential consensus phosphorylation sequence (hydrophobic-X-basic-X-X-ser) for CDPK, (Bachmann et al.1996; Harmon et al., 2000). To test whether LIMP 2 is phosphorylated by CDPK, the CI-14 peptide was tested as a substrate. This peptide, which contains the carboxyl terminal 13 amino acids of LIMP2, includes the region that comprises the CDPK phosphorylation site (**Fig. 28**). This peptide is the same that was used above for the generation of antibodies specific for LIMP2. A recombinant form of an *Arabidopsis* CDPK (KJM23-62H, Harper et al., 1994) was used for this study. CI-14 was readily phosphorylated by CDPK with an apparent K_m of 178 μM (**Fig. 29**). This value is comparable to that obtained for soybean nodulin 26 (Weaver et al., 1991). Thus similar to other characteristics, nodulin 26 and LIMP2 also share the ability to be phosphorylated by a calcium-dependent protein kinase on their carboxyl terminal regions.

Previous work by Chanmanivone (2000), using *Xenopus* oocytes has shown that phosphorylation of soybean nodulin 26 on serine 262 results in an enhanced P_f. Thus, LIMP2 and nodulin 26 are likely targets for regulation by calcium-dependent phosphorylation and phosphorylation may control the flux

A

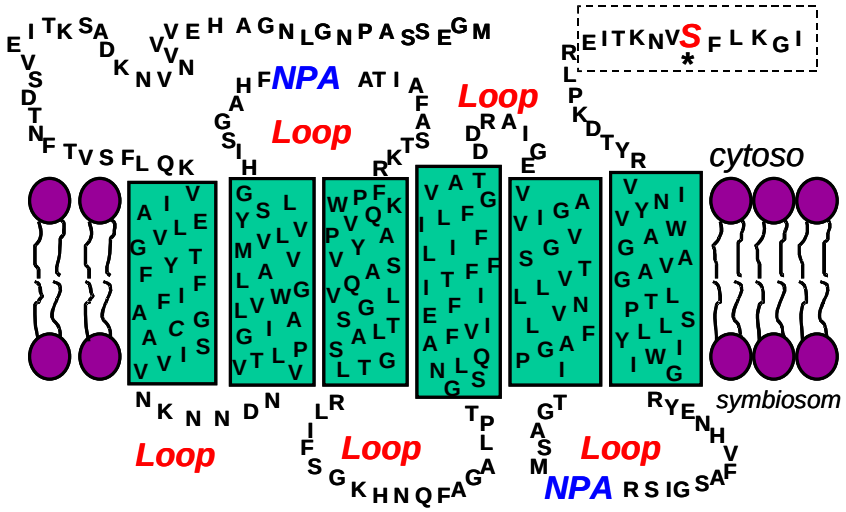

B

CI-14 C-R-E-I-T-K-N-V-S-F-L-K-G-I

GC12P C-E-I-T-K-N-V-S(PO4)-F-L-K-G

Figure 28. Synthetic peptide design for phosphorylation specific epitope recognition. **A**) Topology plot of LIMP2 showing the region in the carboxyl terminal end used for peptide generation (dashed box). **B**) Sequence of CI-14 and GC12P synthetic peptides.

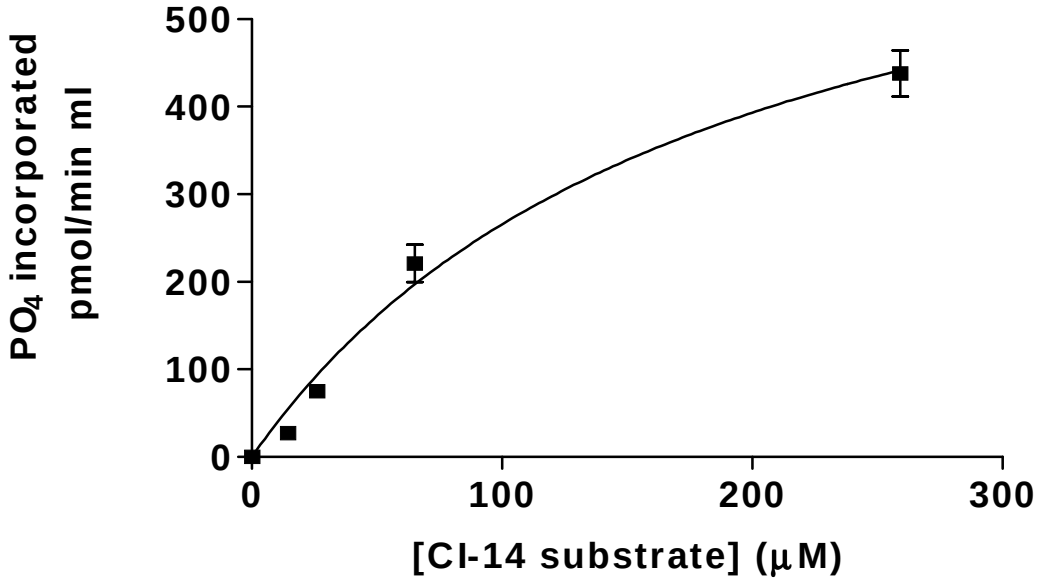

Figure 29. Phosphorylation of the CI-14 peptide of LIMP2. The ability of the LIMP2 synthetic peptide CI-14 to serve as a substrate for a recombinant calcium-dependent protein kinase (*Arabidopsis* CDPK KJM23-6H2, Harper et al. 1994) was tested. Each point is the average of duplicate determinations

of water and solutes through the channel. Generation of an antibody reactive to these MIP proteins which is capable of discriminating between phosphorylation would serve as a useful tool for the elucidation of specific physiological circumstances which modify the phosphorylation state of these proteins.

Generation of a phosphorylation-specific antibody against LIMP2/nodulin26

To prepare a site-specific antibody to probe the phosphorylation state of LIMP2 or nodulin 26, the synthetic peptide GC12P (**Fig. 28**) was synthesized with a phosphate group chemically introduced on the serine within the CDPK phosphorylation site. This peptide was used to elicit antibodies by the standard approaches described above. Initial experiments with antibodies generated to the LIMP2 peptide GC12P demonstrated a preferential reactivity with the phosphopeptide GC12P compared to the corresponding unphosphorylated peptide CI-14 (**Fig. 30**). However the antiserum was not completely specific and still contained antibodies that recognized both peptides (**Fig. 30**). Crossreacting antibodies that react with non-phosphorylated epitopes were removed by passing the GC12P sera over a resin on which the unphosphorylated CI-14 peptide was immobilized. The CI-14 adsorbed antiserum was then affinity purified on GC12P agarose. The treatment resulted in GC12P antibody preparation that showed essentially

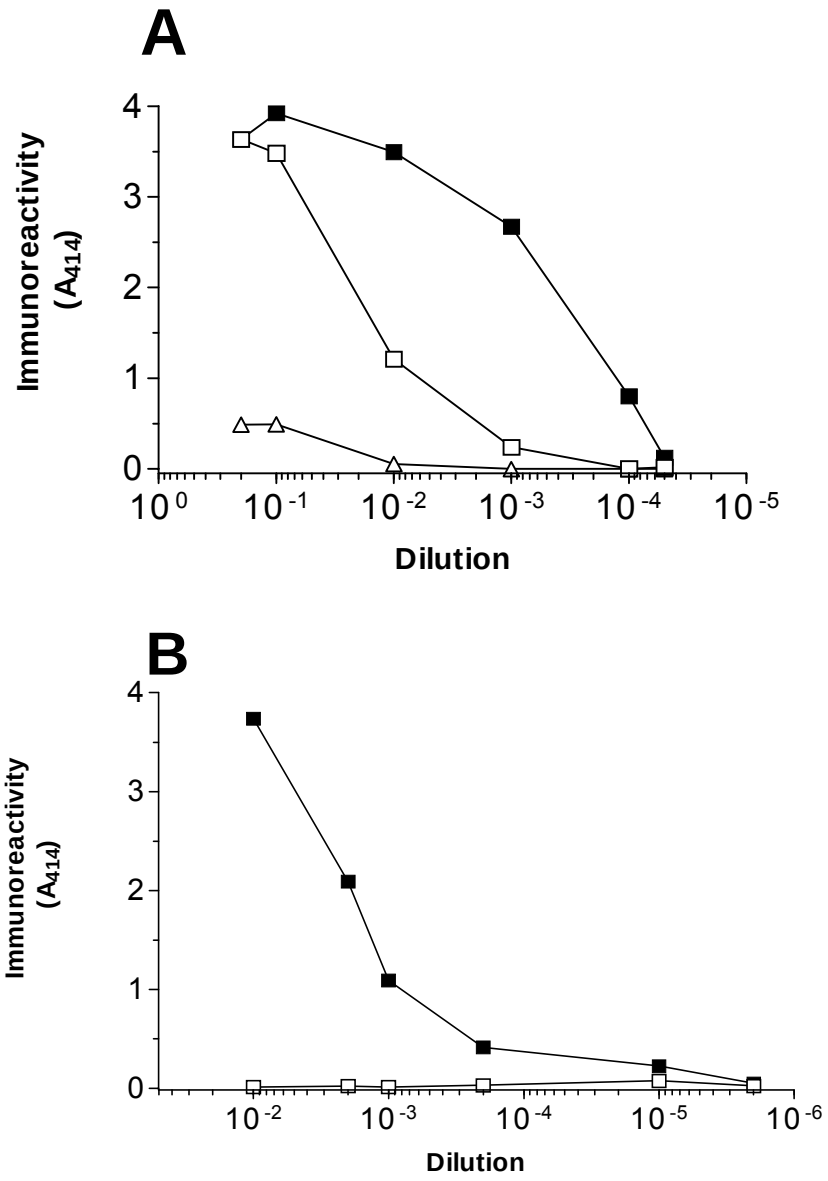

Figure 30. Selectivity of anti-GC-12P antibodies for phosphorylated and unphosphorylated peptides. The results of ELISA assay using either phosphopeptide (GC12P) or unphosphorylated peptide (CI-14) as antigen are shown. The relative immunoreactivity based on the absorbance of peroxidase assay products is plotted against antibody dilution. **A**) Anti-GC12P sera reaction against GC12P (■) and CI-14 (□), and preimmune sera reaction against GC12P(△). **B**) Reactivity of phosphorylation specific anti-GC12P antibodies isolated by affinity purification against GC12P (■) and CI-14 (□).

complete selectivity for the phosphorylated GC12P, and no detectable reaction with the unphosphorylated CI-14 peptide (**Fig. 30**).

To determine whether the anti-GC12P antibodies can distinguish between phosphorylated and unphosphorylated epitopes on the intact nodulin 26 protein, a series of tests were performed. As a negative control, recombinant his-tagged nodulin 26 (RecNodS) purified from *E. coli* was used. Since *E. coli* lacks an endogenous calcium-dependent protein kinase, RecNodS is produced in a nonphosphorylated state (Lee et al., 1995). Consistent with this, Western blot analysis of RecNodS shows no immunoreactivity with the anti-GC12P antibodies whereas immunoreactivity of this protein with antibodies against whole nodulin 26 was unaffected (**Fig. 31**). In contrast, nodulin 26 isolated from 28 day old soybean nodule symbiosomes showed high reactivity with both antibodies (**Fig. 32**). This result suggests that native nodulin 26 is populated by a species which is phosphorylated at ser 262 under normal isolation conditions, and that anti-GC12P antibodies react specifically with this species.

To test this hypothesis further, the effect of in vitro phosphorylation and dephosphorylation of nodulin 26 on immunoreactivity was tested (**Fig. 33**). Incubation of isolated symbiosome membranes with Ca^{2+} and ATP results in the phosphorylation of nodulin 26 by a symbiosome membrane-associated CDPK (**Fig. 33**). Western blot of these membranes shows a high reactivity with anti-nodulin 26 antibodies as well as with the phosphospecific anti-GC12P antibody (**Fig. 33**). Incubation of symbiosome membranes with

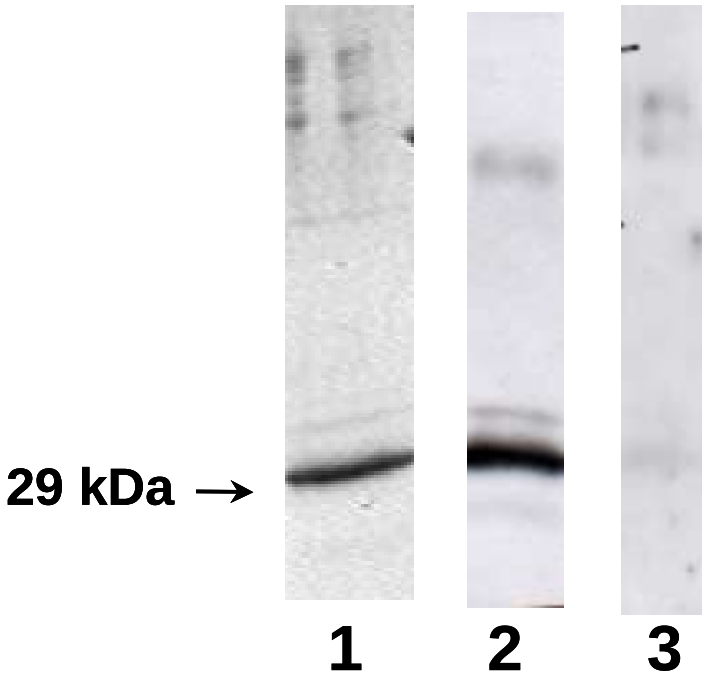

Figure 31. Western blot of recombinant nodulin 26 probed with the phosphorylation specific antibody. Nodulin 26 expressed and purified from *E. coli* (2.3 μg) was subjected to SDS-PAGE on 12.5%(w/v) polyacrylamide gels. **1**) Coomassie blue-stained gel of RecNodS, **2**) Western blot of RecNodS probed with antibodies raised against whole nodulin 26, **3**) Western blot of RecNodS probed with the affinity-purified anti-GC12P antibodies.

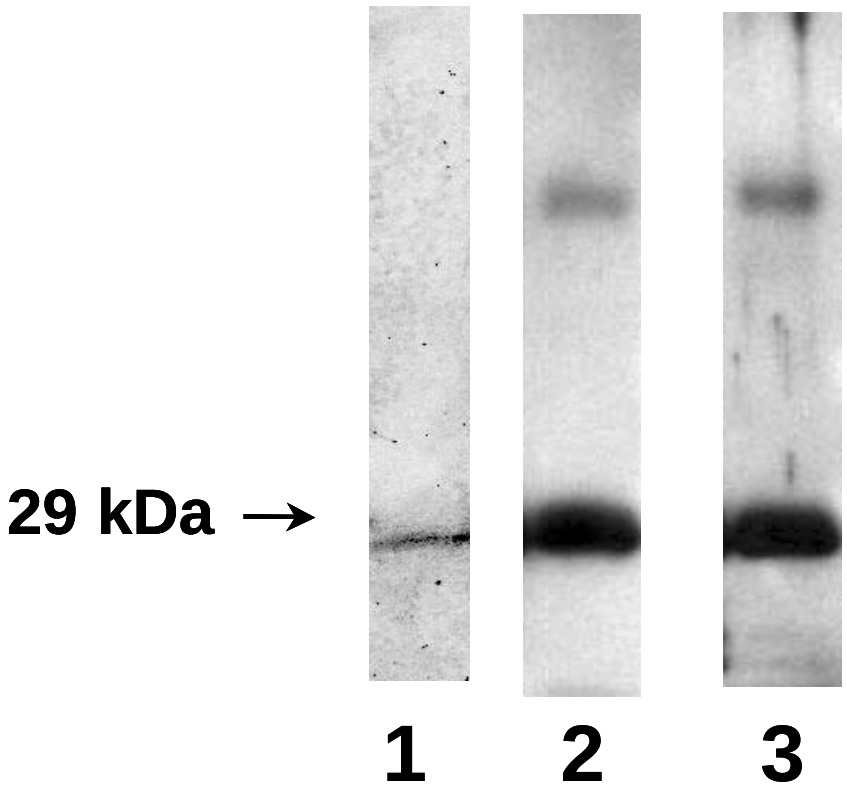

Figure 32. Western blot of native soybean nodule 26 probed with the phosphorylation-specific antibody. Native nodulin 26 was (1.25 μg) purified from soybean symbiosome membranes and was resolved by SDS-PAGE on 12.5% (w/v) polyacrylamide gels. **1**) Coomassie blue-stained gel of nodulin 26, **2**) Western blot of nodulin 26 probed with antibodies raised against whole nodulin 26, **3**) Western blot of nodulin 26 probed affinity-purified anti-GC12P antibodies.

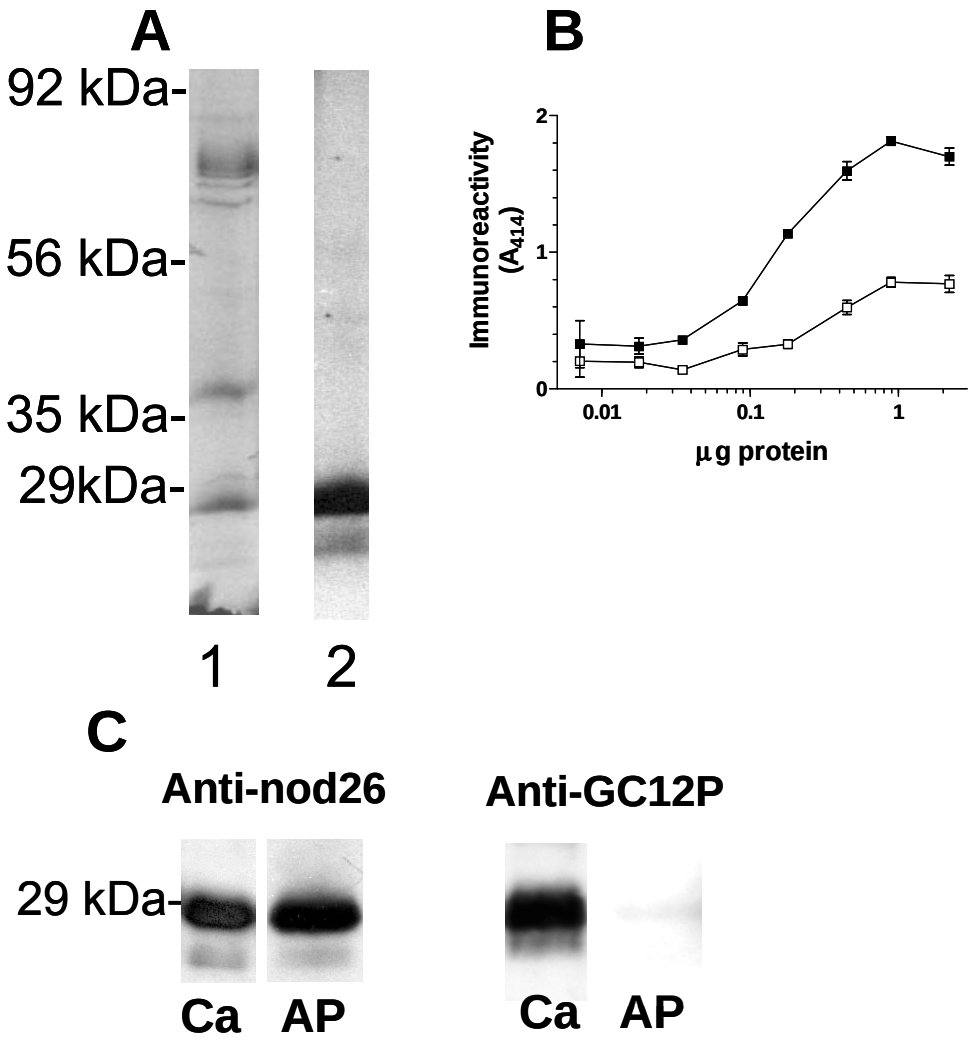

Figure 33. Changes in phosphorylation status of nodulin 26 monitored using the GC12P antibody. Panel A, Nodulin 26 was phosphorylated in situ by CDPK by incubation of soybean symbiosome membranes (4 µg) with 1 mM $CaCl_2$ and γ^{32}P-ATP and was resolved by SDS-PAGE as in Fig. 32. Lane 1) Coomassie blue-stained gel, lane 2) autoradiogram of the gel shown in lane 1. **Panel B**, isolated soybean symbiosome membranes were treated with either $CaCl_2$ and ATP (■), or with alkaline phosphatase (□) and were analyzed by ELISA assay using anti-GC12P antibodies. **Panel C**, Western blot analysis of soybean symbiosome nodulin 26 phosphorylated in situ by CDPK (Ca) or dephosphorylated by alkaline phosphatase treatment (AP). Anti-nod 26, Western blot with antibodies raised against whole nodulin 26; Anti-GC12P, Western blot with affinity purified antibodies raised against the phosphorylation epitope.

alkaline phosphatase, which has been shown to dephosphorylate nodulin 26 (Ou Yang et al., 1991), results in the loss of the Western blot signal with the anti-GC12P antibodies whereas the overall immunoreactivity with anti-nodulin 26 antibodies is not affected (**Fig. 33**).

Collectively, these results show that the anti-GC12P antibodies react with the phosphorylated epitope of native nodulin 26 in a highly specific manner. Further, the data shows that nodulin 26 isolated from soybean symbiosome membranes is phosphorylated on serine 262.

Immunological analysis of the phosphorylation state of nodulin 26 during nodule development

To assay the amount of nodulin 26 and its phosphorylation state in soybean nodules, a rapid procedure for obtaining nodule membranes was adopted. The method is a modification of the differential centrifugation protocol that is part of a two phase partitioning method for symbiosome membrane isolation (Christiansen et al., 1995), with several protease and protein phosphatase inhibitors included in the extraction buffers to preserve nodulin 26 integrity and its phosphorylation state. Further purification of symbiosome membranes can be done by two phase partitioning, but it was found that the 100,000 g membrane pellet obtained prior to phase partitioning gave indistinguishable results from those obtained by further fractionation. Thus, to allow the rapid purification and analysis of multiple nodule samples this method was used.

Western blot analysis of membrane samples from developmental series of soybean nodules using anti-nod26 and anti-GC12P antibodies reveal a pattern for expression and phosphorylation (**Fig. 34**). Consistent with its mRNA expression pattern (i.e., as a late nodulin, Fortin et al., 1987), nodulin 26 protein is not apparent until 16 days after planting and then accumulates to a maximal level in the mature nitrogen-fixing nodules (28 days after planting). Nodulin 26 is sustained at a high level throughout development, even in older flowering soybean plants (100 days after planting) in which nodule senescence is taking place. This argues that nodulin 26 production accompanies the formation of the symbiosome membrane and is an integral component of the symbiosome throughout the lifetime of the nodule.

The phosphorylation pattern of nodulin 26 appears to be different from the protein expression profile. Low levels of nodulin 26 are observed early in nodule development, but the maximal phosphorylation for this protein is not observed until 25 days post inoculation, at a time when nodules mature and are fully developed. Phosphorylation patterns then remain high until very late in development (post flowering) at which time they are virtually undetectable, even though high levels of nodulin 26 are still present.

Regulation of the phosphorylation state of nodulin 26 in response to osmotic stress

Since calcium signaling has been implicated in responses to environmental stress, and considering the high sensitivity of nodules to

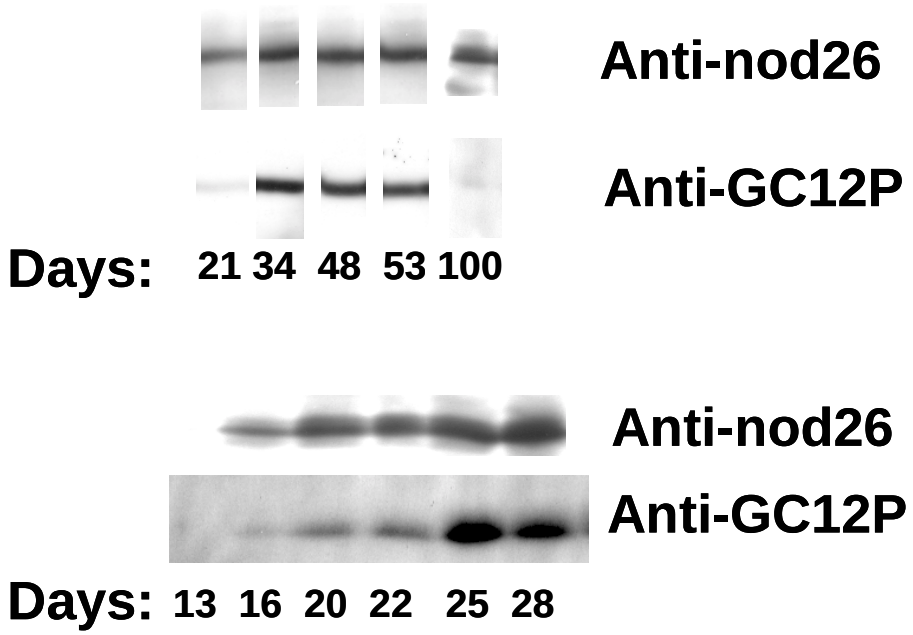

Figure 34. Developmental expression of nodulin 26 protein and determination of its phosphorylation status. Twenty μg samples of soybean nodule membranes were assayed by Western blot for nodulin 26 protein content (anti-nod26) and phosphorylation state (anti-GC12P). The top panel shows the blots from a wide developmental profile (21-100 days after planting). The bottom panel shows a separate experiment with a longer film exposure time focused on the crucial times for the onset of nodulin 26 protein production and the appearance of phosphorylation.

osmotic stress signals, and the fact that nodulin 26 is an aquaglyceroporin facilitating the transport of water and solutes, the effects of water stress on nodulin 26 phosphorylation and expression in mature nodules was addressed. Drought conditions result in little change in nodulin 26 protein levels in nodule membranes, but the level of phosphorylation of the protein increases 3-fold in drought stressed nodules (**Fig. 35**).

Similarly, exposure of 33-day old nodulated soybeans to conditions of high salinity results in little change in nodulin 26 protein levels whereas the levels of phosphorylation increase between 2 to 3 fold by 4 hr after treatment and remain at elevated levels 24 hr after the stimulus (**Fig. 36**). Interestingly, younger plants (<21 days) and older plants (100 days) that show low endogenous levels of phosphorylated nodulin 26 also lack the ability to respond to salinity stress (data not shown). Overall, the results show that phosphorylation of nodulin 26 by an endogenous CDPK is regulated both by the developmental state of the nodule, as well as in response to osmotic stress stimuli (drought or salinity).

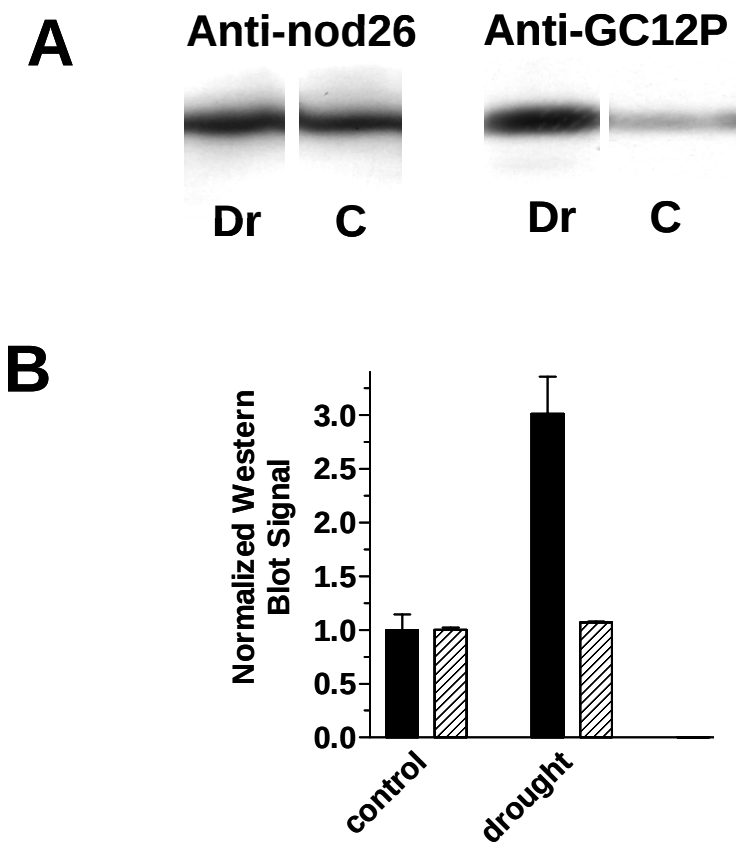

Figure 35. Nodulin 26 phosphorylation in response to drought stress. Membrane samples (20 μg/well) isolated from 48 day soybean nodules harvested from well watered control plants (**C**), or drought stressed plants (**Dr**). **A**) Western blot assay for nodulin 26 protein content (anti-nod26) and phosphorylation state (anti-GC12P). **B**) Densitometry comparison of the relative amounts of nodulin 26 protein (crosshatched bars), and the relative phosphorylation state of nodulin 26 (solid bars). Data was normalized to the average signal obtained for control plants. Error bars show standard error of the mean of three to five replicates.

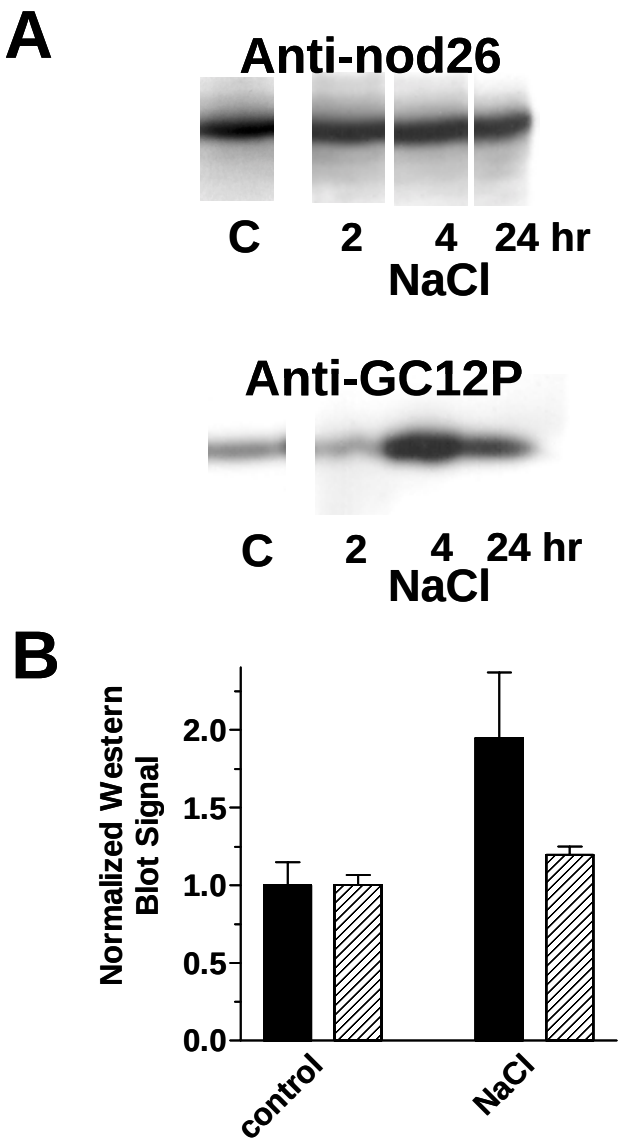

Figure 36. Salinity stress analysis of nodulin 26 levels and phosphorylation state. Symbiosome membranes prepared from nodules of 33 day old soybean plants from control plants (C), or from plants at 2,4,and 24 hr after watering with 0.3M NaCl. **A**) Western blots were probed with Anti-nod26 recognizing total nodulin 26 protein or Anti-GC12P reactive to the phosphorylation specific epitope**.** **B**) Densitometry comparison of the relative amounts of nodulin 26 protein crosshatched bars, and the relative phosphorylation state of nodulin 26. Data was normalized to the average signal obtained for control plants. Error bars show standard error of the mean of two to five replicates.

CHAPTER IV

DISCUSSION

Phylogeny of LIMP1 and LIMP2

The finding of large families of MIP proteins in plants has prompted reorganization of the categorizing system for these proteins culminating in the present model of four distinct phylogenetic branches of MIPs based predominately on the *Arabidopsis* genome sequencing project (*Arabidopsis* genome initiative, 2000; Johanson et al., 2001), and on large expressed sequence tag libraries of maize (Chaumont et al., 2001). Cloning techniques based on the sequence homology found between the signature NPA motifs has allowed the identification of large numbers of MIPs and MIP-like fragments from a broad range of tissues. By using this approach, two previously unknown MIP proteins were identified from mature nodules of the model determinant legume *Lotus japonicus.* These two MIP genes can be placed into two distinct branches of the plant MIP phylogeny based on amino acid sequence identity comparisons (**Fig. 37**).

LIMP1 branches into the plant TIP subclass of MIP proteins, and shows the highest homology to the soybean SPCP1 protein which was identified from a soybean nodule library (Miao and Verma, 1993). Both LIMP1 and SPCP1 show remarkable similarity to the well studied γTIP of *Arabidopsis* and may perform a role in nodule physiology which may be similar in nature to the function of *Arabidopsis* γTIP in vegetative tissues (discussed below).

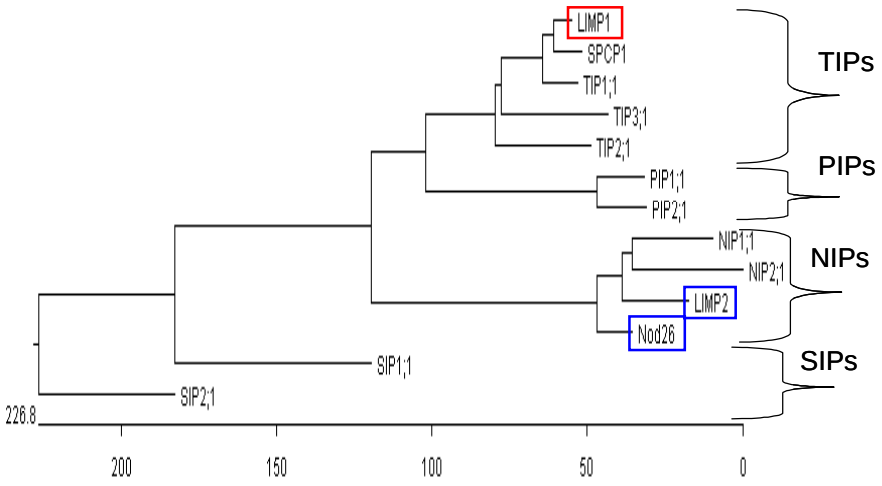

Figure 37. Phylogenetic alignment of selected plant MIP proteins. Sequence comparisons of representative *Arabidopsis* MIP proteins fall into four distinct classes, the TIPs, PIPs, NIPs, and SIPs. Based on amino acid sequence alignments, LIMP1 falls into the TIP branch (red box), while LIMP2, and nodulin 26 are sorted into the NIP subclass (blue boxes). nomenclature for *Arabidopsis* MIPs is from Johanson et al. (2001).

LIMP2 clusters with soybean nodulin 26 and these proteins can be placed into the NIP branch of the plant MIP superfamily (**Fig. 37**). The NIP family was named based on sequence identity to nodulin 26 and all family members show a general grouping with the nodulin 26 protein of soybean. Besides expression in legume nodules, members of the NIP family are also well represented in nonlegume species (Weig et al., 1997; Johanson et al., 2001; Chaumont et al., 2001). For example, of the 36 MIP genes found in *Arabidopsis*, ten encode proteins that cluster within the nodulin 26-like (NIP) subfamily with homology to soybean nodulin 26 ranging from 32 to 62%. Compared to the PIP and TIP subfamilies, the NIP proteins are generally expressed at lower levels in *Arabidopsis*. As yet the subcellular localization and biological functions of these proteins remains a mystery. However the finding of NIP proteins in tissues besides nodules suggest that they have a wider role in plant biology than just rhizobia-legume symbioses.

Sequence divergence between LIMP1 and LIMP2, and the fact that they group with different subfamilies within the plant MIP superfamily, argues that they perform different roles in nodule physiology. As discussed below, analysis of expression, subcellular localization, structure, and transport properties support the proposal that these two proteins have distinct biological roles.

Structure and function of LIMP1 and LIMP2 transport

Sequence comparisons of LIMP1 and LIMP2 argue separate functionalities for these proteins and data generated by heterologous expression in *Xenopus laevis* oocytes supports this hypothesis.

Functionally, LIMP2 shows transport properties highly similar to nodulin 26 (Rivers et al., 1997; Dean et al., 1999; Guenther and Roberts, 2000). Similar to nodulin 26, LIMP2 enhances the flux of water across oocyte plasma membranes several fold (**Fig. 38**). However the P_f of LIMP2 and nodulin 26 is several fold lower than mammalian AQP1 (**Fig. 38**). Thus, although nodulin 26 and LIMP2 are clearly water channels, they apparently show low intrinsic transport rates compared to other MIPs. Studies with nodulin 26 (Chanmanivone, 2000), and another low P_f MIP, AQP0 (Nemeth-Cahalan and Hall, 2000), show that their intrinsic transport rates can be enhanced by regulation by pH as well as by calcium and phosphorylation. Since our findings here show that LIMP2 is phosphorylated, its intrinsic transport properties might be controlled in a similar fashion. This is discussed further below.

In addition to their ability to flux water, both nodulin 26 and LIMP2 are multifunctional aquaglyceroporins that transport glycerol at a rate indistinguishable from the bacterial glyceroporin, GlpF. Recently, *Arabidopsis* NIP1;1 and NIP1;2 were also shown to be multifunctional, exhibiting glycerol transport properties upon expression in yeast (Weig and Jakob, 2000). These findings and our data with LIMP2 suggest that besides their sequence

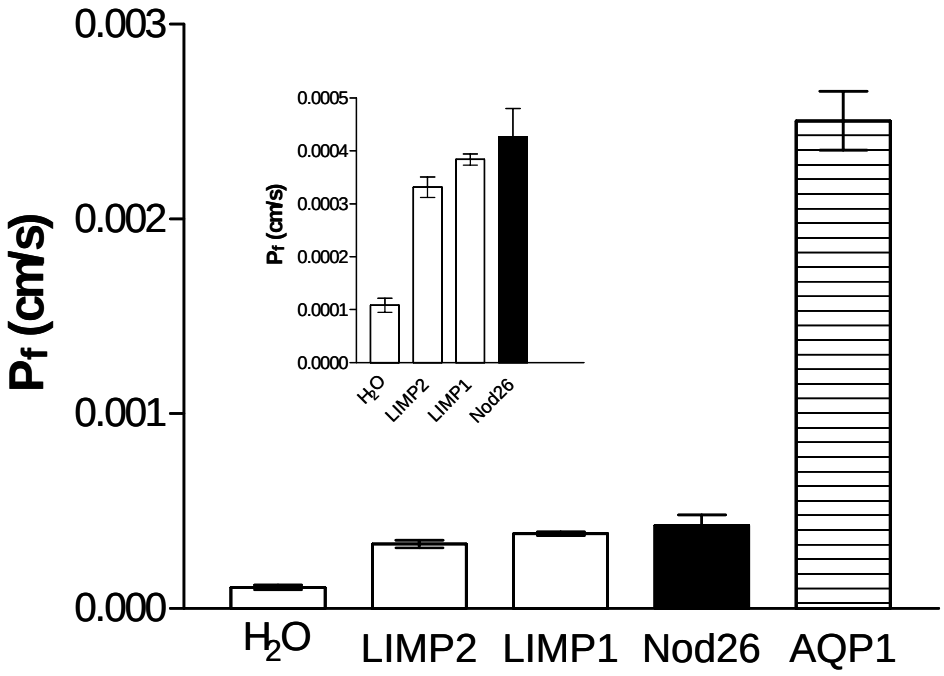

Figure 38. Comparison of osmotic water permeability of oocytes expressing MIP proteins. Oocytes were injected with cRNA for LIMP2, LIMP1, Nod26, AQP1 (46 ng) or water (46 nl), and were assayed for water permeability by using the oocyte swelling assay. Error bars indicate standard error of the mean, (n=5).

similarity and common phylogeny, the NIP subfamily may share similar functional properties as aquaglyceroporins as well.

LIMP1 exhibits aquaporin activity when expressed in *Xenopus* oocytes, but in contrast to nodulin 26 and LIMP2 it appears to be water specific, showing no tendency to flux glycerol. In this regard, LIMP1 is similar to many of the TIP family members characterized which also show water selective transport (Maurel et al., 1993; Maurel et al., 1995). Similar to nodulin 26 and LIMP2, LIMP1 shows a low P_f value compared to AQP1 based on oocyte assays (**Fig. 38**). While absolute differences in transport rate between these various MIPs will have to await the calculation of pf (single channel rate) for LIMP1 and LIMP2, the oocyte data strongly suggest that these proteins have an intrinsic water transport rate that is at the low end of the MIP family.

LIMP1 and LIMP2 possess the structural and functional hallmarks of the subfamilies which they represent: the TIP and NIP subfamilies respectively (Johanson et al., 2001). Questions concerning what structural factors are responsible for functional differences remain to be resolved. To address this molecular modeling analyses of LIMP1 and LIMP2 were conducted by using the two atomic resolution models for the water specific AQP1 (Sui et al., 2001), and the glycerol selective GlpF (Fu et al., 2000).

Before addressing determinants of selectivity in LIMP1 and LIMP2, the current state of functionality of AQP1 and GlpF needs to be revisited. These proteins represent two divergent functional classes of the MIP proteins, the glyceroporins and the aquaporins. However, the overall structural fold seems

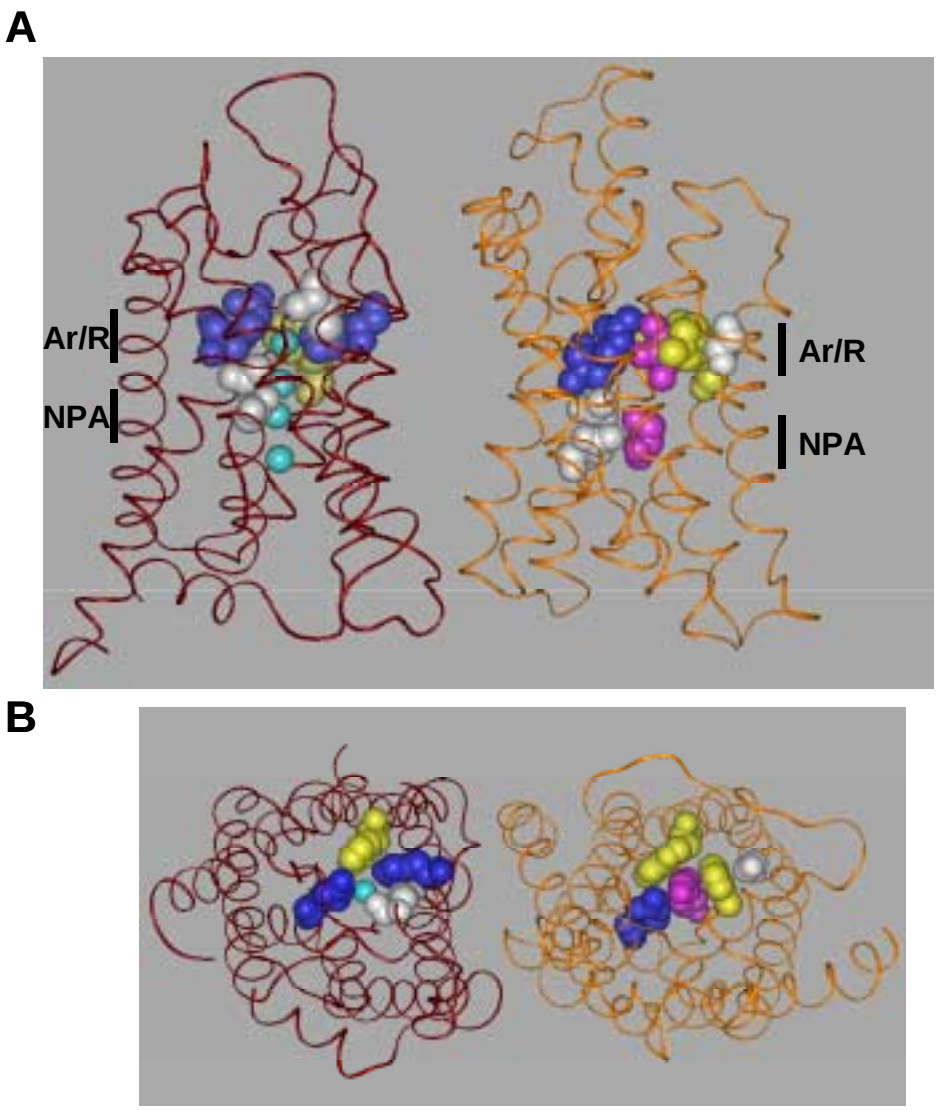

Figure 39. Ribbon diagram of AQP1 and GlpF showing bound substrates and key pore residues. Structures for AQP1 (left) and GlpF (right) were generated based on the published coordinates from the solved crystal structures of these proteins (Fu et al., 2000; Sui et al., 2001). **A)** Structures are viewed in the plane of the membrane, the four water molecules bound in the pore of AQP1 are show in in aqua, while NPA asparagines (bound to water 2 and 3) are shown in white. Basic residues of the aromatic/arginine region (ar/R) are shown in blue, hydrophobic side chains are yellow and hydrophilic side chains are in white. GlpF structure is labeled the same with two of the bound glycerols in the pore shown in magenta. **B)** Structures from the cytoplasmic face looking down through the pore. The four residues forming the narrow ar/R selectivity filter are shown bound to water (AQP1) or glycerol (GlpF).

to be conserved (**Fig. 39**). Both proteins form the general hour glass fold with wide cytoplasmic and extracellular vestibules that constrict to a narrow pore, 20Å in length. The physical size of the pore region at the narrowest point (2.8Å in AQP1, 3.7Å in GlpF) serves as a size selectivity filter to exclude large molecules such as hydrated ions. Amino acid side chains located down the length of the pore are remarkably hydrophobic with “nodes” of hydrophilic residues found that provide hydrogen bonding sites for the coordination of water and glycerol as they permeate the pore (Fu et al., 2000; Sui et al., 2001).

The key for the selectivity properties of GlpF and AQP1 is determined by the narrowest constriction of the pore that occurs near the extracellular vestibule of the channel (**Fig. 39**). This constriction is formed by the confluence of four key residues proposed to be the selectivity filter of the channel. These residues are contributed by conserved amino acids within helix 2, loop E, and helix 6 (**Fig. 40; Table 2**). A space filling model of these four residues with bound transport ligands is shown in **Figure 41**.

In GlpF, these positions are occupied by Trp 48 (helix 2), Phe 200 (loop E), and Arg 206 (loop E), Gly 191 (helix 5) (**Fig. 41**). Trp 48 and Phe 200 form a hydrophobic wedge that forms intimate van der Waals contacts with the carbon backbone of glycerol. Arginine 206 is found on the opposite side of the pore and provides hydrogen bonding stabilization and orientation to the hydroxyl groups 1 and 2 of glycerol, and thus proper orientation of the glycerol backbone within the cleft. Gly 191 is necessary for steric reasons as

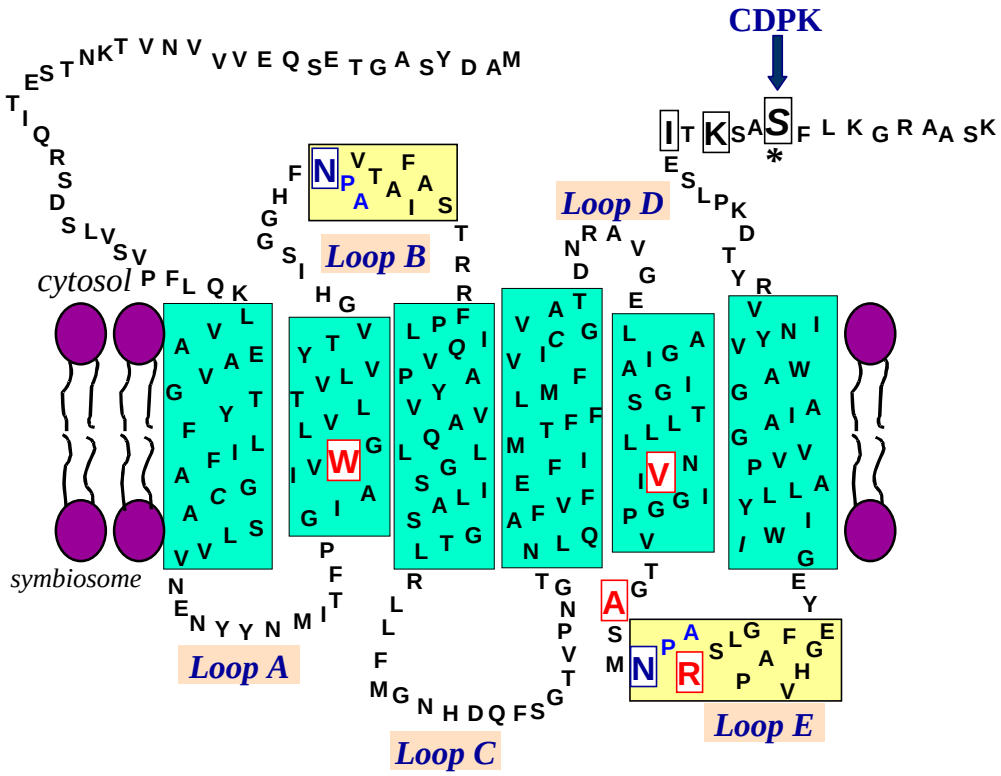

Figure 40. Topology of nodulin 26 showing key functional and regulatory residues. Residues forming the ar/R region are boxed in red. NPA helices are boxed in yellow, asparagine residues are boxed in blue. The consensus sequence for CDPK phosphorylation is boxed in black and the phosphorylated serine is marked with an asterisk.

Table 2: Comparison of ar/R regions and carboxyl terminal phosphorylation site of plant NIP and TIP proteins.

protein	Arabidopsis gene #	Helix 2[a]	Helix 5	Loop E		phos. site (COOH-term)
AQP consensus		F	H	A/C	R	-
Glyceroporin consensus		W	G	F	R	-
Nod 26		W	V	A	R	I-T-K-S-A-S-F-L-K
LIMP2		W	V	A	R	I-T-K-N-V-S-F-L-K-G-I
LIMP1		H	I	A	V	
SPCP1		H	I	A	V	
TIP1;1	2g36830	H	I	A	V	
NIP1:1	4g18030	W	V	A	R	I-T-K-S-G-S-F-L-K
NIP1;2	4g18910	W	V	A	R	I-T-K-S-G-S-F-L-K
NIP2;1	2g34390	W	V	A	R	F-S-K-T-G-S-S-H-K
NIP2;1-like	2g29870	-	V	A	R	F-S-K-T-G-S-S-H-K
NIP3;1	1g31880	W	I	A	R	none found
NIP4;1	5g37810	W	V	A	R	L-T-K-S-A-S-F-L-R
NIP4;2	5g37820	W	V	A	R	L-T-K-S-A-S-F-L-R
NIP5;1	4g10380	A	I	A	R	none found
NIP6;1	1g80760	A	I	A	R	none found
NIP7;1	3g06100	W	V	A	R	T-R-P-C-P-S-P-V-S-P-S

[a] The amino acids which form the ar/R region of LIMP1 and LIMP2/nodulin 26 were compared against the consensus for aquaporins, glyceroporins and members of the *Arabidopsis* NIP and TIP family. Colored residuses indicate: Red, glyceroporin-like; blue aquaporin like; black, no clear preference for either glyceroporin or aquaporin. The conserved carboxyl terminal sites for LIMP2/nodulin 26/NIP is shown, underlined residues are potential

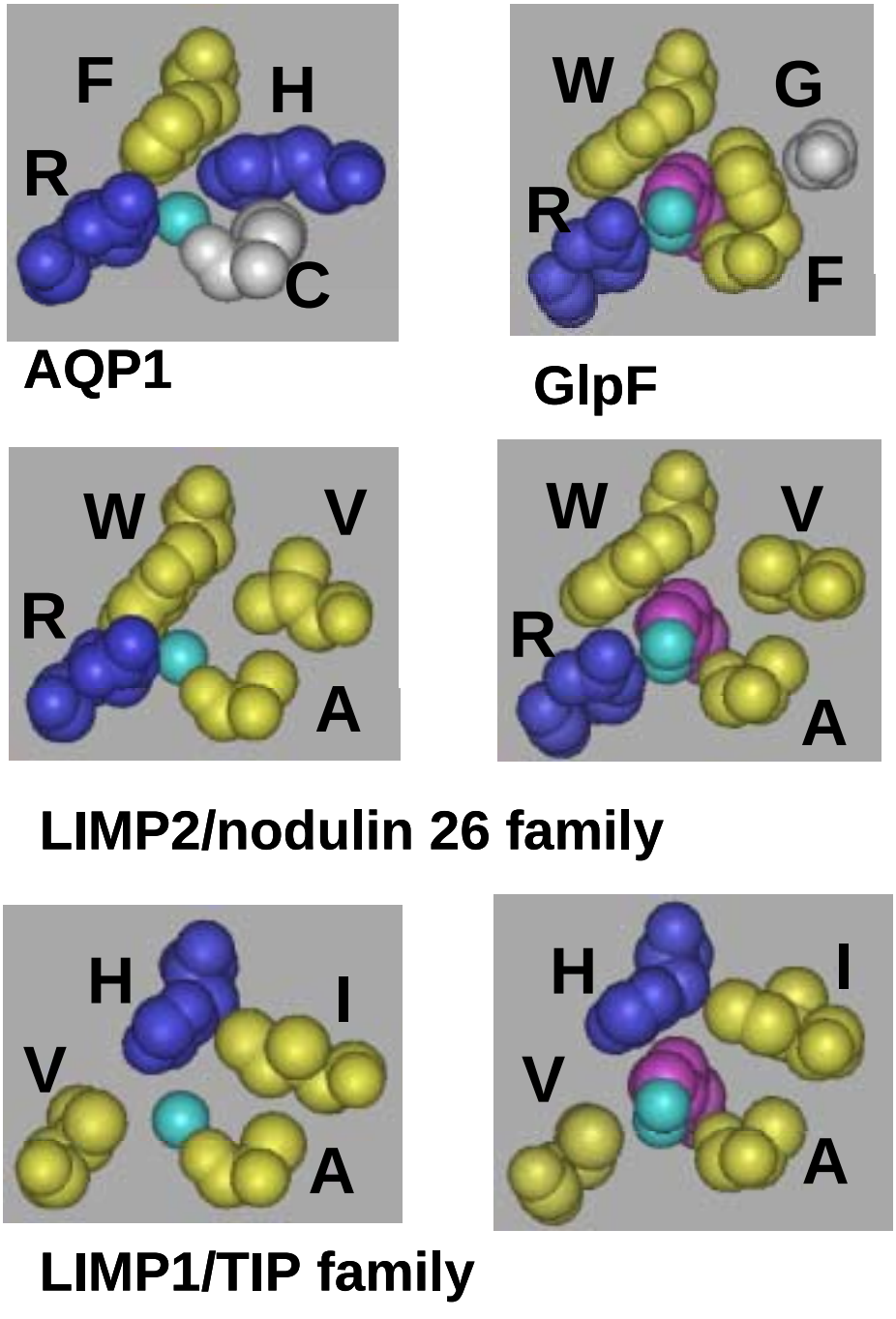

Figure 41. Modeling of the ar/R region of LIMP1 and LIMP2. Shown are space filling models of the side chains of the ar/R region shown in Figure 39. Water in the selectivity filter of AQP1 is show in in aqua, whereas glycerol is shown with carbon backbone in magenta and hydroxyl groups in aqua. Residues are colored as in Figure 39. For LIMP1 and LIMP2 side chain substitutions show divergence of residues forming the ar/R region.

discussed below. This proposed selectivity filter has been termed the "aromatic/arginine (ar/R)" region (Fu et al., 2000; de Groot et al., 2001). The crystal structure of AQP1 reveals that similar mechanics of physical exclusion and biochemical interactions account for the selectivity of this channel. The physical constraints of the AQP1 pore at the ar/R region (2.8 Å vs 3.7 Å for GlpF) are alone enough to account for the exclusion of glycerol. However, additional substitutions of key ar/R residues also contribute to selectivity. The two key residue substitutions that account for the rapid flux and specificity of AQP1 are His 182 and Cys 191 (**Fig. 41**) (Sui et al., 2001). Both residues form hydrogen bonds (Cys 191, peptide carbonyl; His 182, side chain) with the water ligand in the selectivity filter (**Fig. 41**). These residues change both the hydrophobicity, hydrogen bond potential, and geometry of the pore (**Fig. 41**). The third residue of the ar/R region of Glp F, Arg 206, is conserved in the structure of AQP1 and is proposed to serve a similar function as Cys 191 and His 182 in hydrogen bonding to water molecules within the channel (Sui et al., 2001).

To understand how these ar/R residues provide for rapid and selective water transport, one has to consider the energy cost of water transport through the pore (Fu et al., 2000; de Groot and Grubmuller, 2001; Sui et al., 2001). Based on the structure of AQP1, four water molecules are bound at 4 hydrophilic "nodes" within the channel vestibule and pore in an otherwise hydrophobic channel (**Fig. 39**). Since water is transported single file, the pore must provide hydrogen bond compensation to account for the energy cost of

breaking the hydration shell around each water molecule. The hydrogen bonds provided by Cys, Arg, and His provide this compensation at the selectivity filter. In addition, the bulky Phe 58, along with His 182, constrict the pore to the diameter of a water molecule (**Fig. 41**).

In GlpF, Cys191 is replaced by the bulky hydrophobic residue Phe 200 which interacts with the hydrophobic backbone of glycerol. Histidine is replaced by a glycine in GlpF providing a wider pore to accommodate glycerol (**Fig. 41**). The substitution of Cys 191 for a Phe and Phe 58 for a Trp results in a substantially greater hydrophobicity of the ar/R filter and could present an energetic barrier to water flow through this constriction (Fu et al., 2000). This could account for the extremely low water permeability of the GlpF channel despite the larger diameter of the pore.

Analysis of the phylogeny of aquaporins and aquaglyceroporins/glyceroporins shows a high degree of conservation of the ar/R signature residues (**Table 2**). Indeed, Sui et al. (2001) predicts that all water-selective aquaporins have a histidine at an equivalent site in helix 5 whereas glyceroporins possess a glycine at this site. Based on these observations, a model for the selectivity and transport properties of LIMP2/nodulin26/NIPs and LIMP1/TIPs can be made.

In the case of LIMP2, two residues (Trp in helix 2 and Arg in loop E) found in glyceroporins are conserved. These two key residues would provide the amphipathic pore for binding of the carbon backbone as well as the hydroxyls of glycerol. However, unlike GlpF, LIMP2 posesses an alanine

instead of a phenylalanine in loop E, which is more similar to the cysteine/alanine found in aquaporins. The presence of an unusual valine at the important helix 5 position, is a feature unique to the NIP subfamily, and likely aids in glycerol transport through the ar/R region. These substitutions are predicted to increase the pore aperture and hydrophobic qualities of the LIMP2/nodulin 26 ar/R region that could explain its transport properties (an aquaglyceroporin with a low intrinsic water transport rate). Comparison of LIMP2 and nodulin 26 and *Arabidopsis* NIPs show that they have conserved residues at the ar/R region (with the exception of NIP5;1 and 6;1), and thus are predicted to have conserved transport properties. In support of this we have recently found that LIMP2 with a Trp to His substitution retains the ability to transport water but is no longer permeable to glycerol (Wallace, Guenther and Roberts unpublished results).

Analysis of the proposed LIMP1 ar/R region was also intriguing. Nearly all MIP family members possess the conserved arginine (NPA<u>R</u>) in loop E that forms part of the ar/R tetrad. However, this residue is substituted by a valine in the LIMP1/TIP subfamily (**Table 2**). In addition to this, the LIMP1/TIP subfamily displays two unorthodox residue substitutions not found in other MIPs: His for Phe/Trp in helix 2, and Ile for Gly/His in helix 5. Modeling these substitutions on the GlpF and AQP1 structures shows an ar/R region that is more non polar than other water-selective aquaporins with none of the water bonding residues conserved. These properties could account for the low P_f of LIMP1 compared to AQP1. Additionally, the substitution of

histidine within helix 2 as well as the loss of arginine in loop E would explain the inability to interact with glycerol ligands (**Fig. 41**). Clearly the TIP/LIMP1 pore is different from existing aquaporin and glyceroporin models. Preliminary structural analysis of αTIP by electro-cryo crystallography (Daniels et al., 1999) at a resolution of 7.7 Å suggests that the TIPs show the same general tetrameric structure of other MIPs with the same general fold and topology. However analysis of the LIMP1/TIP structure at atomic resolution is necessary to elucidate how these unusual substitutions change the pore architecture and function.

Biological function of nodule MIP proteins

The finding of two MIP proteins with discrete expression patterns, functional properties and subcellular localization in legume nodules suggest that these transport proteins have distinct functions in the nodule. In the case of LIMP2, several observations suggest that this protein is the soybean nodulin 26 ortholog of *Lotus japonicus*. First, LIMP2 exhibits higher homology to soybean nodulin 26 then to any other MIP sequence, and shows nodule-specific expression, suggesting it is a bona fide nodulin. Second, Western blot analysis of isolated *L japonicus* symbiosome membranes shows that LIMP 2 is localized to this membrane. Third, similar to nodulin 26, LIMP2 is phosphorylated on the exact same serine residue within the carboxyl-terminal domain by a calcium-dependent protein kinase. The functional significance of this observation is discussed further below.

The function that LIMP 2/nodulin 26 plays in the nitrogen fixing symbiosis remains an open question. Previous studies with soybean nodulin 26 show that despite its low intrinsic P_f, this protein is responsible for the high permeability of the symbiosome membrane to water (50-fold higher than bare bilayers), and uncharged solutes (Rivers et al. 1997; Dean et al. 1999). Since the symbiosome is the major organelle of the infected cell (**Fig. 6**), nodulin 26 may play an osmoregulatory function, mediating the rapid, reversible uptake and release of water from the symbiosome space to control cytosolic and infected cell volume homeostasis similar to the proposed role of vacuolar water channels (**Fig. 42**) (reviewed in Tyerman et al., 1999). Control of cell shape and volume could also affect intracellular O_2 gradients and nitrogen fixation rates. For example, the infected cell is much larger (30 μm) than most plant cells (5-10 μm) and it has been proposed that the shape and geometry of the infected cells affects O_2 diffusion from the oxygen-rich cell periphery to the symbiosomes located in the cell interior which is the rate limiting step for nitrogen fixation (Thumfort et al., 1994). In addition, an added complexity of the symbiosome is the control of the osmolarity of the symbiosome space, which may be critical for the nitrogen-fixing bacteroid (Gresshoff and Rolfe, 1978). Also, nodules have been found to be highly sensitive to osmotic stresses (drought and salinity) and accumulate osmoprotectant molecules such as proline (Hu et al., 1992). Control of water flux through symbiosome nodulin 26/LIMP2 may be crucial for nodule

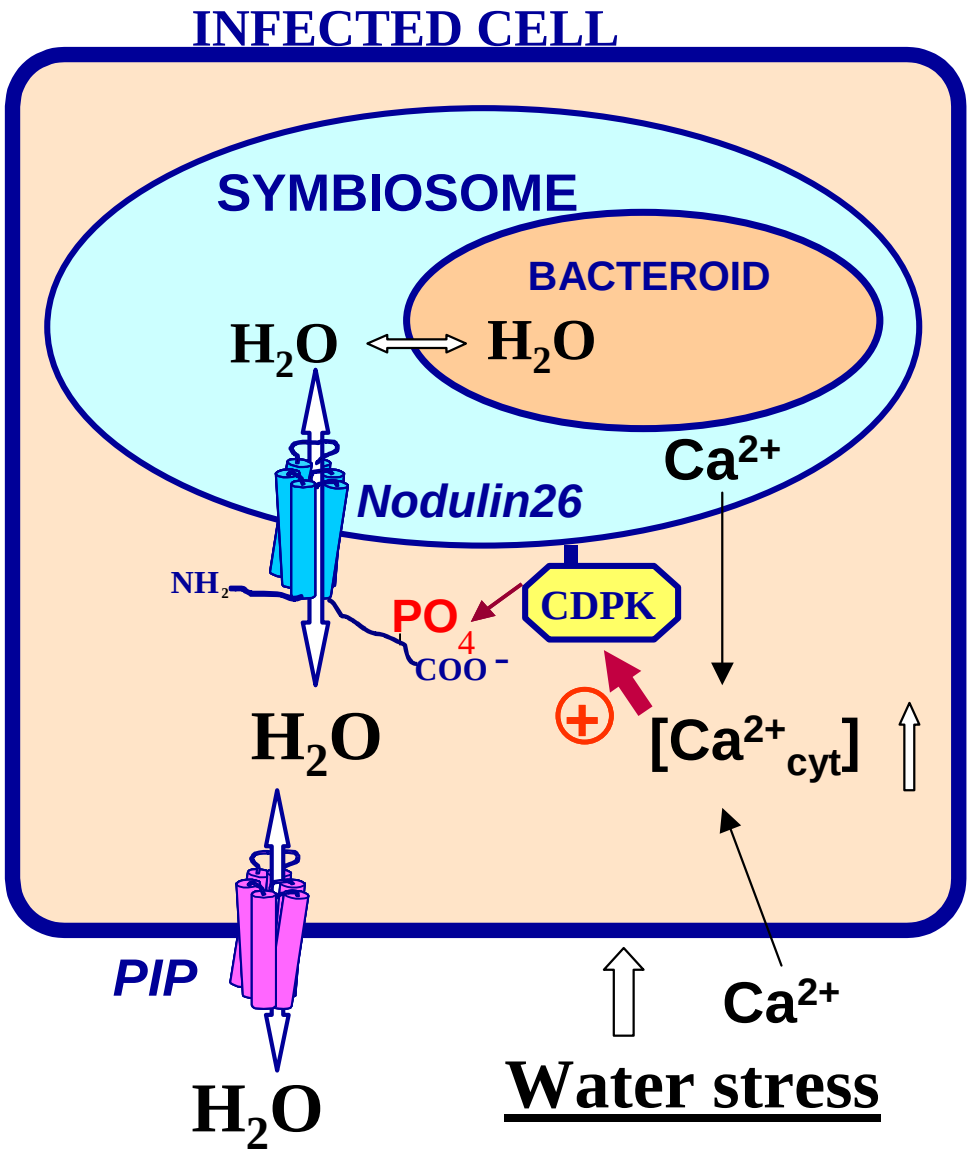

Figure 42. Model for water channel involvement in maintaining infected cell osmotic homeostasis. Modulation of channel activity of nodulin 26 through Ca^{2+} activation of a symbiosome membrane-associated CDPK may be coordinated with the transport activity of other MIP proteins such as plasma membrane PIPs in order to maintain the overall osmotic balance of the infected cell cytosol, the symbiosome space and the enclosed bacteroid.

osmoregulation under these conditions. This is discussed further below.

The potential role of nodulin 26/LIMP 2 becomes even more complex when one considers the added function of solute transport. Based on genetic analyses, roles in mediating glycerol uptake and/or release for metabolic purposes (Sweet et al. 1990; Truniger and Boos, 1993) have been proposed for bacterial glyceroporins. Similarly, mammalian aquaglyceroporins also are thought to be involved in the metabolic shuttling of glycerol (Borgnia et al., 1999). Since the principal carbon metabolite transported and utilized in soybean symbiosomes is malate (Udvardi and Day, 1997), it is not clear what metabolic function that symbiosome membrane transport of glycerol might play. As opposed to a metabolic role, other glycerol transport MIPs such as the yeast Fps1 protein (Luyten et al., 1995; Philips and Herskowitz, 1997) are osmoregulators that compartmentalize or release glycerol from the cell to adapt to changing media osmolarity. Some plants also accumulate glycerol as an osmoprotectant during osmotic and temperature stresses (Goldstein and Noble 1991; Cowan et al., 1992). Whether nodulin 26/LIMP2 has a role in the transport or compartmentalization of glycerol or other osmolytes remains unknown.

In addition, recent evidence suggests that MIP proteins can enhance the permeability of membranes to gases (e.g., CO_2, Nakhoul et al., 1998; Prasad et al., 1998), and it is possible that nodulin 26/LIMP2 aid in the exchange of gases such as CO_2, O_2 and NH_3 across the symbiosome membrane. NH_3 transport is particularly intriguing since the geometry of this

solute is similar to water, and the export fixed nitrogen in the form of NH_3/NH_4^+ across the symbiosome to the cytosol for assimilation is essential to the symbiosis (Day et al., 2001). By using stopped flow methods, Niemietz and Tyerman, (2000) demonstrated a Hg-sensitive facilitated transport in isolated symbiosome membrane vesicles. Whether LIMP2/nodulin 26 is responsible for this flux remains to be addressed.

LIMP1 represents a second major aquaporin expressed in *L. japonicus* that likely plays a role distinct from LIMP2. Besides being a water-specific aquaporin, LIMP1 shows a different expression pattern, showing high mRNA expression in both nodules as well as roots. Analysis with LIMP1-specific antibodies show that its protein expression is detectable in both root and nodule tissues although its levels appear to be much higher in root tissues. Since LIMP1 was not found on isolated symbiosome membranes, it likely is localized to a different cellular/subcellular compartment in nodules. LIMP1 is similar in sequence and its expression patterns to SPCP1 (Miao and Verma 1993), a MIP that may serve a similar function in soybean. While the functional properties of SPCP1 are unknown, Miao and Verma (1993) showed expression of the SPCP1 transcript in all vegetative tissues with the highest amount of expression found in the root elongation zone. This is similar to γTIP, which is transiently expressed at high levels in elongating tissues (Ludevid et al., 1992; Balk and de Boer, 1999; Barrieu et al., 1998; Karlson et al., 2000). In elongating cells, growth is driven by turgor-induced expansion and the high expresson of TIP proteins in these cells may reflect the high

permeability needed for vacuolar water uptake to drive expansion (for review see Johanson et al., 2000).

Although the function of LIMP1 in nodules remains to be established, a role for water transport, perhaps mediated by aquaporins, has been suggested in the regulation of the oxygen diffusion barrier found in nodules (Denison and Kinraide 1995; Serraj et al. 1998). The control of oxygen diffusion and pO_2 within the nodule cortex is critical for the regulation of the rate of nitrogen fixation and is modulated in response to numerous environmental conditions (Hunt and Layzell 1993). The cells of the inner cortex of nodules are proposed to constitute the O_2 diffusion barrier, and are postulated to regulate gas diffusion by reversible uptake and release of water resulting in changes in cell volume and shape that restrict gas flow through the intercellular spaces in accordance with the osmoelectrical model (Denison and Kinraide, 1995). In this model, changes in the activity of a plasma membrane proton pump would modulate an anion (Cl^-) channel altering the membrane potential which in turn would change electrochemical gradient for K^+. A directional flow of ions would result in the generation of an osmotic gradient that would drive water either into or out of the cell depending on the directionality of the ion fluxes. This would cause cell shrinkage or swelling and modulating the gas permeability across the inner cortex (Denison and Kinraide, 1995). Interestingly, nodule permeability to O_2 has been strongly implicated as the mechanism by which the plant can regulate the overall nitrogen fixation process (Hunt and Layzell, 1993), and cell volume changes

may be a mechanism for the overall control of the nitrogen fixation process. Recently, high levels of MIP in these inner cortical cells has been proposed based immunostaining of soybean nodules with antibodies raised against radish γTIP (Serraj et al. 1998). One possibility is that LIMP1 or TIP proteins play a role in enhancing the water permeability of vacuoles in cortical cells to allow regulation of gas diffusion by altering the cell and interstitial space volume.

To gain insight into the multiple potential biological roles of LIMP1 and LIMP2 it is necessary to develop an approach to perturb their expression and investigate the resulting phenotype. Aquaporin null mutations obtained either by pathological states or gene knockout have been invaluable in revealing the role of mammalian, yeast, and bacterial MIP proteins (Agre, 1998). Cases where this approach are successful in plants are rarer. By using antisense techniques Kaldenhoff et al. (1998) successfully showed the importance of PIP1b and 1a in regulating the P_f of root cell plasma membranes, and phenotypes of abnormal root mass (5x wildtype) resulted. In another case, the involvement of a plant MIP in the self-incompatibility response (rejection of self-related pollen) was shown in a recessive *Brassica* mutant (Ikeda et al., 1997). Our approaches using antisense with transgenic *Lotus* plants were largely unsuccessful presumably because the constructs had a modest effect on LIMP1 and LIMP2 expression. Recently, plasmids for the production of large amounts of double stranded RNAi (which triggers post transcriptional gene silencing) have been developed which are more effective suppresser of

mRNA expression in *Lotus* nodules (Kapranov et al., 2001). Hopefully, by using this modified approach, more successful suppression of LIMP1 and LIMP2 expression might be obtained.

Regulation of nodule MIP proteins

Analysis of the LIMP1 transcripts in nodules show that they vary during the diurnal light dark cycle with levels decreasing during the dark period. In this regard, LIMP1 is similar to another *Lotus japonicus* MIP, a PIP ortholog of *Arabidopsis* PIP1 which shows a similar pattern of diurnal variation (Clarkson et al., 2000; Henzler et al., 1999). This variation in expression is correlated with a decrease in the hydraulic conductivity (L_p) of *Lotus* roots at night time hours, perhaps reflecting a decreased need for transcellular water flow that is normally associated with transpiration during the light cycle. Clarkson et al. (2000), also noted that root L_p was very sensitive to metabolic deprivation (low nitrate, phosphate, or sulfate). Since nodule gas permeabilities and nitrogen fixation rates are sensitive to numerous metabolic signals (Vessey et al., 1988; Sung et al., 1991) it will be interesting to determine whether these nutrient conditions affect LIMP1 expression in roots or nodules.

A common feature of LIMP2 and other members of the nodulin 26 subfamily is the presence of a conserved phosphorylation motif for calcium-dependent protein kinases: hydrophobic-X-basic-X-X-ser/thr within the hydrophilic carboxyl terminal region of the protein (**Table 2**). Previous work shows that soybean nodulin 26 is the major substrate of a CDPK that is co-localized to the symbiosome membrane (Weaver et al.,1991) and that

phosphorylation occurs on the serine within this conserved motif (Weaver and Roberts, 1992). Several animal and plant MIP proteins are phosphorylated by various protein kinases. Reports of the effects of phosphorylation on MIP transport activity are varied, including the stimulation of activity (Kuwahara et al. 1995; Maurel et al. 1995; Johansson et al. 1998), the inhibition of activity (Han et al. 1998), and modulation of membrane targeting (Fushimi et al.1997). The conservation of this CDPK phosphorylation site among nodulin 26 subfamily members suggest that regulation by calcium-dependent phosphorylation may be another shared characteristic. In the case of soybean nodulin 26, previous oocyte expression studies shows that reagents that stimulate phosphorylation of serine 262 (eg., TPA and okadaic acid) also enhance P_f 2-3 fold. In addition it was found that reduction in pH has a similar affect on the water permeability of nodulin 26 (increasing P_f). These observations suggest that symbiosome water and solute permeability might be subject to dual control, by calcium signaling through phosphorylation of nodulin 26, as well as by pH, possibly via the H^+-ATPase that resides in the symbiosome membrane (Udvardi and Day, 1989). Since LIMP2 shows similar functional properties and is phosphorylated on the same serine residue, it is likely that this protein is subject to the same regulation.

Interestingly, nodulin 26 was among the first endogenous substrates demonstrated for CDPK (Weaver et al., 1991). This multifunctional calcium dependent protein kinase is now recognized to phosphorylate multiple protein

targets including membrane channels, pumps and a number of metabolic enzymes (Harmon et al., 2000).

Early metabolic labeling studies with ^{32}P-phosphate showed that nodulin 26 is phosphorylated in vivo (Weaver et al., 1991). However, these studies required the detachment of symbiosome membrane nodules to obtain adequate labeling of the phosphate pool. Detachment of nodules is itself a drastic environmental stress that causes significant disruption of nodule physiology (Sung et al., 1991) and the nature of developmental and environmental signals that regulate nodulin 26 phosphorylation has remained obscure. In this study this technical problem was circumvented by generating a specific antibody probe selective for phosphorylation of serine 262 of nodulin 26. By using this probe the phosphorylation state of native nodulin 26 was assessed.

The first finding shows that nodulin 26 is phosphorylated in response to its developmental state. Nodulin 26 expression is first detected at 15 days after planting. However, phosphorylation of the protein lags behind this step, with levels rising on day 25. Analysis of nodules during this period shows that at day 15 a clear differentiation of the infected zone surrounded by defined inner and outer cortical cells is apparent (Galetovic, Guenther and Roberts, unpublished). However, electron micrographs show that infected cells have few symbiosomes with single bacteroids at these early stages. Thus, nodulin 26 protein appears early in infected cell development prior to the burst of membrane biogenesis that accompanies symbiosome formation (Verma and

Hong, 1996). Phosphorylation however, does not become apparent until the time when mature infected cells (**Fig. 6**) are developed with multiple symbiosomes. At late stages, after flowering, at a time when nodules are reported to be entering the senescence phase, the level of phosphorylation decreases substantially even though the protein level of nodulin 26 changes little. The results argue that in normal mature nitrogen-fixing root nodules a steady state population of nodulin 26 is phosphorylated by CDPK. Whether symbiosome membrane CDPK is developmentally regulated as well needs to be investigated further. If phosphorylation regulates the rate of water or solute flux as we propose (Chanmanivone, 2000), then within wild type nodules this would serve to attenuate the rate of flux in response to the osmoregulatory, and metabolic needs of the nodule (**Fig. 42**)

Interestingly, two environmental signals apparently upregulate nodulin 26 phosphorylation state further: drought and salinity. Previous work with soybean nodules show that nodule physiology is exquisitely sensitive to these environmental cues which trigger a rapid cessation of nitrogen fixation by affecting gas diffusion (O_2) through the nodule inner cortex. (Diaz del Castillo et al., 1994; Serraj and Sinclair, 1996). Since phosphorylation of nodulin 26 enhances water permeability, phosphorylation might be part of the adaptive response to these stresses, altering the water permeability of the symbiosome membrane, perhaps in coordinate regulation with the accumulation of osmolytes to aid in osmoregulation and stress adaptation (**Fig. 42**).

Calcium signaling is known to be involved in mediating plant responses to osmotic stress (Knight et al., 1997), and CDPKs have been shown to be involved in salt and osmotic stress adaptation (Urao et al., 1994; Sheen, 1996; Saijo et al., 2000). Furthermore, as discussed in the introduction section, numerous MIP proteins are subject to regulation by osmotic signaling. In the case of one plant MIP, spinach PM28A, phosphorylation is modulated by changing water potential resulting in attenuation of plasma membrane P_f in response to water deficit (Johansson et al., 1998). The present work provides evidence for an osmoregulatory role for LIMP2/nodulin 26 and suggests that this protein plays a role in stress adaptation in the infected cell of the nodule.

LIST OF REFERENCES

Agre, P. (1997). Molecular physiology of water transport: aquaporin nomenclature workshop. Mammalian aquaporins. *Biol Cell* **89,** 255-7.

Agre, P. (1998). Aquaporin null phenotypes: the importance of classical physiology. *Proc Natl Acad Sci U S A* **95,** 9061-3.

Agre, P., Bonhivers, M. and Borgnia, M. J. (1998). The aquaporins, blueprints for cellular plumbing systems. *J Biol Chem* **273,** 14659-62.

Agre, P., Lee, M. D., Devidas, S. and Guggino, W. B. (1997). Aquaporins and ion conductance. *Science* **275,** 1490; discussion 1492.

Agre, P., Saboori, A. M., Asimos, A. and Smith, B. L. (1987). Purification and partial characterization of the Mr 30,000 integral membrane protein associated with the erythrocyte Rh(D) antigen. *J Biol Chem* **262,** 17497-503.

Aguilar, J. M. M., Ashby, A. M., Richards, A. J. M., Loake, G. J., Watson, M. D., and Shaw, C. H. (1988). Chemotaxis of *Rhizobium leguminosarum* biovar *phaseoli* towardars flavonoid inducers of the symbiotic nodulation genes. *J Gen Microbiol* **134,** 2741-46.

Ausubel, F. M., Brent, R., Kingston, R. E., Moore, D.D., Seidman, J. G., Sith, J. A., and Struhl, K. eds. (1987). Current protocols in molecular biology. Greene Pub. Associates and Wiley-Interscience: J. Wiley, New York.

Bachmann, M., Shiraishi, N., Campbell, W. H., Yoo. B. C., Harmon, A. C., and Huber, S. C. (1996). Identification of Ser-543 as the major regulatory phosphorylation site in spinach leaf nitrate reductase. *Plant Cell* **8,** 505-17.

Bai, L., Fushimi, K., Sasaki, S. and Marumo, F. (1996). Structure of aquaporin-2 vasopressin water channel. *J Biol Chem* **271,** 5171-6.

Balk, P. A., and de Boer, A. D. (1999). Rapid stalk elongation in tulip (*Tulipa gesneriana* L. cv. Apeldoorn) and the combined action of cold-induced invertase and the water-channel protein gammaTIP. *Planta* **209,** 346-54.

Barkla, B. J., Vera-Estrella, R., Pantoja, O., Kirch, H. H. and Bohnert, H. J. (1999). Aquaporin localization - how valid are the TIP and PIP labels? *Trends Plant Sci* **4,** 86-8.

Barrieu, F., Chaumont, F. and Chrispeels, M. J. (1998). High expression of the tonoplast aquaporin ZmTIP1 in epidermal and conducting tissues of maize. *Plant Physiol* **117,** 1153-63.

Barrieu, F., Marty-Mazars, D., Thomas, D., Chaumont, F., Charbonnier, M. and Marty, F. (1999). Desiccation and osmotic stress increase the abundance of mRNA of the tonoplast aquaporin BobTIP26-1 in cauliflower cells. *Planta* **209,** 77-86.

Berry, V., Francis, P., Kaushal, S., Moore, A., and Bhattacharya, S. (2000). Missense mutations in MIP underlie autosomal dominant 'polymorphic' and lamellar cataracts linked to 12q. *Nature Genet* **25**, 15-7.

Biela, A., Grote, K., Otto, B., Hoth, S., Hedrich, R. and Kaldenhoff, R. (1999). The *Nicotiana tabacum* plasma membrane aquaporin NtAQP1 is mercury- insensitive and permeable for glycerol. *Plant J* **18,** 565-70.

Borgnia, M., Nielsen, S., Engel, A. and Agre, P. (1999). Cellular and molecular biology of the aquaporin water channels. *Annu Rev Biochem* **68,** 425-58.

Borgnia, M. J. and Agre, P. (2001). Reconstitution and functional comparison of purified GlpF and AqpZ, the glycerol and water channels from Escherichia coli. *Proc Natl Acad Sci U S A* **98,** 2888-93.

Calamita, G., Bishai, W. R., Preston, G. M., Guggino, W. B. and Agre, P. (1995a). Molecular cloning and characterization of AqpZ, a water channel from Escherichia coli. *J Biol Chem* **270,** 29063-6.

Calamita, G., Mola, M. G., Gounon, P., Jouve, M., Bourguet, J. and Svelto, M. (1995b). Aquaporin-CHIP-related protein in frog urinary bladder: localization by confocal microscopy. *J Membr Biol* **143,** 267-71.

Carbrey, J. M., Cormack, B. P. and Agre, P. (2001). Aquaporin in *Candida*: characterization of a functional water channel protein. *Yeast* **18,** 1391-6.

Chandy, G., Zampighi, G. A., Kreman, M. and Hall, J. E. (1997). Comparison of the water transporting properties of MIP and AQP1. *J Membr Biol* **159,** 29-39.

Chanmanivone, N. (2000). The Nodulin 26 Aquaglyceroporin Transporter: Influence of Transmembrane Mutations, pH, Calcium, and Phosphorylation. Masters Thesis, University of Tennessee, Knoxville.

Chaumont, F., Barrieu, F., Jung, R. and Chrispeels, M. J. (2000). Plasma membrane intrinsic proteins from maize cluster in two sequence subgroups with differential aquaporin activity. *Plant Physiol* **122,** 1025-34.

Chirgwin, J. M., Przybyla, A. E., MacDonald RJ., and Rutter, W. J. (1979). Isolation of biologically active ribonucleic acid from sources enriched in ribonuclease. *Biochemistry* **18,** 5294-5299.

Chaumont, F., Barrieu, F., Wojcik, E., Chrispeels, M. J., and Jung, R. (2001). Aquaporins constitute a large and highly divergent protein family in maize. *Plant Physiol* **125,** 1206-15.

Chollet, R., Vidal, J., and O'Leary, M.H. (1996). Phosphoenolpyruvate carboylase: A ubiquitous,highly regulated enzyme in plants. *Annu Rev Plant Physio Plant Mol Biol* **47,** 273-98.

Christiansen, J. H., Rosendahl, L., and Widel, l. S. (1995). Preparation and characterization of sealed inside-out peribacteroid membrane vesicles from *Pisum sativum* L. and *Glycine max* L root nodules by aqueous polymer two-phase partitioning. *Journal of Plant Physiology* **147,** 175-81.

Clarkson, D. T., Carvajal, M., Henzler, T., Waterhouse, R. N., Smyth, A. J., Cooke, D. T. and Steudle, E. (2000). Root hydraulic conductance: diurnal aquaporin expression and the effects of nutrient stress. *J Exp Bot* **51,** 61-70.

Cowan, A. K., Rose, P, D., and Horne, L. G., (1992). *Dunaliella salina* A model system for studying the response of plant cells to stress. *J Exp Bot* **43**, 1535-47.

Daniels, M. J., Chrispeels, M. J. and Yeager, M. (1999). Projection structure of a plant vacuole membrane aquaporin by electron cryo-crystallography. *J Mol Biol* **294,** 1337-49.

Day, D. A., and Copeland, L. (1991). Carbon metabolism and compart-mentation in nitrogen fixing legumes nodules. *Plant Physiol. Bio-chem.* **29,**185-201.

Day, D. A., Poole, P. S., Tyerman, S. D. and Rosendahl, L. (2001). Ammonia and amino acid transport across symbiotic membranes in nitrogen-fixing legume nodules. *Cell Mol Life Sci* **58,** 61-71.

Deamer, D. W., Mahon, E. H., and Bosco, G. (1994). Self-assembly and function of primitive membrane structures. Early life on earth. Nobel Symposium No. 84, ed. by S. Bengtson (Columbia University Press, New York, 1994).

de Groot, B. L., Engel, A. and Grubmuller, H. (2001). A refined structure of human aquaporin-1. *FEBS Lett* **504,** 206-11.

de Groot, B. L. and Grubmuller, H. (2001). Water permeation across biological membranes: mechanism and dynamics of aquaporin-1 and GlpF. *Science* **294,** 2353-7.

de Groot, B. L., Heymann, J. B., Engel, A., Mitsuoka, K., Fujiyoshi, Y. and Grubmuller, H. (2000). The fold of human aquaporin 1. *J Mol Biol* **300,** 987-94.

Dean, R. M., Rivers, R. L., Zeidel, M. L., and Roberts, D. M. (1999). Purification and functional reconstitution of soybean nodulin 26. An aquaporin with water and glycerol transport properties. *Biochemistry* **38,** 347-353.

Deen, P. M., Verdijk, M. A., Knoers, N. V., Wieringa, B., Monnens, L. A., van Os, C. H. and van Oost, B. A. (1994). Requirement of human renal water channel aquaporin-2 for vasopressin- dependent concentration of urine. *Science* **264,** 92-5.

Denison, R. F., and Kinraide, T. B. (1995). Oxygen-induced membrane depolarizations in legume root nodules. Possible evidence for an osmoelectrical mechanism controlling nodule gas permeability. *Plant Physiol* **208**: 235-40.

Diaz del Castillo, L., Hunt, S., and Layzell, D. B. (1994). The role of oxygen in the regulation of nitrogenase activity in drought-stressed soybean nodules. *Plant Physiology*. **106,** 949-55.

Dix, J. A. and Solomon, A. K. (1984). Role of membrane proteins and lipids in water diffusion across red cell membranes. *Biochim Biophys Acta* **773,** 219-30.

Dixit, R., Rizzo, C., Nasrallah, M., and Nasrallah, J. (2001). The brassica MIP-MOD gene encodes a functional water channel that is expressed in the stigma epidermis. *Plant Mol Biol* **45,** 51-62.

Dordas, C., Chrispeels, M. J., and Brown, P. H. (2000). Permeability and channel-mediated transport of boric acid across membrane vesicles isolated from squash roots. *Plant Physiol* **124,** 1349-62.

Ehring, G. R., Zampighi, G., Horwitz, J., Bok, D. and Hall, J. E. (1990). Properties of channels reconstituted from the major intrinsic protein of lens fiber membranes. *J Gen Physiol* **96,** 631-64.

Ellman, G. L. (1959). Tissue sulfhydryl groups. *Arch Biochem Biophys* **82**, 70-7.

Engelke, T., Jagadish, M. N., and Puhler, A. (1987). Biochemical and genetical analysis of *Rhizobium meliloti* mutants defective in C_4 -dicarboxylate transport. *J Gen Microbiol* **133,** 3019-29.

Finkelstein, A. (1987) *Water Movement Through Lipid Bilayers, Pores and Plasma Membranes, Theory and Reality*. Wiley and Sons, New York.

Fischer, H. M. (1994). Genetic regulation of nitrogen fixation in rhizobia. *Microbiol Rev* **58,** 352-86.

Fortin, M. G., Morrison, N. A. and Verma, D. P. (1987). Nodulin-26, a peribacteroid membrane nodulin is expressed independently of the development of the peribacteroid compartment. *Nucleic Acids Res* **15,** 813-24.

Fortin, M. G., Zelechowska, M., and Verma, D. P. S. (1985). Specific targeting of membrane nodulins to the bacteroid-enclosing compartment in soybean nodules. *EMBO J* **4,** 3041-6.

Franssen, H. J., Vijn, I., Yang, W. C., and Bisseling, T. (1992). Developmental aspects of the *Rhizobium*-legume symbiosis. *Plant Mol. Biol*.**19,** 89-107.

Froger, A., Tallur, B., Thomas, D. and Delamarche, C. (1998). Prediction of functional residues in water channels and related proteins. *Protein Sci* **7,** 1458-68.

Fu, D., Libson, A., Miercke, L. J., Weitzman, C., Nollert, P., Krucinski, J. and Stroud, R. M. (2000). Structure of a glycerol-conducting channel and the basis for its selectivity. *Science* **290,** 481-6.

Fushimi, K., Sasaki, S., and Marumo, F. (1997). Phosphorylation of serine 256 is required for cAMP-dependent regulatory exocytosis of the aquaporin-2 water channel. *J Biol Chem* **272,** 14800-4.

Gamborg, O. (1970). The effects of amino acids and ammonium on the growth of plant cells in suspension culture. *Plant Physiol* **45,** 372-5.

Garcia, F., Kierbel, A., Larocca, M. C., Gradilone, S. A., Splinter, P., LaRusso, N. F., and Marinelli, R. A. (2001). The water channel aquaporin-8 is mainly intracellular in rat hepatocytes, and its plasma membrane insertion is stimulated by cyclic AMP. *J Biol Chem* **276,** 12147-52.

Gerbeau, P., Guclu, J., Ripoche, P., and Maurel, C. (1999). Aquaporin Nt-TIPa can account for the high permeability of tobacco cell vacuolar membrane to small neutral solutes. *Plant J* **18,** 577-87.

Gietz, R. D., and Sugino, A. (1988). New yeast-*Escherichia coli* shuttle vectors constructed with in vitro mutagenized yeast genes lacking six-base pair restriction sites. *Gene* **74,** 527-34.

Goldstein, G., and Nobel, P. S. (1991). Changes in osmotic pressure and mucilage during low temperature accimation of *Opuntia ficus*. *Plant Physiol*. **97**, 954-61.

Gooden, M. M., Takemoto, L. J. and Rintoul, D. A. (1985). Reconstitution of MIP26 from single human lenses into artificial membranes. I. Differences in pH sensitivity of cataractous vs. normal human lens fiber cell proteins. *Curr Eye Res* **4,** 1107-15.

Gresshoff, P. M., and Rolfe, B. G. (1978). Viability of Rhizobium japonicum bacteroids isolated from soybean nodules*. Planta* **142**, 329-34.

Guenther, J. F. and Roberts, D. M. (2000). Water-selective and multifunctional aquaporins from *Lotus japonicus* nodules. *Planta* **210,** 741-8.

Han, Z., Wax, M. B. and Patil, R. V. (1998). Regulation of aquaporin-4 water channels by phorbol ester-dependent protein phosphorylation. *J Biol Chem* **273,** 6001-4.

Harlow, E., and Lane, D. (1988) Antibodies, A Laboratory manual. Cold Spring Harbor Laboratory Press, Cold Spring Harbor, N.Y.

Hamann, S., Zeuthen, T., La Cour, M., Nagelhus, E. A., Ottersen, O. P., Agre, P. and Nielsen, S. (1998). Aquaporins in complex tissues: distribution of aquaporins 1-5 in human and rat eye. *Am J Physiol* **274,** C1332-45.

Harmer, S. L., Hogenesch, J. B., Straume, M., Chang, H. S., Han, B., Zhu, T., Wang, X., Kreps, J. A. and Kay, S. A. (2000). Orchestrated transcription of key pathways in Arabidopsis by the circadian clock. *Science* **290,** 2110-3.

Harmon, A. C., Yoo, B. C. and McCaffery, C. (1994). Pseudosubstrate inhibition of CDPK, a protein kinase with a calmodulin- like domain. *Biochemistry* **33,** 7278-87.

Harmon, A. C., Gribskov, M., and Harper, J. M., (2000). CDPKs: A kinase for every Ca^{2+} signal. *Trends Plant Sci*. **5,** 154-9.

Handberg, K., and Stougaard, J. (1992). *Lotus japonicus*, an autogamous, diploid legume species for classical and molecular genetics. *Plant J* **2**, 487-96.

Harper, J. F., Huang, J. F. and Lloyd, S. J. (1994). Genetic identification of an autoinhibitor in CDPK, a protein kinase with a calmodulin-like domain. *Biochemistry* **33,** 7267-77.

Harvengt, P., Vlerick, A., Fuks, B., Wattiez, R., Ruysschaert, J. M. and Homble, F. (2000). Lentil seed aquaporins form a hetero-oligomer which is phosphorylated by a Mg(2+)-dependent and Ca(2+)-regulated kinase. *Biochem J* **352,** 183-90.

Heller, K. B., Lin, E. C. and Wilson, T. H. (1980). Substrate specificity and transport properties of the glycerol facilitator of *Escherichia coli*. *J Bacteriol* **144,** 274-8.

Henzler, T., Waterhouse, R. N., Smyth, A. J., Carvajal, M., Cooke, D. T., Schaffner, A. R., Steudle, E. and Clarkson, D. T. (1999). Diurnal variations in hydraulic conductivity and root pressure can be correlated with the expression of putative aquaporins in the roots of *Lotus japonicus*. *Planta* **210,** 50-60.

Höfte, H., Hubbard, L., Reizer, J., Ludevid, D., Herman, E. M., and Chrispeels, M. J. (1992). Vegetative and seed forms of the tonoplast intrinsic protein in the vacuolar membrane of *Arabidopsis thaliana*. *Plant Physiol* **99**, 561-70.

Hozawa, S., Holtzman, E. J., and Ausiello, D. A. (1996). cAMP motifs regulating transcription in the aquaporin 2 gene. *Am J Physiol* **270,** C1695-702.

Hu, C. A., Delauney, A. J., and Verma, D. P. (1992). A bifunctional enzyme (delta 1-pyrroline-5-carboxylate synthetase) catalyzes the first two steps in proline biosynthesis in plants. *Proc Natl Acad Sci U S A* **89,** 9354-8.

Hill, E. A., (1995). Osmotic flow in Membrane Pores. *Int Rev Cytol* **163,** 1-41.

Hunt ,S., and Layzell, D.B. (1993). Gas exchange of legume nodules and the regulation of nitrogenase activity. *Annu Rev Plant Physiol Plant Mol Biol* **44,** 483-511.

Ikeda, S., Nasrallah, J. B., Dixit, R., Preiss, S. and Nasrallah, M. E. (1997). An aquaporin-like gene required for the *Brassica* self-incompatibility response. *Science* **276,** 1564-6.

Jauh, G. Y., Phillips, T. E. and Rogers, J. C. (1999). Tonoplast intrinsic protein isoforms as markers for vacuolar functions. *Plant Cell* **11,** 1867-82.

Jensen, M. O., Tajkhorshid, E. and Schulten, K. (2001). The mechanism of glycerol conduction in aquaglyceroporins. *Structure (Camb)* **9,** 1083-93.

Johanson, U., Karlsson, M., Johansson, I., Gustavsson, S., Sjovall, S., Fraysse, L., Weig, A. R. and Kjellbom, P. (2001). The complete set of genes encoding major intrinsic proteins in Arabidopsis provides a framework for a new nomenclature for major intrinsic proteins in plants. *Plant Physiol* **126,** 1358-69.

Johansson, I., Karlsson, M., Johanson, U., Larsson, C. and Kjellbom, P. (2000). The role of aquaporins in cellular and whole plant water balance. *Biochim Biophys Acta* **1465,** 324-42.

Johansson, I., Karlsson, M., Shukla, V. K., Chrispeels, M. J., Larsson, C. and Kjellbom, P. (1998). Water transport activity of the plasma membrane aquaporin PM28A is regulated by phosphorylation. *Plant Cell* **10,** 451-9.

Johansson, I., Larsson, C., Ek, B. and Kjellbom, P. (1996). The major integral proteins of spinach leaf plasma membranes are putative aquaporins and are phosphorylated in response to Ca2+ and apoplastic water potential. *Plant Cell* **8,** 1181-91.

Johnson, K. D., Höfte, H., and Chrispeels, M. J. (1990). An intrinsic tonoplast protein of protein storage vacuoles in seeds is structurally related to a bacterial solute transporter (GIpF). *Plant Cell* **2,** 525-32.

Johnson, K. D., and Chrispeels, M. J. (1992). Tonoplast-bound protein kinase phosphorylates tonoplst intrinsic protein. *Plant Physiol* **100**, 1787-95.

Jung, J. S., Preston, G. M., Smith, B. L., Guggino, W. B., and Agre, P. (1994). Molecular structure of the water channel through aquaporin CHIP. The hourglass model. *J Biol Chem* **269,** 14648-54.

Kaldenhoff, R., Grote, K., Zhu, J. J., and Zimmermann, U. (1998). Significance of plasmalemma aquaporins for water-transport in *Arabidopsis thaliana*. *Plant J* **14,** 121-8.

Kaldenhoff, R., Kolling, A., and Richter, G. (1996). Regulation of the *Arabidopsis thaliana* aquaporin gene AthH2 (PIP1b). *J Photochem Photobiol B* **36,** 351-4.

Kammerloher, W., Fischer, U., Piechottka, G. P., and Schaffner, A. R. (1994). Water channels in the plant plasma membrane cloned by immunoselection from a mammalian expression system. *Plant J* **6,** 187-99.

Kapranov, P., Routt, S. M., Bankaitis, V. A., de Bruijn, F. J., and Szczyglowski, K. (2001). Nodule-specific regulation of phosphatidylinositol transfer protein expression in *Lotus japonicus*. *Plant Cell* **13,** 1369-82.

Karlsson, M., Johansson, I., Bush, M., McCann, M. C., Maurel, C., Larsson, C., and Kjellbom, P. (2000). An abundant TIP expressed in mature highly vacuolated cells. *Plant J* **21,** 83-90.

Kuwahara, M., Fushimi, K., Terada, Y., Bai, L., Marumo, F., and Sasaki, S. (1995). cAMP-dependent phosphorylation stimulates water permeability of aquaporin-collecting duct water channel protein expressed in *Xenopus* oocytes. *J Biol Chem* **270,** 10384-7.

King, L. S. and Agre, P. (1996). Pathophysiology of the aquaporin water channels. *Annu Rev Physiol* **58,** 619-48.

Kijne, W. J. (1992). Physiology of Nitrogen-fixing legume nodules: compartments and functions. In *Biological Nitrogen Fixation*,

G. Stacey, R. H. Burris, H. J. Evans, eds. Chapman and Hall, New York. pp 349-98

Kirch, H. H., Vera-Estrella, R., Golldack, D., Quigley, F., Michalowski, C. B., Barkla, B. J. and Bohnert, H. J. (2000). Expression of water channel proteins in Mesembryanthemum crystallinum. *Plant Physiol* **123,** 111-24.

Knight, H., Trewavas, A. J. and Knight, M. R. (1997). Calcium signalling in Arabidopsis thaliana responding to drought and salinity. *Plant J* **12,** 1067-78.

Kyte, J., and Doolittle, R.F. (1982). A simple method for displaying the hydropathic character of a protein. *J Mol Biol* **157,**105-32.

Lazo, G. R., Stein, P. A., and Ludwig, R. A. (1991). A DNA transformation-competent Arabidopsis genomic library in Agrobacterium. *Biotechnology* **9,** 963-7.

Laemmli, U.K. (1970). Cleavage of structural proteins during the assembly of the head of bacteriophage T4. *Nature* **227,** 680-5.

Lee, J. W., Zhang, Y., Weaver, C. D., Shomer, N. H., Louis, C. F., and Roberts, D. M. (1995). Phosphorylation of nodulin 26 on serine 262 affects its voltage- sensitive channel activity in planar lipid bilayers. *J Biol Chem* **270,** 27051-7.

Legocki, R. P., and Verma, D. P. (1980). Identification of "nodule-specific" host proteins (nodulins) involved in the development of rhizobium-legume symbiosis. *Cell* **20,** 153-63.

Li, J., Patil, R. V., and Verkman, A. S. (2002). Mildly abnormal retinal function in transgenic mice without Muller cell aquaporin-4 water channels. *Invest Ophthalmol Vis Sci* **43,** 573-9.

Louis, C. F., Hogan, P., Visco, L., and Strasburg, G. (1990). Identity of the calmodulin-binding proteins in bovine lens plasma membranes. *Exp Eye Res* **50,** 495-503.

Ludevid, D., Höfte, H., Himelblau, E., and Chrispeels, M.J. (1992). The expression pattern of the tonoplast intrinsic protein γ-TIP in *Arabidopsis thaliana* is correlated with cell enlargment, *Plant Physiol*. **100**, 1633-39.

Luyten, K., Albertyn, J., Skibbe, W. F., Prior, B. A., Ramos, J., Thevelein, J. M., and Hohmann, S. (1995). Fps1, a yeast member of the MIP family

of channel proteins, is a facilitator for glycerol uptake and efflux and is inactive under osmotic stress. *EMBO J* **14,** 1360-71.

Macey, R. I. (1984). Transport of water and urea in red blood cells. *Am J Physiol* **246,** C195-203.

Marinelli, R. A., Tietz, P. S., Pham, L. D., Rueckert, L., Agre, P., and LaRusso, N. F. (1999). Secretin induces the apical insertion of aquaporin-1 water channels in rat cholangiocytes. *Am J Physiol* **276,** G280-6.

Marin-Olivier, M., Chevalier, T., Fobis-Loisy, I., Dumas, C., and Gaude, T. (2000). Aquaporin PIP genes are not expressed in the stigma papillae in *Brassica oleracea*. *Plant J* **24,** 231-40.

Mathai, J. C., Mori, S., Smith, B. L., Preston, G. M., Mohandas, N., Collins, M., van Zijl, P. C., Zeidel, M. L., and Agre, P. (1996). Functional analysis of aquaporin-1 deficient red cells. The Colton-null phenotype. *J Biol Chem* **271,** 1309-13.

Maurel, C., Reizer, J., Schroeder, J. I., and Chrispeels, M. J. (1993). The vacuolar membrane protein gamma-TIP creates water specific channels in *Xenopus* oocytes. *EMBO J* **12,** 2241-7.

Maurel, C., Reizer, J., Schroeder, J. I., Chrispeels, M. J., and Saier, M. H. (1994). Functional characterization of the *Escherichia coli* glycerol facilitatior, GlpF, in *Xenopus* oocytes. *J Biol Chem* **269**, 11869-72.

Maurel, C., Kado, R. T., Guern, J., and Chrispeels, M. J. (1995). Phosphorylation regulates the water channel activity of the seed-specific aquaporin alpha-TIP. *EMBO J* **14,** 3028-35.

Maurel, C. (1997). Aquaporins and water permeability of plant membranes. *Annu. Rev. Plant Physiol. Plant Mol. Biol*. **48**,399-429.

Maurel, C., Tacnet, F., Guclu, J., Guern, J., and Ripoche, P. (1997). Purified vesicles of tobacco cell vacuolar and plasma membranes exhibit dramatically different water permeability and water channel activity. *Proc Natl Acad Sci U S A* **94,** 7103-7108.

Maurel, C., and Chrispeels, M. J. (2001). Aquaporins. A Molecular Entry into Plant Water Relations. *Plant Physiol* **125,** 135-138.

Miao, G. H., and Verma, D. P. (1993). Soybean nodulin-26 gene encoding a channel protein is expressed only in the infected cells of nodules and is

regulated differently in roots of homologous and heterologous plants. *Plant Cell* **5,** 781-94.

Mohr, H., and Schopfer, P. (1995). *Plant Physiol*. Springer, New York.

Mulders, S. M., Preston, G. M., Deen, P. M., Guggino, W. B., van Os, C. H., and Agre, P. (1995). Water channel properties of major intrinsic protein of lens. *J Biol Chem* **270,** 9010-16.

Murata, K., Mitsuoka, K., Hirai, T., Walz, T., Agre, P., Heymann, J. B., Engel, A., and Fujiyoshi, Y. (2000). Structural determinants of water permeation through aquaporin-1. *Nature* **407,** 599-605.

Nakhoul, N. L., Davis, B. A., Romero, M. F., and Boron, W. F. (1998). Effect of expressing the water channel aquaporin-1 on the CO_2 permeability of *Xenopus* oocytes. *Am J Physiol* **274,** C543-8.

Németh-Cahalan, K. L., and Hall, J. E. (2000). pH and calcium regulate the water permeability of aquaporin 0. *J Biol Chem* **275,** 6777-82.

Nielsen, S., and Agre, P. (1995). The aquaporin family of water channels in kidney. *Kidney Int* **48,** 1057-68.

Nielsen, S., Chou, C. L., Marples, D., Christensen, E. I., Kishore, B. K., and Knepper, M. A. (1995). Vasopressin increases water permeability of kidney collecting duct by inducing translocation of aquaporin-CD water channels to plasma membrane. *Proc Natl Acad Sci U S A* **92,** 1013-7.

Niemietz, C. M., and Tyerman, S. D. (1997). Characterization of water channels in wheat root membrane vesicles. *Plant Phys* **115**, 561-67.

Niemietz, C. M., and Tyerman, S. D. (2000). Channel-mediated permeation of ammonia gas through the peribacteroid membrane of soybean nodules. *FEBS Lett* **465,** 110-4.

Nollert, P., Harries, W. E., Fu, D., Miercke, L. J., and Stroud, R. M. (2001). Atomic structure of a glycerol channel and implications for substrate permeation in aqua(glycero)porins. *FEBS Lett* **504,** 112-7.

Oppermann, C. H., Taylor, C. G., and Conkling, M. A. (1994). Root-knot nematode-directed expression of a plant root-specific gene. *Science* **263,** 221-3.

Ou Yang, L. J., Udvardi, M. K., and Day, D. A. (1990). Specificity and regulation of the dicarboxylate carrier on the peribacteroid membrane soybean nodules. *Planta* **182,** 434-44.

Ou Yang, L. J., Whelan, J., Weaver, C. D., Roberts, D. M., and Day, D. A., (1991). Protein phosphorylation stimulates the rate of malate uptake across the peribacteroid membrane of soybean nodules. *FEBS Lett* **293,** 188-90.

Pao, G. M., Wu, L. F., Johnson, K. D., Höfte, H., Chrispeels, M. J., Sweet, G., Sandal, N. N., and Saier, M. H., Jr. (1991). Evolution of the MIP family of integral membrane transport proteins. *Mol Microbiol* **5,** 33-7.

Park, J. H., and Saier, M. H., Jr. (1996). Phylogenetic characterization of the MIP family of transmembrane channel proteins. *J Membr Biol* **153,** 171-80.

Parniske, M. C., Zimmermann, P., Cregan, B., and Werner, D. (1990). Hypersensitive reaction of nodule cells in the *Glycine sp./Bradyrhizobium japonicum*-symbiosis occurs at the genotype-specific level. *Botanica Acta* **103,**143-8.

Parsons, L.R., and Kramer, P.J. (1974). Diurnal cycling in root resistance to water movement. *Physiol. Plant* **30,**19-23.

Peterson, G. (1977). A simplification of the protein assay method of Lowry *et al.* which is more generally applicable. *Anal Biochem* **83,** 346-56.

Philips, J., and Herskowitz, I. (1997). Osmotic balance regulates cell fusion during mating in *Saccharomyces cerevisiae*. *J Cell Biol* **138,** 961-74.

Prasad, G. V., Coury, L. A., Finn, F., and Zeidel, M. L. (1998). Reconstituted aquaporin 1 water channels transport CO_2 across membranes. *J Biol Chem* **273,** 33123-6.

Preston, G. M., Carroll, T. P., Guggino, W. B., and Agre, P. (1992). Appearance of water channels in Xenopus oocytes expressing red cell CHIP28 protein. *Science* **256,** 385-7.

Reizer, J., Reizer, A., and Saier, M. H., Jr. (1993). The MIP family of integral membrane channel proteins: sequence comparisons, evolutionary

relationships, reconstructed pathway of evolution, and proposed functional differentiation of the two repeated halves of the proteins. *Crit Rev Biochem Mol Biol* **28,** 235-57.

Ren, G., Reddy, V. S., Cheng, A., Melnyk, P., and Mitra, A. K. (2001). Visualization of a water-selective pore by electron crystallography in vitreous ice. *Proc Natl Acad Sci U S A* **98,** 1398-403.

Rivers, R. L., Dean, R. M., Chandy, G., Hall, J. E., Roberts, D. M., and Zeidel, M. L. (1997). Functional analysis of nodulin 26, an aquaporin in soybean root nodule symbiosomes. *J Biol Chem* **272**, 16256-61.

Roberts, D. M., and Harmon, A. C. (1992). Calcium-modulated proteins: targets of intracellular calcium signals in higher plants. *Annu Rev Plant Physiol Plant Mol Biol* **43,** 375-414.

Roberts, D.M., and Tyerman, S.D. (2002). Voltage-dependent cation channels permeable to NH_4^+, K^+, and Ca^{2+} in the symbiosome membrane of the model legume *Lotus japonicus*. *Plant Physiol*. **128,** 370-8.

Roth, E., Jeon, K., and Stacey, G. (1988). Homology in endosymbiotic systems: The term 'symbiosome'. Molecular genetics of plant microbe interactions (eds), Palcios, R., Verma, D.P.S., ADS Press, St. Paul. 220-5.

Saijo, Y., Hata, S., Kyozuka, J., Shimamoto, K. and Izui, K. (2000). Over-expression of a single Ca2+-dependent protein kinase confers both cold and salt/drought tolerance on rice plants. *Plant J* **23,** 319-27.

Sambrook, J., Fritsch, E. F., Maniatis, T. (1989). Molecular cloning : a laboratory manual. Cold Spring Harbor Laboratory Press, Cold Spring Harbor, N.Y.

Sandal, N. N. and Marcker, K. A. (1988). Soybean nodulin 26 is homologous to the major intrinsic protein of the bovine lens fiber membrane. *Nucleic Acids Res* **16,** 9347.

Sansom, M. S., and Biggin, P. C. (2001). Water at the nanoscale. *Nature* **414,** 156-9.

Sansom, M. S., and Law, R. J. (2001). Membrane proteins: Aquaporins--channels without ions. *Curr Biol* **11,** R71-3.

Sarda, X., Tousch, D., Ferrare, K., Legrand, E., Dupuis, J. M., Casse-Delbart, F. and Lamaze, T. (1997). Two TIP-like genes encoding aquaporins are expressed in sunflower guard cells. *Plant J* **12,** 1103-11.

Schoenbeck, M. A., Temple, S. J., Trepp, G. B., Blumenthal, J. M., Samac, D. A., Gantt, J. S., Hernandez, G., and Vance, C. P. (2000). Decreased NADH glutamate synthase activity in nodules and flowers of alfalfa (*Medicago sativa* L.) transformed with an antisense glutamate synthase transgene. *J Exp Bot.* **342,** 29-39.

Serraj, R., Frangne, N., Maeshima, M., Fleurat-Lessard, P., and Drevon, J.J. (1998). A γ-TIP cross-reacting protein is abundant in the cortex of soybean N_2-fixing nodules. *Planta* **206**: 681-4.

Serraj, R., and Sinclair, T. R., (1996). Inhibition of nitrogenase activity and nodule oxygen permeability by water deficit. *J Exp Bot* **47**, 1067-73.

Sheen, J. (1996). Ca^{2+}-dependent protein kinases and stress signal transduction in plants. *Science* **274,** 1900-2.

Shiels, A., Kent, N. A., McHale, M., and Bangham, J. A. (1988). Homology of MIP26 to Nod26. *Nucleic Acids Res* **16,** 9348.

Sikorski, R. S., and Hieter, P. (1989). A system of shuttle vectors and yeast host strains designed for efficient manipulation of DNA in *Saccharomyces cerevisiae*. *Genetics* **122,** 19-27.

Sinclair, T.R., and Serraj, R. (1995). Dinitrogen fixation sensitivity to drought among grain legume species. *Nature* **378,** 344.

Smart, L. B., Moskal, W. A., Cameron, K. D., and Bennett, A. B. (2001). MIP genes are down-regulated under drought stress in *Nicotiana glauca*. *Plant Cell Physiol* **42,** 686-93.

Smith, B. L. and Agre, P. (1991). Erythrocyte Mr 28,000 transmembrane protein exists as a multisubunit oligomer similar to channel proteins. *J Biol Chem* **266,** 6407-15.

Steudle, E. (1994). Water transport across roots. *Plant and Soil* **167**, 79-90.

Steudle, E., and Henzler, T. (1995). Water channels in plants: do basic concepts of water transport change. *J Exp Bot* **46**, 1067-76.

Steudle, E. (1997). Water transport across plant tissue: Role of water channels. *Biology of the Cell* **89**, 259-73.

Steudle, E. (2000). Water uptake by roots: effects of water deficit. *J Exp Bot* **51,** 1531-42.

Steudle, E. (2001). The cohesion-tension mechanism and the acquisition of water by plant roots. *Annu Rev Plant Physiol Plant Mol Biol* **52,** 847-75.

Stiller, J., Martirani, L., Tuppale, S., Chian, R., Chiurazzi, M., and Gresshoff, P. M. (1997). High frequency transformation and regeneration of transgenic plants in the model legume *Lotus japonicus*. *J Exp Bot* **48,** 1357-65.

Stougaard, J. (2001). Genetics and genomics of root symbiosis. *Curr Opin Plant Biol* **4**, 328-35.

Sui, H., Han, B. G., Lee, J. K., Walian, P., and Jap, B. K. (2001). Structural basis of water-specific transport through the AQP1 water channel. *Nature* **414,** 872-8.

Sung, L. Moloney, A. H. M., Hunt, S., and Layzell, D. B. (1991). The effect of excision on O_2 diffusion and metabolism in soybean nodules. *Plant Physiol* **83**, 67-74.

Sweet, G., Gandor, C., Voegele, R., Wittekindt, N., Beuerle, J., Truniger, V., Lin, E. C., and Boos, W. (1990). Glycerol facilitator of Escherichia coli: cloning of glpF and identification of the glpF product. *J Bacteriol* **172,** 424-30.

Szczyglowski, K., Hamburger, D., Kapranov, P., and de Bruijn, F. J. (1997). Construction of a *Lotus japonicus* late nodulin expressed sequence tag library and identification of novel nodule-specific genes. *Plant Physiol* **114,** 1335-46.

Szczyglowski, K., Kapranov, P., Hamburger, D., and de Bruijn, F. J. (1998). The *Lotus japonicus* LjNOD70 nodulin gene encodes a protein with similarities to transporters. *Plant Mol Biol* **37,** 651-61.

Tamas, M. J., Luyten, K., Sutherland, F. C., Hernandez, A., Albertyn, J., Valadi, H., Li, H., Prior, B. A., Kilian, S. G., Ramos, J., Gustafsson, L., Thevelein, J. M., and Hohmann, S. (1999). Fps1p controls the accumulation and release of the compatible solute glycerol in yeast osmoregulation. *Mol Microbiol* **31,** 1087-104.

Thumfort, P. P., Atkins, C. A., and Layzell, D. B. (1994). A re-evaluation of the role of the infected cell in the control of O_2-diffusion in legume nodules. *Plant Physiol*. **105**, 1321-33.

Truniger, V., and Boos, W. (1993). Glycerol uptake in *Escherichia coli* is sensitive to membrane lipid composition. *Res Microbiol* **144,** 565-74.

Tyerman, S.D., Whitehead, L.F., and Day, D.A. (1995). A channel-like transporter for NH_4 on the symbiotic interface of N_2- fixing plants. *Nature* **378,** 629-32.

Tyerman, S. D., Bohnert, H. J., Maurel, C., Steudle, E., and Smith, J. A. C. (1999). Plant aquaporins: their molecular biology, biophysics, and significance for plant water relations. *J Exp Bot* **50,** 1055-71.

Tyerman, S. D., Niemietz, C. M. and Bramley, H. (2002). Plant aquaporins: multifunctional water and solute channels with expanding roles. *Plant Cell Environ* **25,** 173-94.

Udvardi, M. K., and Day, D. A. (1997) Metabolite transport across symbiotic membranes of legume nodules. *Annu Rev Plant Physiol Plant Mol Biol* **48,** 493-523.

Udvardi, M. K., and Day, D. A. (1989). Electrogenic ATPase activity on the peribacteroid membrane of soybean (*Glycine max* L.) root nodules . *Plant Physiol* **90,** 982-7.

Udvardi, K. M., Price, G. D., Gresshoff, P. M., and Day, A. D., (1988). A dicarboxylate transporter on the peribacteroid membrane of soybean nodules. *FEBS Lett* **231,** 36-40.

Unger, V. M. (2000). Fraternal twins: AQP1 and GlpF. *Nat Struct Biol* **7,** 1082-4.

Urao, T., Katagiri, T., Mizoguchi, T., Yamaguchi-Shinozaki, K., Hayashida, N., and Shinozaki, K. (1994). Two genes that encode Ca^{2+}-dependent protein kinases are induced by drought and high-salt stresses in *Arabidopsis thaliana*. *Mol Gen Genet* **244,** 331-40.

Van Brussel, A. A., Zaat, S. A., Cremers, H. C., Wijffelman, C. A., Pees, E., Tak, T., and Lugtenberg, B. J. (1986). Role of plant root exudate and Sym plasmid-localized nodulation genes in the synthesis by Rhizobium leguminosarum of Tsr factor, which causes thick and short roots on common vetch. *J Bacteriol* **165,** 517-22.

van Hoek, A. N., Hom, M. L., Luthjens, L. H., de Jong, M. D., Dempster, J. A., and van Os, C. H. (1991). Functional unit of 30 kDa for proximal tubule water channels as revealed by radiation inactivation. *J Biol Chem* **266,** 16633-5.

van Hoek, A. N., and Verkman, A. S. (1992). Functional reconstitution of the isolated erythrocyte water channel CHIP28. *J Biol Chem* **267,** 18267-9.

Verbavatz, J. M., Brown, D., Sabolic, I., Valenti, G., Ausiello, D. A., Van Hoek, A. N., Ma, T., and Verkman, A. S. (1993). Tetrameric assembly of CHIP28 water channels in liposomes and cell membranes: a freeze-fracture study. *J Cell Biol* **123,** 605-18.

Verma, D.P., and Hong, Z. (1996). Biogenesis of the peribacteroid membrane in root nodules. *Trends Microbiol*. **4,** 354-8.

Verwoerd, T. C., Dekker, B. M., and Hoekema, A. (1989). A small-scale procedure for the rapid isolation of plant RNAs. *Nucleic Acids Res* **17,** 2362.

Vessey, J. K., York, E. K., Henry, L. T., and Raper, C. D., Jr. (1988). Uniformity of environmental conditions and plant growth in a hydroponic culture system for use in a growth room with aerial CO_2 control. *Biotronics* **17,** 79-94.

Vessey, J. K., Walsh, K. B., and Layzell, D. B. (1991). Oxygen limitation of nitrogen fixation in stem girdled and nitrate-treated soybean nodules. *Plant Physiol* **73**, 113-21.

Volschenk, H., Viljoen, M., Grobler, J., Petzold, B., Bauer, F., Subden, R. E., Young, R. A., Lonvaud, A., Denayrolles, M., and van Vuuren, H. J. (1997). Engineering pathways for malate degradation in *Saccharomyces cerevisiae*. *Nature Biotechnol* **15,** 253-7.

Walz, T., Hirai, T., Murata, K., Heymann, J. B., Mitsuoka, K., Fujiyoshi, Y., Smith, B. L., Agre, P., and Engel, A. (1997). The three-dimensional structure of aquaporin-1. *Nature* **387,** 624-7.

Wayne, R., and Tazawa, M. (1990). Nature of the water channels in the internodal cells of *Nitellopsis*. *J Membr Biol* **116,** 31-9.

Weaver, C. D., and Roberts, D. M. (1992). Determination of the site of phosphorylation of nodulin 26 by the calcium-dependent protein kinase from soybean nodules. *Biochemistry* **31,** 8954-9.

Weaver, C. D., Crombie, B., Stacey, G., and Roberts, D. M. (1991). Calcium-dependent phosphorylation of symbiosome membrane proteins from nitrogen-fixing soybean nodules. Evidence for phosphorylation of nodulin 26. *Plant Physiol* **95**, 222-7.

Weaver, C. D. (1994). Structural and functional characterization of the nodulin 26 ion channel and the calmodulin-like domain protein kinase from soybean. Doctor of Philosophy Dissertation, University of Tennessee, Knoxville.

Weaver, C.D., Shomer, N.H., Louis, C.F., and Roberts, D.M. (1994). Nodulin 26, a nodule-specific symbiosome membrane protein from soybean, is an ion channel. *J Biol Che.* **269,** 17858-62.

Werner, D. (1992). Physiology of nitrogen-fixing legume nodules: compartments and functions. In *Biological Nitrogen Fixation*, G. Stacey, R. H. Burris, H. J. Evans, eds. Chapman andd Hall, New York. pp 399-431.

Weig, A., Deswarte, C., and Chrispeels, M. J. (1997). The major intrinsic protein family of Arabidopsis has 23 members that form three distinct groups with functional aquaporins in each group. *Plant Physiol* **114,** 1347-57.

Weig, A. R., and Jakob, C. (2000). Functional identification of the glycerol permease activity of Arabidopsis thaliana NLM1 and NLM2 proteins by heterologous expression in Saccharomyces cerevisiae. *FEBS Lett* **481,** 293-8.

Yamada, S., Katsuhara, M., Kelly, W. B., Michalowski, C. B., and Bohnert, H. J. (1995). A family of transcripts encoding water channel proteins: tissue- specific expression in the common ice plant. *Plant Cell* **7,** 1129-42.

Yang, B., and Verkman, A.S. (1997). Water and glycerol permeabilities of aquaporins 1-5 and MIP determined quantitatively by expression of epitope-tagged constructs in *Xenopus* oocytes*. J Biol Chem* **272,** 16140-6.

Yang, B., van Hoek, A. N., and Verkman, A. S. (1997). Very high single channel water permeability of aquaporin-4 in baculovirus-infected insect cells and liposomes reconstituted with purified aquaporin-4. *Biochemistry* **36,** 7625-32.

Yasui, M., Hazama, A., Kwon, T. H., Nielsen, S., Guggino, W. B., and Agre, P. (1999). Rapid gating and anion permeability of an intracellular aquaporin. *Nature* **402,** 184-7.

Zampighi, G. A., Kreman, M., Boorer, K. J., Loo, D. D., Bezanilla, F., Chandy, G., Hall, J. E., and Wright, E. M. (1995). A method for determining the unitary functional capacity of cloned channels and transporters expressed in *Xenopus laevis* oocytes. *J Membr Biol* **148,** 65-78.

Zarembinski, T. I., and Theologis, A. (1993). Anaerobiosis and plant growth hormones induce two genes encoding 1- aminocyclopropane-1-carboxylate synthase in rice (*Oryza sativa* L.). *Mol Biol Cell* **4**, 363-73.

Zeidel, M. L., Ambudkar, S. V., Smith, B. L., and Agre, P. (1992). Reconstitution of functional water channels in liposomes containing purified red cell CHIP28 protein. *Biochemistry* **31,** 7436-40.

Zeuthen, T., and Klaerke, D. A. (1999). Transport of water and glycerol in aquaporin 3 is gated by H^+. *J Biol Chem* **274,** 21631-6.

Zhang, Y., and Roberts, D. M. (1995). Expression of soybean nodulin 26 in transgenic tobacco. Targeting to the vacuolar membrane and effects on floral and seed development. *Mol Biol Cell* **6,** 109-17.

VITA

James F. Guenther was born on October 4, 1970 in New Orleans Louisiana to Julian Frederick, and Tenie Mae Guenther. He received his Bachelor of Science degree in May 1996 from Southeastern Louisiana University. He was accepted to the Biochemistry and Cellular and Molecular Biology program at The University of Tennessee the following fall of 1997. He joined the laboratory of Dr. Daniel M. Roberts where he received his Doctor of Philosophy degree in Biochemistry and Cellular and Molecular Biology in May 2002.